GRAVIMETRIC, ELECTROCHEMICAL AND QUANTUM CHEMICAL STUDIES OF SOME NAPHTHALOCYANINE AND PHTHALOCYANINE DERIVATIVES AS CORROSION INHIBITORS FOR ALUMINIUM IN ACIDIC MEDIUM

Masego Dibetsoe

B.Sc (NWU), B.Sc.Hons (NWU)

A thesis submitted in fulfilment of the requirements for the degree of

Master of Science (Physical Chemistry)

in the

Department of Chemistry

Faculty of Agriculture, Science and Technology,

North-West University (Mafikeng Campus)

Supervisor: Prof Eno. E. Ebenso

Co-Supervisor: Dr M.M Kabanda

May 2014

DECLARATION

I declare that this project which is submitted in fulfilment of the requirements for the degree of Master of Science in Chemistry (M.Sc) at the North West University, Mafikeng Campus has not been previously submitted for a degree at this university or any other university.

The following research was compiled, collated and written by me. All the quotations are indicated by appropriate punctuation marks. Sources of my information are acknowledged in the reference pages.

M. Dibetsoe

.....

Masego Dibetsoe

ACKNOWLEDGEMENTS

First and foremost, I would like to take all glory and honour to my Lord and Saviour Jesus Christ, for not only blessing me with the opportunity to further my education, but also seeing me through it and providing for all my need. Thank you.

I would like to thank my supervisor Professor E.E Ebenso for leading me with excellence throughout my course, his constant support and believing in me. I have truly learned a lot from you and I am very grateful to have had you as my supervisor.

I also greatly appreciate the input and support I have received from my co-supervisor Dr Mwadham. M. Kabanda. Not only did you teach me about quantum chemical studies, but you also pushed me to do my best. For that I thank you.

Thank you so much Babatunde Obadele from TUT for the help teaching us how to use the AUTOLAB and assisting further with the electrochemical studies. It's much appreciated.

I would like to acknowledge SASOL INZALO Foundation for funding my studies. Thank you for the financial support, the workshops and conferences you sent me to, the mentorship and the endless support. My studies would have not been the same if it wasn't for this opportunity. I am truly grateful.

I would also like to thank the Chemistry department of North West University for having me. It really felt like home.

Last but certainly not least, I would not have made it this far without my beautiful family. To my parents; I know all you wanted was to give me the life and opportunities that you never had and to watch me shine. Well, I am where I am today because of your love, support (even financially) and fervent prayers. To my sister; you didn't always understand why I had to go to school for so long, but now I can see that you are following in my footsteps. I'm very proud of you. I love you all more than words can express, and I pray that the good Lord keeps you for me even as I continue in this journey. Thank you.

ABSTRACT

The corrosion inhibition behaviour of seven macrocyclic compounds (including phthalocyanines and naphthalocyanines) namely 1,4,8,11,15,18,22,25-Octabutoxy-29*H*,31*H*-phthalocyanine(Pc1), 2,3,9,10,16,17,23,24-Octakis(octyloxy)-29*H*,31*H*-phthalocyanine(Pc2), 2,9,16,23-Tetra-*tert*-butyl-29*H*,31*H*-phthalocyanine 29*H*,31*H*-phthalocyanine(Pc3), 5,9,14,18,23,27,32,36-Octabutoxy-2,3-naphthalocyanine(nPc1), 2,11,20,29-Tetra-tert-butyl-2,3-naphthalocyanine(nPc2) and 2,3-naphthalocyanine(nPc3) on the corrosion of aluminium in 1M HCl was studied by means of weight loss, electrochemical, quantum chemical and quantitative structure activity relationship(QSAR) techniques. The inhibition efficiencies and corrosion rates were evaluated at temperatures ranging from 30°C - 70°C. The results suggest that inhibition efficiencies are relatively low but increased on the addition of potassium iodide (KI) due to synergistic effect. Langmuir isotherm agrees well with the experimental data. The individual quantum chemical parameters and combined ones (in a QSAR study) suggest strong interactions between the inhibitor and the metal surface. The results also point to the fact that 1,4,8,11,15,18,22,25-Octabutoxy-29*H*,31*H*-phthalocyanine and 5,9,14,18,23,27,32,36-Octabutoxy-2,3-naphthalocyanine have the highest tendency to donate electrons to an electron poor species. The results are indicative of the possible role of macrocyclic compounds as corrosion inhibitors for Al surface.

LIST OF ABBREVIATIONS

Al	Aluminium
Pc	Phthalocyanine
nPc	Naphthalocyanine
PPM	Parts Per Million
HCl	Hydrochloric acid
MIC	Microbial corrosion
IE	Inhibition efficiency
$[(CH_2)_{12}]$	Cyclododecane
Cu-PC	Copper Phthalocyanine
EIS	Electrochemical Impedance Spectroscopy
TGA	Thermogravimetric Analysis
BTSPA	bis-[trimethoxysilypropyl]amine
DMAE	2-N,N dimethylaminoethanol
UV	Ultraviolet spectrometry
VIS	Visible
Py	Pyridine
Pc1	1,4,8,11,15,18,22,25-Octabutoxy-29*H*,31*H*-phthalocyanine
Pc2	2,3,9,10,16,17,23,24-Octakis(octaloxy)-29*H*,31*H*-phthalocyanine
Pc3	2,9,16,23-Tetra-*tert*-butyl-29*H*,31*H*-phthalocyanine
Pc4	29*H*,31*H*-Phthalocyanine
nPc1	5,9,14,18,23,27,32,36-Octabutoxy-2,3-naphthalocyanine
nPc2	2,11,20,29-Tetra-*tert*-butyl-2,3-naphthalocyanine
nPc3	2,3-Naphthalocyanine
THF	Tetrahydrofuran
PDP	Potentiostatic polarization
KCl	Potassium chloride
SSE	Reference electrode

OCP	Open circuit potential
SCE	Saturated calomel electrode
KI	Potassium Iodide
E_a	Activation Energy
ΔH	Enthalpy
ΔS	Entropy
K_{ads}	Equilibirium adsorption constant
C_{inh}	Inhibitor Corrosion
HOMO	Highest Occupied Molecular Orbital
LUMO	Lowest Unoccupied Molecular Orbital
EA	Electron Affinity
IP	Ionization Potential
QSAR	Quantitative Structure Activity Relationship
DFT	Density Functional Theory
MNDO	Modified neglect of differential overlap
AM1	Austin model 1
PM3	Parameterized model number 3
HF	Hartree-Fock
MP	Møller-Plesset
B3LYP	The Becke's Three Parameter Hybrid Functional using the Lee-Yang-Parr Correlation Functional Theory
MV	Molecular Volume
RMSE	Root Mean Square Error
SSE	Sum of Squared Errors
EQCM	Electrochemical Quartz Crystal Microbalance
ICP-OES	Inductively Coupled Plasma Optical Emission Spectrometry

TABLE OF CONTENTS

LIST OF FIGURES

LIST OF TABLES

CHAPTER 1

INTRODUCTION

1.1 Definition of Corrosion

Corrosion is the disintegration of any material into its constituent atoms due to chemical reaction with its surroundings. This means electrochemical oxidation of metal in reaction with an oxidant such as oxygen. The formation of an oxide iron due to oxidation of the iron atoms is a well-known example of electrochemical corrosion, commonly known as rusting. This type of damage typically produces oxides and/or salts of the original metal. Corrosion can also refer to other materials than metals, such as ceramics or polymers, although in this context, the term degradation is more common [1]. Degradation means deterioration of physical properties of the material. This can be a weakening of the material due to a loss of cross-sectional area, shattering of a metal due to hydrogen embrittlement, or it can be the cracking of a polymer due to sunlight exposure. Materials can be metals, polymers, ceramics or composites-mechanical mixtures of two or more materials with different properties [2].

The corrosion of metals has been and still is a huge problem in industries all over the world as the use of metals is inevitable. Iron is the most widely used metal (usually as steel) in the world and the following process explain the step in which it corrodes.

1.2. Corrosion Mechanism

Corrosion processes and their characterization are complex mechanisms which require crucial experimental techniques. These processes on metallic materials are always electrochemical processes. Electrochemical reaction is a reaction which the electron can flow from certain areas of the metal to other areas through a solution which can conduct electric currents [3,4]. The process of rusting or corrosion takes place in a few steps.

Oxidation reaction: Firstly, iron is oxidized to ferrous (Fe^{2+}) ions, according to reaction 1 given below:

$$Fe_{(s)} \rightarrow Fe^{2+}_{(aq)} + 2e- \quad (1)$$

Then the (Fe^{2+}) ions are oxidized to ferric ions (Fe^{3+}), as indicated by reaction 2:

$$Fe^{2+}_{(aq)} \rightarrow Fe^{3+}_{(aq)} + e- \quad (2)$$

Reduction reaction: The third step is the reduction of oxygen by the electrons from reactions (1) and (2). This reduction is summarized by reaction 3:

$$O_{2\,(g)} + 2H_2O_{(l)} + 4e- \rightarrow 4OH^-_{(aq)} \quad (3)$$

The last step involves the reaction between Fe^{2+} and O_2 to produce ferric oxide (ion (lll) oxide). Equation 4 illustrates this:

$$4Fe^{2+}_{(aq)} + O_2 + XH_2O_{(l)} \rightarrow 2Fe_2O_3.XH_2O_{(s)}\,(rust) + 8H^+_{(aq)} \quad (4)$$

Electrochemical corrosion involves two half-cell reactions i.e. an oxidation reaction at the anode and a reduction reaction at the cathode. Both anodic and cathodic reactions have to balance each other out, resulting in a neutral reaction. Both anodic and cathodic reactions occur simultaneously at the same rates [5].

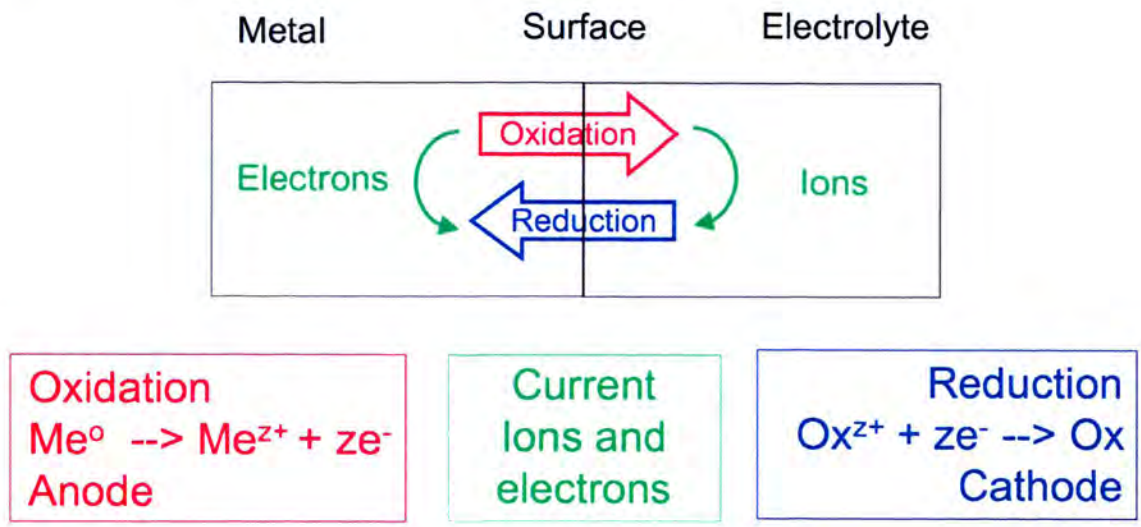

Figure 1.1: Corrosion cycle (the letter Z represent the number of electrons that can be released or taken up by the metal) [5].

1.3 Causes for metal corrosion

Metals corrode mainly because they are used in environments where they are chemically unstable. This instability is what causes the process of corrosion, and it results from the fact that a refined metal is continually trying to revert to its natural state (the mineral) [6]. It is much more natural for a metal to exist in the form of a compound, since the compounds contain less energy than the metal, therefore, more stable.

Mineral (oxide) ^{stable} --------→ Metal (e.g steel) ^{unstable} (5)

Only copper and the precious metals (gold, silver, platinum, etc.) are found in nature in their metallic state. All other metals, including iron (the metal commonly used) are processed from minerals or ores into metals which are unstable in their environments [7]. Water, air, chemical environmets (e.g. acid), etc. are among the many causes of corrosion.

1.4 Types of corrosion

Many different kinds of corrosion have been discovered, namely:

1.4.1 Galvanic corrosion: Also known as "bimetallic corrosion" is an aggressive kind of corrosion due to the electrochemical reaction between two different metals. Basically, galvanic corrosion occurs when two dissimilar/unlike metals having different electrical potentials are electrically connected [8].

1.4.2 Cavitation corrosion: corrosion that is enhanced through the formation and collapse of gas or vapor bubbles at or near the metal surface. Cavitation corrosion occurs when fluids operational pressure causing gas pockets and bubbles to form and collapse.

1.4.3 Microbial corrosion (MIC): Also called bacterial corrosion is a type of corrosion caused by microorganisms, i.e. bacteria, moulds or fungi. There are many kinds of bacteria that can cause Microbiologically Influenced Corrosion (MIC) on carbon steels, stainless steels, aluminium and copper alloys. It can apply to both metals and non-metallic materials [9].

1.4.4 Pitting corrosion: Pitting corrosion is a localized corrosion that causes holes on the metal. Pitting corrosion occurs in materials that have a protective film such as a corrosion product or when a coating breaks down. The exposed metal gives up electrons easily and the reaction initiates tiny pits [10].

1.4.5 Uniform corrosion: The uniform reduction of thickness over the surface of the corroding metal. Uniform corrosion occurs over the majority of the surface of a metal at a steady and often predictable rate. Although it is unsightly its predictability facilitates easy control, the most basic method being to make the material thick enough to function for the lifetime of the component [11].

1.4.6 Concentration cell corrosion (Crevice corrosion): This type of corrosion occurs when two or more areas of a metal surface are in contact with different concentrations of the same solutions. If two areas of a component in close proximity differ in the amount of reactive constituent available the reaction in one of the areas is speeded up. An example of this is crevice corrosion which occurs when oxygen cannot penetrate a crevice and a differential aeration cell is set up. Corrosion occurs rapidly in the area with less oxygen [12].

1.4.7 Filiform corrosion: takes place on substances that are painted. When moisture finds its way in the coating of the surface that is painted. This pattern of corrosion is characterized by the appearance of filaments. Filiform corrosion can be visually observed under a microscope and can occur on the surfaces of coated steel, magnesium, silver, gold, enamel, etc.

1.4.8 Intergranular corrosion (intercrystalline corrosion): The microstructure of metals is made up of grains, separated by grain boundaries. Cracking may occur along boundaries in the presence of tensile stress. It is caused by the physical and chemical differences between the centers and edges of the grain [11].

1.4.9 Stress corrosion cracking: the formation of cracks on a normal material through the simultaneous action of a tensile stress. It is the combined action of a static tensile stress and corrosion which forms cracks and eventually catastrophic failure of the component. This is specific to a metal material paired with a specific environment.

1.4.10 Erosion corrosion: the acceleration of the rate of corrosion attack on metal due to the motion of a corrosive fluid and a metal surface. The increased turbulence caused by pitting on the internal surfaces of a tube can result in rapidly increasing erosion rates and eventually a leak. Erosion corrosion can also be aggravated by faulty workmanship. For example, burrs left at cut tube ends can upset smooth water flow can cause localized turbulence and high flow velocities, resulting in erosion corrosion. A combination of erosion and corrosion can lead to extremely high pitting rates.

1.4.11 Dealloying corrosion: Dealloying is a selective corrosive attack by one or more constituents of a metallic alloy. This type of corrosion occurs when the alloy losses its atomic component of the metal and retains its corrosion resistant component on the metal surface.

1.4.12 Fretting corrosion. Relative motion between two surfaces in contact by a stick-slip action causing breakdown of protective films or welding of the contact areas allowing other corrosion mechanisms to operate[13].

1.5 Rate of corrosion

The rate at which metals corrode is simplified as the weight loss per unit time. The simplest way of measuring the corrosion rate of a metal is to expose the sample to the test medium (e.g. acid) for a specific time and taking the difference of the weight of the metal before and after corrosion [14].
Corrosion rate is calculated assuming uniform corrosion over the entire surface of the coupon and following equation is used;

$$\rho = (\Delta W/St) \tag{6}$$

where ΔW = weight loss, s = area of the corrosion material and t = immersion time [15].

1.6 Factors that influence corrosion rate

There are many factors that influence the rate of corrosion. Amongst the most common are the temperature and concentration of the medium. However, there are other factors which play an important role in determining the rate of corrosion of metals and these factors can be divided into two:

Factors on the metal:

- **The nature of the metal**. Metals that have low electrode potential (e.g. K, Na) are more reactive and more subject to corrosion. On the other hand, metal with high electrode potential (e.g. Al, Ti) are less reactive and are not easy to corrode.
- **Surface state of the metal**. Usually, the corrosion product is the oxide of the metal. Aluminium and Titanium are some of the metals which have an oxide layer which is highly insoluble, with low ionic and electronic conductivity. The oxide layer forms on the surface of the metal, acts as a protective film and prevents/reduces the corrosion rate. This behavior is known as 'Passivation'. Passivation generally means to make something chemically passive. Metals such as Al and Ti are self-passivating and can effectively with-stand corrosion. If the oxide layer on the metal is soluble and conductive, then the metal is not protected and is more vulnerable to corrosion (e.g. Zn and Fe).
- **Anodic and Cathodic area**. Another important factor is the ratio of anodic to cathode area [8]. For corrosion to occur there must be an anodic and cathodic reaction. Metals which have a smaller anodic area and a larger cathodic area will corrode faster and intensively than metals with a larger anodic area and smaller cathodic area.

Factors on the environment:

- **Temperature**. Most electrochemical reactions proceed at faster rates with increasing temperature. An increase in temperature will tend to stimulate corrosion attack by increasing the rate of electrochemical reactions and diffusion processes [16,17].
- **Humidity**. One of the most important factors that affect the rate of corrosion in the humidity of the atmosphere. Humidity can be defined as the amount of water vapor or moisture in the air. In the absence of moisture, most contaminant would have little or no corrosive effect.
- **pH of the medium**. Generally, the rate of corrosion is higher in acidic pH than in neutral and alkaline pH. Low pH of acid accelerates corrosion by providing a plentiful supply of hydrogen ions [18].

1.7 Corrosion Processes

Research on corrosion has shown that there are two main mechanisms/processes of corrosion. Electrochemical and chemical oxidation.

1.7.1 Electrochemical processes. Corrosion is a naturally occurring electrochemical process. The presence of a tiny amount of electrolyte on an unprotected metal surface can cause electrons to flow from a higher energy area (anode) to a lower energy area (cathode) initiating and sustaining corrosion. Microscopic droplets of water that are present in the air at 70-85% relative humidity serve as the electrolyte. The anode is the site at which the metal is corroded; the electrolyte is the corrosive medium; and the cathode (part of the same metal surface or of another metal surface in contact with it) forms the other electrode in the cell and is not consumed in the corrosion process. At the anode the corroding metal passes into the electrolyte as positively charged ions, releasing electrons which participate in the cathodic reaction. Hence the corrosion current between anode and the cathode consists of electrons flowing within the metal and ions flowing within the electrolyte [19].

1.7.2 Chemical oxidation. Chemical oxidation, unlike electrochemical, can occur in the lack of oxygen and does not need a complex cell to be in place. Chemical oxidation is caused by a substance which can be categorized as either an acid or an alkali. A general rule is that the more acidic a substance is, the more corrosive it will be and the more alkaline the less corrosive [20,21].

1.8 Kinetics and Thermodynamics of Adsorption

Adsorption is a natural process in which atoms, ions or molecules of a substance adhere to a surface of the adsorbent e.g. metal surface.

Kinetics[22]. Chemical kinetics is the study of the rates of chemical processes. These include investigations of how different experimental conditions can influence the rate of a chemical reaction and gives information about the mechanism of the reaction. Kinetics in corrosion is needed to predict the evolution of a system. Activation parameters for some systems can be estimated from the Arrhenius equation [23]:

$$k = Ae^{-E_a / RT} \tag{7}$$

where: k = the rate constant
A = the pre-exponential factor or the pre-factor
R = time gas constant
E_a = the activation energy
T = the absolute temperature

Generally, as the temperature of the corrosive acid medium increases, the corrosion rate also increases[24].

Thermodynamics[25]. The thermodynamic principles are used to explain corrosion in terms of the stability of chemical species and reactions associated with the corrosion process.

Thermodynamics can be used to evaluate the theoretical activity of a particular metal in a corrosion situation, provided the chemical make-up of the environment/medium is known. Thermodynamic considerations of an adsorption process are necessary to conclude whether the process is spontaneous or not. Gibb's free energy change, $\Delta G°$, is the fundamental criterion of spontaneity. Reactions occur spontaneously at a given temperature if $\Delta G°$ is a negative value. The thermodynamic parameters of Gibb's free energy change, $\Delta G°$, enthalpy change, $\Delta H°$, and entropy change, $\Delta S°$, for the adsorption processes are calculated using the following equations[26]:

$$\Delta G° = -RT\ln K_a \quad (8)$$

and

$$\Delta G° = \Delta H° - T\Delta S° \quad (9)$$

Generally, $\Delta G°$ values of up to -20 $kJ.mol^{-1}$ are consistent with electrostatic interaction between the charged molecules and the charged metal (physisorption), while those around -40 $kJ.mol^{-1}$ or higher are associated with chemisorption as a result of sharing or transfer of electrons from the organic molecules to the metal surface to form a coordinate type of bond[27].

1.9 The effects of corrosion

The effects of corrosion in our daily lives are both direct and indirect. Some of these effects are:

1.9.1 Economic effects [28]: Many industries shut down. This results in replacement of corroded material, preventive maintenance, loss of valuable products, etc. Several studies over the past 30 years have shown that the direct annual cost of corrosion to an industrial economy is approximately 3.1% of the company's Gross National Product (GNP). Corrosion has caused the US economy about $ 300 billion in prices per year at the current prices.

1.9.2 Health effects: Metal objects are commonly used by human beings for consumption purposes e.g. plates and cups. A corroded cup may contaminate its contents (e.g. water), which may cause health problems [29]. Corrosion of copper pipe can lead to levels of copper in the drinking water which may cause a bitter or metallic taste. The water industry will have to consider the effects of corrosion on water quality.

1.9.3 Safety effects: The effect of acid deposition on buildings is significantly damaging to the building. Sudden failure in equipment can cause fire, explosion, and release of toxic product or construction collapse.

1.10 The Corrosion of Aluminium

Aluminium is used excessively in the modern world and the uses of the metal are extremely diverse due to its many unusual combination of properties e.g. ductility and malleability, high

hardness, low density, high electrical conductivity. One of the most common uses of aluminium is packaging: drinks cans, foil wrapping, bottle tops, etc. [7]. Aluminium forms a diversity of alloys, which gives a wide range of properties and uses. It is also easy to form and recycle; the recycling of aluminium requires only 5% of the energy it takes to extract the metal from its ore. Aluminium has good corrosion resistance, especially in the atmosphere, due to the natural oxide layer [30]. Aluminum owes its excellent corrosion resistance and its usage as one of the primary metals of commerce to the barrier oxide film that is bonded strongly to its surface and, that if damaged, re-forms immediately in most environments. On a surface freshly abraded and then exposed to air, the barrier oxide film is only 1 nm thick but is highly effective in protecting the aluminum from corrosion. Aluminium has many advantageous properties such as lightness, suitability for surface treatments, functional advantages of extruded and cast semi-products, high thermal and electrical conductivity.
Although aluminium can be passive, it is a very reactive metal. However, aluminium reacts differently in different media:

Aluminium in air: Aluminium can be made to corrode quickly in air but it does not usually react, lasting longer than the less reactive iron in normal environments. The presence of salts in the air reduce the stability of aluminium, but not as much as it would do so on other material e.g. carbon steel. Aluminium reacts relatively slowly to form oxides and corrode. The reactions can be represented by this chemical equation:

$$4Al + 3O_2 \rightarrow 2Al_2O_3 \quad (10)$$

Aluminium in water: In oxygen containing environments (e.g.water), aluminium is rapidly covered with a dense oxide layer. The oxide layer is essentially inert, and prevents corrosion. When unoxidized aluminum is immersed in pure water, it will form a white hydroxide film, which remains more or less constant in thickness once equilibrium is reached. The equilibrium thickness of the layer depends on temperature. The film is stable in natural water with a pH in the neutral range from 4.5 to 8.5. However, water with a lower pH (more acidic) may attack some aluminum alloys, and water with higher pH (more basic) will attack all aluminum alloys. In the system aluminium and water, the metal is the anode and the water is the electrolyte. The oxidation is coupled with a reduction reaction.

Oxidation: $Al \rightarrow Al^{3+} + 3e^-$ (11)

Reduction: $2H^+ + 2e^- \rightarrow H_2$ (12)

$O_2 + 2H_2O + 4e^- \rightarrow 4OH^-$ (13)

$O_2 + 4H^+ 4e^- \rightarrow 2H_2O$ (14)

Formation of the corrosion product: $Al^{3+} + 3OH^- \rightarrow Al(OH)_3$ (15)

The rate of corrosion of aluminium in water depends on several parameters coupled to water: pH, temperature, electric conductivity.

Aluminium in acidic medium: In the case of corrosion in an acidic medium, the corrosion rate increases with temperature increase because the hydrogen evolution overpotential decreases. Temperature has a great effect on acidic corrosion, most often in hydrochloric and sulphuric acid [31]. The corrosion of Al in the presence of HCl is due to the migration of chloride ions through the oxide film or due to the chemisorbed chloride ions onto the oxide surface where they act like reaction partners, aiding dissolution via the formation of oxide–chloride complexes. Chloride ion is bonded chemically in the interface as an initial step of the formation of different mixed oxo-, hydro- and chlorocomplexes according to the following equations [32]:

$$Al[Ox\ (OH)y\ (H_2O)z\ ] + Cl^- \rightarrow Al[Ox\ (OH)y{-}1\ Cl\ (H_2O)z\ ] + OH^- \quad (16)$$

$$(AlOOH)_4\ xH_2O + Cl^- \rightarrow (AlOOH)_3\ xAlOClxH_2O + HO^- \quad (17)$$

$$AlOOH + Cl^- \rightarrow AlOCl + HO^- \quad (18)$$

$$Al\ (OH)_3 + Cl^- \rightarrow Al\ (OH)2\ Cl + OH^- \quad (19)$$

1.11 Corrosion Protection Methods

Corrosion affects most of the industrial sector and may cost billions of dollars each year for prevention and replacement maintenance [33].

Corrosion prevention can take a number of forms depending on the circumstances of the metal being corroded.

1.11.1 Environmental Modifications: Corrosion is caused by chemical interactions between metal and gases in the surrounding environment. Evaluating the environment in which a structure is or will be located is very important to corrosion control, no matter which control method or combination of methods is used. Modifying the environment immediately surrounding a structure, such as reducing moisture or improving drainage, can be a simple and effective way to reduce the potential for corrosion. This may be as simple as limiting contact with rain or seawater by keeping metal materials indoors or could be in the form of direct management of the environmental affecting the metal.

1.11.2 Material Selection: All metal are subject to corrosion but through monitoring and understanding the environmental conditions that are the cause of corrosion, changes to the type of metal being used can also lead to significant reductions in corrosion. Some of the most common materials used in constructing a variety of facilities, such as steel and steel-reinforced concrete, can be severely affected by corrosion.

1.11.3 Cathodic protection: Cathodic protection is a technique that uses direct electrical current to counteract the normal external corrosion of a structure that contains metal. Cathodic protection works by converting unwanted anodic (active) sites on a metal's surface

to cathodic (passive) sites through the application of an opposing current. This opposing current provides free electrons and forces local anodes to be polarized to the potential of the local cathodes. It has had widespread application on underground pipelines, and ever increasing use as the most effective corrosion control method for numerous other underground and underwater structures such as lead cables, water storage tanks, lock gates and dams, steel pilings, underground storage tanks, well casings, ship hulls and interiors, water treatment equipment, trash racks and screens. It is a scientific method which combats corrosion by use of the same rules which cause the corrosion process.

1.11.4 Coating: Coating is a principal tool for defending against corrosion. These substances are often applied in combination with cathodic protection systems to provide the most cost-effective protection for a metal. Paints and other organic coatings are used to protect metals from the degradative effect of environmental gases. Corrosion resistant coatings protect metal components against degradation due to moisture, salt spray, oxidation or exposure to a variety of environmental or industrial chemicals. Anti-corrosion coating allows for added protection of metal surfaces and act as a barrier to inhibit the contact between chemical compounds or corrosive materials.

1.11.5 Corrosion Inhibitors: Corrosion inhibitors are chemicals that react with the metal's surface or the environmental gases causing corrosion, thus, disturbing the chemical reaction that causes corrosion. Theses are substances that, when added to a particular environment, decrease the rate of attack of that environment on a material such as metal. They can help extend the life of equipment, prevent system shutdowns and failures, avoid product contamination, prevent loss of heat transfer, and preserve a metal in good condition. Inhibitors can work by adsorbing themselves on the metal's surface and forming a protective film.

Due to the challenges posed by the corrosion of metals, several steps have been designed to protect metals against corrosion. However, one of the best options involves the use of corrosion inhibitors. A corrosion inhibitor retards the rate of corrosion of a metal by being adsorbed on its surface through the transfer of charge/electron from the inhibitor to the metal surface [34].

There are different methods in which corrosion inhibitors are used. A large number of corrosion inhibitors have been developed and used for application to various systems depending on the medium treated, the type of surface that is subject to corrosion, the type of corrosion encountered, and the conditions to which the medium is exposed [35].

1.12 Corrosion Inhibitors

A corrosion inhibitor is a chemical compound that slows down or stops the corrosion (normally rusting) of a metal; a substance which when added in a small concentration to an environment effectively reduces the corrosion rate of a metal exposed to that environment. The choice of an inhibitor can be considered in two ways. Firstly, some inhibitors are

obtained from living organisms and are referred to as green corrosion inhibitors. Secondly, compounds containing hetero atoms in their aromatic or long carbon chain are capable of being adsorbed on the metal surface and can protect the metal against corrosion [34]. The inhibition of these reactions can be controlled by many types of organic and inorganic compounds, but organic compounds are the more common type of corrosion inhibitors. Most organic compounds which are efficient corrosion inhibitors contain functional groups which incorporate phosphorus, oxygen, nitrogen, sulfur atoms and multiple bonds. The action of these inhibitors are closely related to factors such as: the types of functional groups, the number and type of adsorption sites, the charge distribution in the molecules and the type of interaction between the inhibitors and the metal surface. A large number of organic compounds have been investigated as corrosion inhibitors for different types of metals.

With increased awareness towards environmental pollution and control, the search for less toxic and environment friendly corrosion inhibitors are becoming increasingly important [35]. The mechanism by which inhibitors protect the metal is by adsorbing onto the surface of the metal. Adsorption is a phenomenon in which molecules adhere to the surface of the material.

Inhibitors have always been considered to be the first line of defense against corrosion. A great number of scientific studies have been devoted to the subject of corrosion inhibitors.

A large number of corrosion inhibitors have been developed and used for application to various systems depending on the medium treated, the type of surface that is susceptible to corrosion, the type of corrosion encountered, and the conditions to which the medium is exposed. The efficiency and usefulness of a corrosion inhibitor under one set of circumstances often does not imply the same for another set of circumstances [36].

1.12.1 Types of corrosion inhibitors

a) Anodic inhibitors: Anodic inhibitors mainly slow the reaction kinetics of the anodic reaction. The corrosion potential is usually shifted in the positive direction. Anodic inhibitors usually act by forming a protective oxide film on the surface of the metal causing a large anodic shift of the corrosion potential. This shift forces the metallic surface into the passivation region. They are also sometimes referred to as passivators. Some examples of anodic inhibitors are chromates, nitrates, tungstate, molybdates.

b) Cathodic inhibitors: Cathodic inhibitors primarily slow the reaction kinetics of the cathodic reaction. The corrosion potential is usually shifted in the negative direction. Cathodic inhibitors are generally less effective than the anodic type. In contrast, they often form a visible film along the cathode surface, which polarizes the metal by restricting the access of dissolved oxygen to the metal substrate. The film also acts to block hydrogen evolution sites and prevent the resultant depolarizing effect. Cathodic inhibitors can provide inhibition by three different mechanisms as:

- Cathodic poisons: Cathodic reactions rates can be reduced by the use of cathodic poisons. Nonetheless, cathodic poisons can also increase the susceptibility of a metal to hydrogen induced cracking since hydrogen can also be absorbed by the metal during aqueous corrosion.

- Oxygen scavenger: The rates of corrosion can also be reduced by the use of oxygen scavengers that react with dissolved oxygen. Sulfite and bisulfite ions are examples of oxygen scavengers that can combine with oxygen to form sulfate.

c) Mixed Inhibitors: Mixed inhibitors work by reducing both the cathodic and anodic reactions. They are naturally film forming compounds that cause the formation of precipitates on the surface obstructing both anodic and cathodic sites. Mixed inhibitors tend to slow the reaction kinetics of both the anodic and cathodic reactions about equally. The corrosion potential may or may not shift. The most common inhibitors of this category are the silicates and the phosphates [37].

d) Volatile corrosion Inhibitors: VCIs have been used for years to temporarily protect metals from corrosion in extreme conditions found on automobile underbodies, offshore drilling decks, storage tanks, naval vessels and in the petrochemical industry [38]. Volatile compounds, such as morpholine or hydrazine, are transported with steam to prevent corrosion in the condenser tubes by neutralizing acidic carbon dioxide or by shifting surface pH towards less acidic and corrosive values.

e) Organic Inhibitors: Organic inhibitors are commonly used in acid solutions and they usually act by inhibiting the cathodic reaction. A common application is acid pickling which is used to remove oxide scale from steel ingots. Acids chemically dissolve the oxide scales, and inhibitors are needed to inhibit the electrochemical dissolution of the metal after the scale is removed [39]. Organic Corrosion Inhibitors can improve wetting and adhesion over traditional corrosion inhibitors. They can also be formed to provide coatings with high gloss as well as corrosion-resistant clear coats. The environmental toxicity of organic corrosion inhibitors has prompted the search for green corrosion inhibitors as they are biodegradable, do not contain heavy metals or other toxic compounds. As in addition to being environmentally friendly and ecologically acceptable, plant products are inexpensive, readily available and renewable. Investigations of corrosion inhibiting abilities of tannins, alkaloids, organic, amino acids, and organic dyes of plant origin are of interest [35]. It is seen that presence of heteroatoms such as nitrogen, sulphur, phosphorous in the organic compound molecule improves its action as copper corrosion inhibitor [40].

f) Inorganic Inhibitors: Inorganic inhibitors are usually used in neutral to alkaline environments and they usually act by forming a film and inhibiting the anodic reaction. Chromate is a common inorganic inhibitor that is a film former (but it also inhibits the cathodic reaction). The use of inorganic inhibitors as an alternative to organic compounds is based on the possibility of degradation of organic compounds with time and temperature [40].

1.13 Inhibition Mechanism

Corrosion inhibitors are needed to reduce the corrosion rates of metallic materials in corrosive media. The process of inhibition happens through adsorption. The adsorption mechanism is classified into two categories:

1.13.1 Physisorption: is a process where-by the electron structure of the atom or molecule is barely distressed upon adsorption.

1.13.2 Chemisorption: Chemisorption is a sub-class of adsorption, driven by a chemical reaction occurring at the exposed surface.

Table 1.1: Differences between Physisorption and Chemisorption.

Physisorption	Chemisorption
Low heat of adsorption usually in range of 20-40 kJ/mol.	High heat of adsorption in the range of 50-400 kJ/mol.
Occurs only at the temperature below the boiling point of the adsorbate (molecule).	Can occur at all temperatures.
Force of attraction are Vander Waal's forces.	Forces of attraction are chemical bond forces.
No appreciable activation energy is required.	An appreciable activation energy may be invovled in the process.
Usually takes place at low temperature and decreases with increasing temperature.	It takes place at high temperature.
The adsorbed amount increases when the pressure of the adsorbate increases.	Pressure is insignificant.
It forms multimolecular layers.	It forms monomolecular layers.

1.14 Corrosion Inhibition Efficiency

The traditional approach to evaluate the viability of corrosion inhibition combines an assessment of corrosion inhibitor efficiency and availability. The environmental parameters (e.g. temperature) have a great effect on inhibitor performance which affect the inhibition efficiency. The inhibition efficiency has been closely related to the inhibitor adsorption abilities and the molecular properties for different kinds of organic compounds. The power of the inhibition depends on the molecular structure of the inhibitor. Organic compounds, which can donate electrons to unoccupied d orbital of metal surface to form coordinate covalent bonds and can also accept free electrons from the metal surface by using their anti bonding orbital to form feedback bonds, constitute excellent corrosion inhibitors [41].
The efficiency of a inhibitor is thus expressed by this equation:

$$\%IE = \left(\frac{\rho 1 - \rho 2}{\rho 1}\right) \times 100 \qquad (20)$$

Where, ρ_1 and ρ_2 are the corrosion rates of the metal sheets in the absence and presence of inhibitor, respectively.

In general, the efficiency of an inhibitor increases with an increase in inhibitor concentration.

1.15 Research Aim and Objectives

1.15.1 Aim

The main aim of this study is to investigate the inhibiting effect of some naphthalocyanine and phthalocyanine derivatives as corrosion inhibitors of aluminium in acidic medium namely:

(i) 1,4,8,11,15,18,22,25-Octabutoxy-29*H*,31*H*-phthalocyanin(Pc1);
(ii) 2,3,9,10,16,17,23,24-Octabutoxy(octyloxy)-29*H*,31*H*-phthalocyanine(Pc2);
(iii) 2,9,16,23-Tetra-*tert*-butyl-29*H*,31*H*-phthalocyanine(Pc3);
(iv) 29*H*,31*H*-Phthalocyanine(Pc4);
(v) 2,3-Naphthalocyanine(nPc3);
(vi) 2,11,20,29-Tetra-*tert*-butyl-2,3-naphthalocyanine(nPc2);
(vii) 5,9,14,18,23,27,32,36-Octabutoxy-2,3-naphthalocyanine(nPc1);

This study employs gravimetric methods, electrochemical techniques and quantum chemical methods [42].

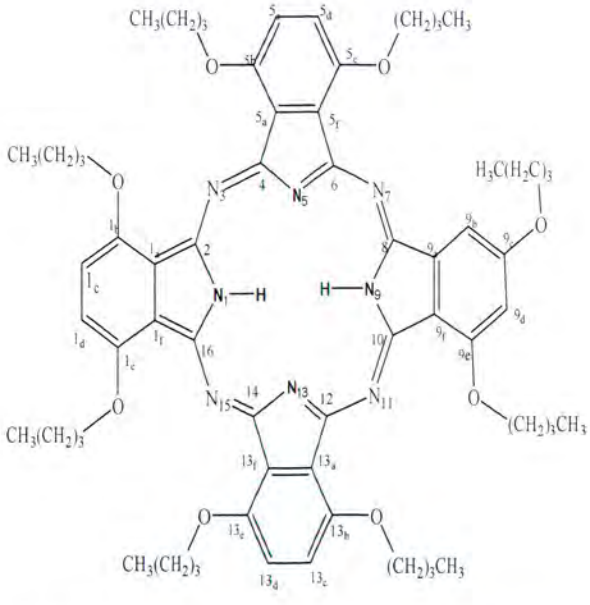

1,4,8,11,15,18,22,25-Octabutoxy-29*H*,31*H*-phthalocyanine

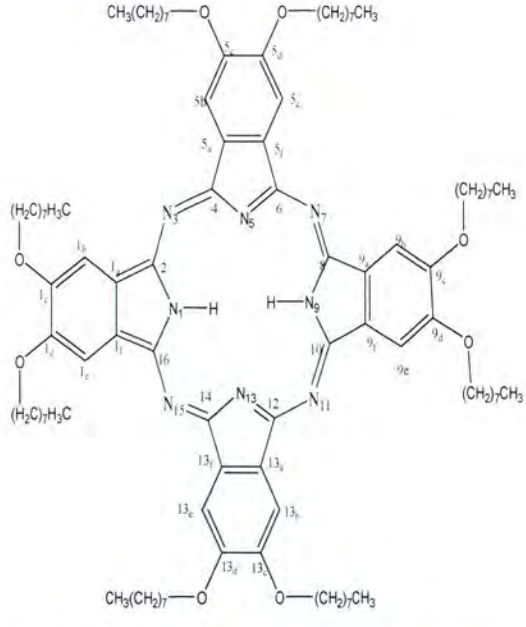

2,3,9,10,16,17,23,24-Octakis(octaloxy)-29*H*,31*H*-phthalocyanine

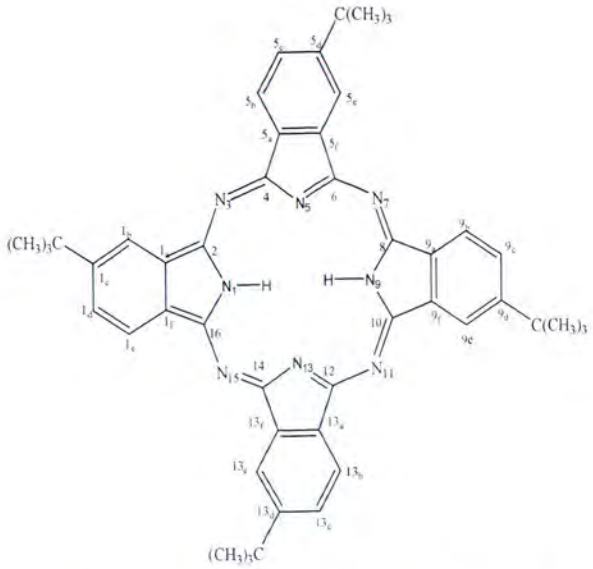

2,9,16,23-Tetra-*tert*-butyl-29*H*,31*H*-phthalocyanine

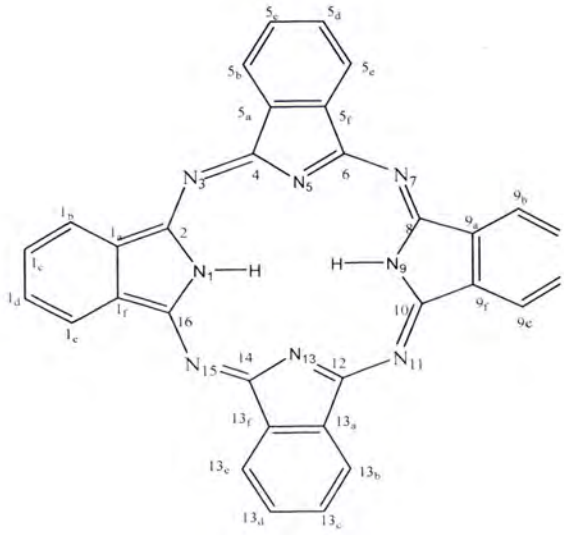

29*H*,31*H*-Phthalocyanine

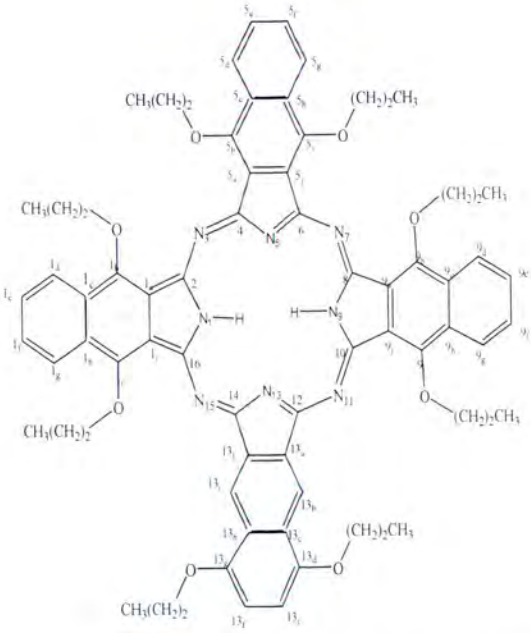

5,9,14,18,23,27,32,36-Octabutoxy-2,3-naphthalocyanine

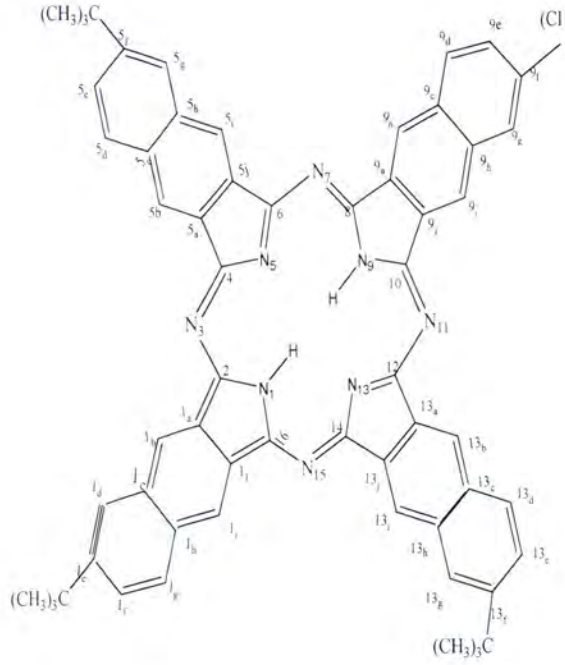

2,11,20,29-Tetra-*tert*-butyl-2,3-naphthalocyanine

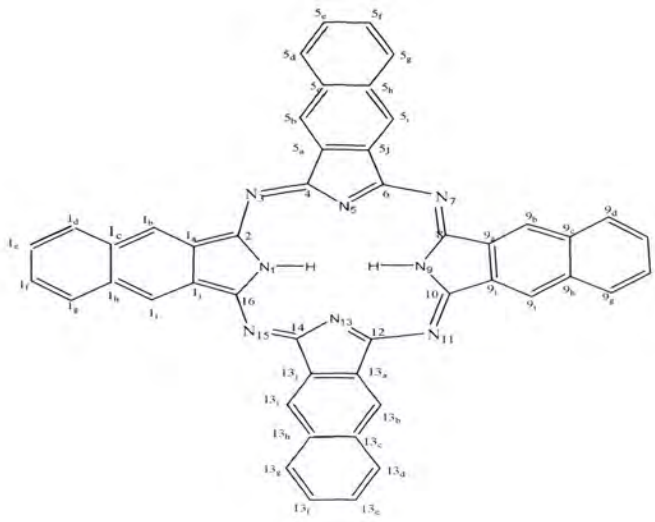

2,3-Naphthalocyanine

Figure 1.2: Structures of the naphthalocyanine and pthalocyanine derivatives used as inhibitors.

1.15.2 Objectives

The objectives of this research are to:

- Employ gravimetric and electrochemical techniques to study the corrosion inhibition process.
- Find the inhibiting potential of the inhibitors and the effect of their concentrations and temperature on the corrosion rate using thermodynamics, kinetics and adsorption principles.
- Study the synergistic or antagonistic effect of the addition of KI on the inhibitors.
- Employ quantum chemical method to optimize the geometry, calculate the quantum chemical descriptors and determine the relationship between inhibition efficiency and structural properties of macrocyclic compounds [43].

CHAPTER 2

LITERATURE REVIEW

2.1 Macrocyclic compounds

A macrocycle is a cyclic macromolecule or a macromolecular cyclic portion of a molecule. It is a molecule containing a ring of nine or more atoms. It is a cyclic molecule with three or more potential donor atoms that can coordinate to a metal center.

Macrocyclic compounds may be single, continuous thread of atoms as in cyclododecane $[(CH_2)_{12}]$, or they may incorporate more than one strand or other ring system (subcyclic units) with the macrocycle. These macrocycles may be composed of aromatic rings that confer considerably rigid structure upon the cyclic system. These aromatic rings may be joined together or coupled by spacer units consisting of one or more carbon atoms. Macrocyclic compounds and their derivatives are interesting ligand system because they are good hosts for metal anions, neutral molecules and organic cation guests. Macrocycles are important and powerful ligands, ubiquitous in transition metal coordination chemistry for the following reasons:

a) They mimic important biological ligands developed long ago by nature, for example the porphyrin prosthetic group of many metalloproteins.

b) They impart thermodynamic and kinetic stabilities to their metal complexes uncommon or non-existent with ligands of lessor types.

Synthetic macrocyclic complexes mimic some naturally occurring macrocycles because of their resemblance to many natural macrocycles, such as metalloproteins, porphyrins and cobalamine [44]. Macrocyclic compounds are uncharged and contain a cavity in which a cation can be encapsuled. The complexes thus formed are of great analytical interest, but relatively few papers dealing with these compounds have been published in analytical journals as compared to hundreds of publications in a variety of nonanalytical journals [45]. As early as 1939, a few macrocyclic compounds have been prepared by organic chemists, but their complexing properties with cations were not recognized until in the sixties. There are natural macrocyclic compounds which are antibiotics which have remained in the center of interest of biochemical, physical and electroanalytical chemists [45]. It was in 1967 when Pedersen[46] published his first paper on crown ethers under the title "Cyclic Polyethers and Their Complexes with Metal Salts". Since then, these ligands and related synthetic macrocyclic compounds have been in the center of interest for physical, organic, inorganic, and biochemists and, to a lesser extent, for analytical chemists. Soon after Pedersen's publication, Lehn *et al* [47] in Strasbourg started their large series on papers on the analytically very important macrobicyclic compounds called cryptands by Lehn. Their

properties and applications are presented in the present paper in the section on "Bicyclic, Tricyclic, and Tetracyclic Cryptands" [45].

2.2 Macrocyclic compounds as corrosion inhibitors

Macrocyclic compounds constitute a potential class of corrosion inhibitors. Most of the research work on macrocyclic compounds has been done on synthesis, design, and characterization of metal complexes. A survey of the literature revealed that despite the high ability of macrocyclic compounds to interact strongly with metal surfaces, little investigation has been made of the compounds used as corrosion inhibitors. Agarwala and coworkers studied the inhibitive action of porphyrins and some phthalocyanins and found them to be potential inhibitors for steel in acid chloride environments [48]. Recently, macrocyclic compounds have emerged as a new and potential class of corrosion inhibitors. Their ability to act as corrosion inhibitors are attributed to their fascinating molecular structure, the presence of π electrons or nonbonding electrons. In addition to these structural features planarity of these molecules further facilitates the formation of a strong bond between metal and macrocyclic molecules. A survey of literature shows that despite the high ability of macrocyclic compounds to interact strongly with metal surface, little attention has been made on the use of these compounds as corrosion inhibitors [49/50].

2.3 Phthalocyanine

Phthalocyanine is a beautifully symmetrical 18π-electron aromatic macrocycle. Phthalocyanine is an intensely blue-green coloured macrocyclic compound that is widely used in dyeing. Phthalocyanines form coordination complexes with most elements of the periodic table [51]. All phthalocyanine compounds absorb light on both sides of the blue-green portion of the visible spectrum. Therefore, "phthalocyanine" is an apt nomenclature for all members of the phthalocyanine class [52]. Phthalocyanines are large p-planar compounds composed of four isoindole groups that are linked by nitrogen atoms. Phthalocyanines have been most commonly used as pigments and dyes because of their intense color and resistance to photo-bleaching. Some phthalocyanines including zinc, silicon, and aluminum phthalocyanines have been tested in clinical studies [53].

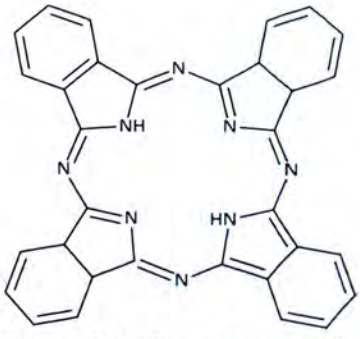

Figure 2.1: The structrure of phthalocyanine

Figure 2.2: An image of phthalocyanine blue

The word phthalocyanine is derived from the Greek terms for naphtha (rock oil) and for cyanine (dark blue)[52].

2.3.1 Historical background

Phthalocyanines (PcH_2) and its metal complexes (MPcs) were accidentally discoverd in the early 1900s[54]. In 1907, Braun and Tchernia, at the Metropolitan Gas company in London, upon examining the properties of a cyanobenzamide which they made from the reaction of phthalocyanine and acetic anhydride, found an amount of blue substance after heating o-cyanobenzamide, cooling, dissolving in alcohol and filtration[52]. This substance was undoubtedly phthalocyanine. Professor Reginal P.Linstead of the Imperial college of Science and Technology first used the term "phthalocyanine" in 1933 to describe this class of organic compounds. They are an important class of organic materials, which have attracted wide range of research interests because of their peculiar and unconventional chemical and physical properties such as chemical inertness, semi-conductivity, photoconductivity, and catalytic activity[55].

In 1934, onwards many attempts have been made by different scientists and dye companies of the world to construct the phthalocyanine colouring mater but it was the Imperial chemical industries, London which in the year 1935 started a full manufacture of the principal colouring blue pigment "copper – phthalocyanine" and named it Monstral Fast Blue BS. In 1936, I.G. Farben industry at Ludwigshaten and in the late 1930's du point and deep water point New Jersey began to produce Cu-PC. The standard ultramarine and colour company began production of this substance (pigment blue) in 1949. Successive chemical and physical studies of these chromogens by the world scholars have opened many new horizons for the utility of these pigments in variety of important fields other than colouring and now presently phthalocyanines occupy almost 60-70 of the total words production of the pigment and dyes [32].

2.3.2 The uses of Phthalocyanine

In recent years, phthalocyanines (Pcs) found more special interest as new materials in optical, electronic and photo-electronic components. [54]
Not only are the phthalocyanine a new class of organic compounds but also they constitute a new class of color matter of chromogen. Moderate cost of manufacture, good stability and properties in a region of visible spectrum which had been lacking in chromogen. The phthalocyanine class of compounds also consists of metal derivatives. The two hydrogen atoms in the center of the molecule could be replaced by metals from every group of the Periodic table to form the group of compounds known as the metal phthalocyanines. More than 40 metal phthalocyanines have been prepared and several thousand different phthalocyanine compounds have been synthesized[52]. The phthalocyanine macrocycle can play host to over seventy different metal ions in its central cavity. Since discovery, phthalocyanines and its derivatives have been extensively used as colourants (dyes or pigments). More recently, they have been employed in several 'hi-tech' applications such as the photoconducting material in laser printers and the light absorbing layer in recordable CDs (compact discs). They are also used as photosensitisers in laser cancer therapy, as nonlinear

optical materials and as industrial catalyst. The synthesis and application of phthalocyanine material is a very dynamic and multidisciplinary field of research [55].

Approximately 25% of all artificial organic pigments are phthalocyanine derivatives. These dyes find extensive use in various areas of textile dyeing, for spin dyeing and in the paper industry. Due to its stability, phthalo blue is used in inks, coatings and many plastics. The pigment is insoluble and has no tendency to migrate in the material. It is a standard pigment used in printing ink and the packaging industry.

Phthalocyanines are the second most important class of colorant and copper phthalocyanine is the single largest-volume colorant sold. Traditional uses of phthalocyanine colorants are as blue and green pigments for automotive paints and printing inks. Phthalocyanines have also found extensive use in many of the modern high technologies e.g. as cyan dyes for ink jet printing, in electrophotography as charge generation materials for laser printings and as colorants for cyan toners [56]. In the visible spectrum, phthalocyanines are limited to blue, cyan and green colors. However, their adsorption may be extended into the near infrared and by suitable chemical engineering it is possible to fingerprint the 700-1000 nm region [57]. The properties and effects of these infrared-absorbing include important hi-tech applications, photodynamic therapy, optical data storage, reverse saturable absorbers and solar screen [56]. Phthalocyanine derivatives, which have a similar structure to porphyrin, have been utilized in important functional materials in many fields. Their useful properties are attributed to their efficient electron transfer abilities [58].

2.3.3 Phthalocyanine structure

The common feature of this macrocycle is a basic structure consisting of 4 pyrrole units, which are linked in a circular manner by the methine or azamethine bridges. Phthalocyanine has the same structure as porphyrin. Their useful properties are attributed to their efficient electron transfer abilities. The central cavity of phthalocyanine is known to be capable of accomodating 63 different elemental ions, including hydrogen[59], where the central atom coordinates with the pyrrole nitrogens. The size of the hole depends on the kind of bridges connecting the pyrrole units. Naphthalocyanine is a phthalocyanine derivative.

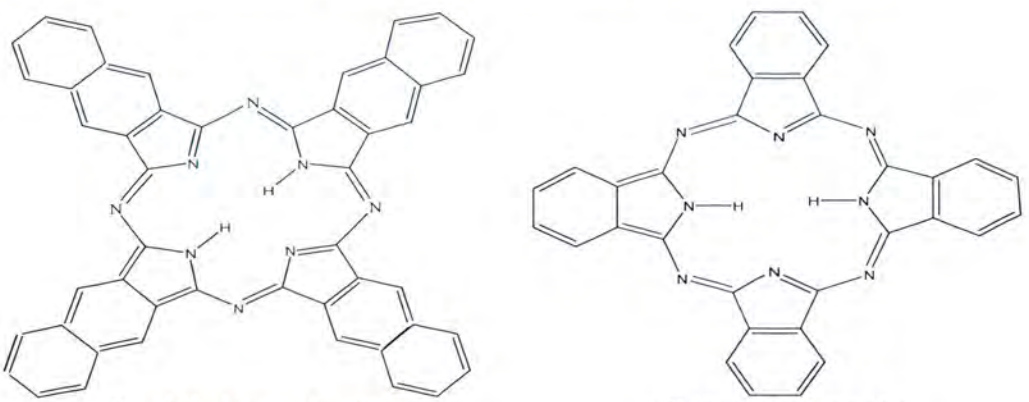

Naphthalocyanine (a) Phthalocyanine (b)

Figure 2.3: Structures of Naphthalocyanine and Phthalocyanine

Pthalocyanines with a metal or semi-metal at the center are called metallophthalocyanines or metal phthalocyanine [60]. Metal phthalocyanine have been utilized in many fields such as molecular electronics, optelectronics, photonics, etc. The functions of metal phthalocyanine are based on electron transfer reactions because of the 18 π electron conjugated ring system found in their molecular structure[59]. Phthalocyanines containing certain transition metals (e.g. Cr, Mn, Fe, Co) have more complex electronic structures because the open (n-1) d shell may result in a number of energetically close-lying electronic states [61].

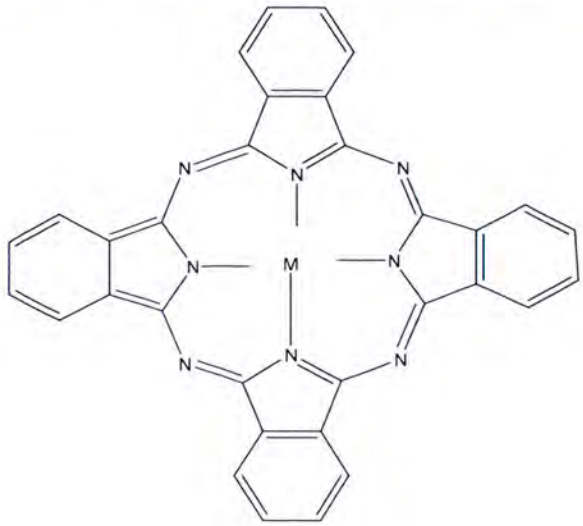

Figure 2.4: Metallophthalocyanine

2.3.4 Phthalocyanines as corrosion inhibitors

Phthalocyanines exhibit several interesting properties and applications due to their highly delocalized conjugated π electron system. The high inhibition action of the phthalocyanines is attributed to their strong chemical adsorption on the metal surface, which is determined by planarity and lone pairs of electrons in heteroatoms. Generally, localized corrosion can be prevented by the action of adsorption and aggressive anions, or by the formation of a more resistant oxide film on the metal surface. In the last few years, there has been increasing interests in macrocyclic compounds as corrosion inhibitors in acidic environments [57]. The effectiveness of some phthalocyanines as acid corrosion inhibitors have been studied [62].

Ozdemir et al [63] studied the corrosion inhibition of aluminium by novel phthalocyanines in hydrochloric acid solution. This was carried out by means of potentiodynamic polarization and electrochemical impedance spectroscopy (EIS) techniques. Langmiur adsorption isotherm fitted well with all their experimental data. The inhibition efficiency increased with increase in the phthalocyanine concentration, but decreased with an increase in temperature.

Quraishi and Rawat [50] investigated the inhibition of mild steel corrosion by some macrocyclic compounds in hot and concentrated hydrochloric acid by weight loss and potentiodynamic polarization studies. Inhibition efficiencies (IE) and corrosion rates (CR) of

these compounds were evaluated at three different temperatures ranging from 25 to 70°C. Enhancement of IE of these compounds was observed on addition of potassium iodide (KI) due to synergism. Adsorption studies showed that all of these compounds inhibit corrosion of mild steel in 5N HCl by adsorption mechanism.

Hettiachchi *et al* [62] believe that phthalocyanine would be an effective corrosion inhibitor due to planarity of the molecules, the stability as well as the possibility of interaction between the π electrons of the macrocycle with conduction band of metal. The planar molecule is expected to provide a high degree of coverage and hence a higher inhibition efficiency. Their range of good properties have led the phthalocyanines to become the object of intensive world-wide investigation.

In 2005, Zhao *et al* [64] also studied the inhibition effect of metal-free phthalocyanine (H_2Pc), copper phthalocyanine (CuPc) and copper phthalocyanine tetrasulfuric tetrasodium ($CuPc{\cdot}S_4{\cdot}Na_4$) on mild steel in 1mol/l HCl in the concentration range of 1.0×10^{-5} to 1.0×10^{-3} mol/l by electrochemical test, scanning electron microscope with energy disperse spectrometer (SEM/EDS) and quantum chemical method. The potentiodynamic polarization curves of mild steel in hydrochloric acid containing these compounds showed both cathodic and anodic processes of steel corrosion were suppressed, and the Nyquist plots of impedance expressed mainly as a capacitive loop with different compounds and concentrations. For all these phthalocyanines, the inhibition efficiency increased with the increase in inhibitor concentration, while the inhibition efficiencies for these three phthalocyanines with the same concentration decreased in the order of $CuPcS_4Na_4$ > CuPc > H_2Pc according to the electrochemical measurement results. The SEM/EDS analysis indicated that there are more lightly corroded and oxidative steel surface for the specimens after immersion in acid solution containing 1.0×10^{-3} mol/l phthalocyanines than that in blank. The quantum chemical calculation results showed that the inhibition efficiency of these phthalocyanines increased with decrease in molecule's LUMO energy, which was different from the micro-cyclic compounds.

Seugama and Aoki prepared bis-[trimethoxysilypropyl]amine (BTSPA) film filled with copper phthalocyanice (CuPc) by adding different concentrations of copper pthalocyanine and placed it on a carbon steel substrate using 120°C and 150°C as curing temperatures. For samples cured at 150 °C a second layer was also placed. The electrochemical behavior of carbon steel coated with BTSPA filled with CuPc was studied by electrochemical measurements, electrochemical impedance spectroscopy (EIS) and polarization curves, in aerated 0.1 mol L^{-1} NaCl solution. Physical and chemical characterization was made by thermogravimetric analysis (TGA), scanning electron microscopy, contact angle measurements and infrared spectroscopy. TGA showed no decomposition of CuPc during the curing process. CuPc added into the silane film showed a strong influence on its corrosion resistance, mainly when the samples are cured at 150 °C. The results showed that lower inhibitor concentrations led to a higher corrosion resistance and the second layer increased by one order of magnitude the corrosion resistance[65].

2.4 Synthesis of Phthalocyanine

Classically, phthalocyanine have been prepared by high temperature (200 to 300°C) fusion methods from phthalic anhydride or its derivatives or by condensation of phthalonitriles with lithium pentan-1-olate in refluxing pentan-1-ol (135°C). 1,3-Diiminisoindolines, prepared from phthalonitriles, are ready condensed to phthalocyanines in refluxing 2-N,N dimethylaminoethanol (DMAE) (135°C). Lower temperature synthesis of phthalocyanines in refluxing butan-1-ol (80°C) using DBU6.7 as a base is also common. Other low temperature synthesis include the use of 1,3,3trichloroisoindolines, 1-imino-3-methylthio-6-neopentoxyisoindoline, or UV methods but all give phthalocyanine at low yields [66].

Phthalocyanines with almost all metals of the periodic table in their centre are prepared by slight variation in the following methods of preparation:

a. The reaction of phthalonitrile with metal or metal salts.

4 moles of phthalonitrile are heated with one of the metal or metal chloride to 180- 1900C for atleast 2 hrs in quinoline or a mix of quinoline and trichlorobenzene. Co, Ni, Cr, Fe, Vanadyl, Chloroaluminium, and Ti-phthalocyanines have been made by this method. Quinoline or urea decomposition products act as halogen absorbing matrials in the absence of which the halogen atom enters in the PC Molecules.

b. The reaction of phthalic anhydride, phthalic acid or phthalimide, urea, metal salt and catalyst.

This method uses, the phthalic anhydride/imide, a metal salt, urea and a catalyst. The reaction here completes in about four hours heating at 170-200°C. A reaction medium such as trichlorobenzene, nitrobenzene or chloronaphthalene is generally used in the reaction. The yields in this reaction are generally about 85%. Catalysts include Am. molybdate, boric acid, ferric chloride or the pre-made metal PC itself. Cu, Co, Ni, Fe, Sn etc metal phthalocyanines are generally prepared by this method.

c. The reaction of (metalless) phthalocyanine or replaceable metal phthalocyanine with a higher metal in the periodic table.

The method involves boiling of phthalocyanine and a metal in quinoline or benzophenone. A variation of this method is a double decomposition of a labile metal phthalocyanine with a metal salt forming its more stable metal phthalocyanine molecule. For example a dilithium metal phthalocyanine complex soluble in alcohol is added $CuCl_2$ and the Cu-Phthalocyanine which precipitates immediately is filtered and dried. Reaction medium other than alcohol, such as dimethyl formamide and dimethyl sulphoxide are also equally effective. Heavy metal phthalocyanines from uranium, lead, thorium, lanthanum, gadolinium etc. metalsare prepared by thus method. The chemistry of the formation of phthalocyanine involving the union of four isoindoline units symmetrically about a centre atom in one reaction system (step) is indeed a remarkable process[67]. Kopylovich *et al* report that the most important method is based on the template reaction between a source of metal (metal, salt, alkoxide, metal-salt, etc)[68].

2.5 Solubility of Phthalocyanine

Solubility of phthalocyanines has different origins. It resides in the substituent groups or the coordinated ligands. Peripheral groups are primarily designed to promote solubility in particular solvents so that the phthalocyanine chromophore may be manipulated. Aggregation resides in the phthalocyanine chromophore and results primarily from attractive interactions between two or more of them. Solvents that will have the pronounced effects on reducing aggregation will be those which compete with aggregative interaction. While the aggregated interaction is modified by the nature of a complexed ion in the cavity and by the electronic and steric effects of peripheral groups, the interaction remains one of π-π and π-σ interactions on the frame of an organic molecule. Phthalocyanine compounds with nonionic peripheral groups in organic solutions display dependence on solvents that is influenced by the peripheral group and correlates with solvent polarity [69].

The low solubility of unsubstituted metal phthalocyanine is also a huge problem. The low solubility of common organic solvents can be overcome by introduction of suitable substituents onto the ring system. For example, quarternization of the pyridine nitrogen of metal phthalocyanine analogues containing a pyridine (Py) ring in the place of one or more of the benzoid rings is expected to confer solubility in aqueous media [70]. Introduction of peripheral substituents can dramatically increase the solubility of the target phthalocyanine in water or common organic solvents. Almost all early phthalocyanine complexes were unsubstituted on the periphery and had a low solubility in most known solvents even in such high-boiling aromatic solvents as 1-chloro- or 1-bromonaphthalene and quinoline, with sulfuric acid was found to be the best solvent for them [71].

CHAPTER 3

METHODOLOGY

3.1 EXPERIMENTAL WORK

3.1.1 Materials

Tests were performed on freshly prepared sheets 100% aluminium. The metal specimen were prepared, degreased and cleaned. Glass hooks and rods were used to suspend the metal sheet.

3.1.2 Reagents

The Hydrochloric acid (HCl) corrodent, tetrahydrofuran (THF) solvent and acetone solvents for this study were obtained from MERCK CHEMICALS.

3.1.3 Inhibitors

The phthalocyanines under study were obtained commercially from SIGMA-ALDRICH CHEMICALS. These are: 1,4,8,11,15,18,22,25-Octabutoxy-29*H*,31*H*-phthalocyanine (Pc1); 2,3,9,10,16,17,23,24-Octakis(octaloxy)-29*H*,31*H*-phthalocyanine (Pc2); 2,9,16,23-Tetra-*tert*-butyl-29*H*,31*H*-phthalocyanine (Pc3); 29*H*,31*H*-Phthalocyanine (Pc4); 5,9,14,18,23,27,32,36-Octabutoxy-2,3-naphthalocyanine (nPc1); 2,11,20,29-Tetra-*tert*-butyl-2,3-naphthalocyanine (nPc2) and 2,3-Naphthalocyanine (nPc3).

3.1.4 Gravimetric method

The gravimetric method (weight loss technique) is the most widely used method of inhibition assessment. The simplicity and reliability of the measurement offered by the weight loss method is such that the technique forms the baseline method of measurement in many corrosion monitoring programmes [72;73]. The following steps were followed:

1. Aluminium sheets were weighed using a weighing balance.
2. The aluminium sheets were completely immersed in 100 ml of solution containing various concentrations of the studied inhibitors and 1M HCl, for a period of 12 hours.
3. The immersion was maintained at a specific temperature e.g 30°C.
4. The aluminium sheets were then washed with distilled water and brushed.
5. Rinsed with acetone to remove all the impurities and to speed up the drying process.
6. These were then dried over-night and re-weighed.

Figure 3.1: Immersion set-up.

The materials used throughout the experiments were aluminium metal sheets of 1 x 8 cm surface area. The corrosive solution of 1M HCl was prepared using 32% hydrochloric acid and distilled water. Stock solutions of all the phthalocyanines were prepared by dissolving 0.1g of the inhibitor in 10 ml tetrahydrofuran (THF), then transferred to a 250 ml volumetric flask and diluted to the mark with distilled water to make a 400 ppm stock solution. The concentrations required (25, 50, 75, 100 ppm) were then prepared. After weighing precisely, the specimen were immersed in 200 ml beakers containing 1M HCl and different concentrations of the inhibitor. The beakers were placed in a water bath set a specific temperature which was monitored by a thermometer.

The corrosion rate, percent inhibition efficiency (%IE) and the surface coverage (θ) were calculated from the weight loss.

The corrosion rate (ρ) in g cm^{-2} h^{-1} was calculated from the following equation [23]:

$$\rho = \frac{\Delta W}{St} \tag{21}$$

where W is the average weight loss of the aluminium sheets, S the total area of the aluminium specimen, and t is the immersion time in hours (h).

With the calculated corrosion rate, the inhibition efficiency (%IE) and the degree of surface coverage (θ) were calculated as follows [74]:

$$\%IE = \left(\frac{\rho 1 - \rho 2}{\rho 1}\right) \times 100 \tag{22}$$

$$\theta = \left(\frac{\rho 1 - \rho 2}{\rho 1}\right) \tag{23}$$

where ρ_1 and ρ_2 are the corrosion rates of the aluminium sheets in the absence and presence of inhibitor, respectively.

3.2 Electrochemical techniques

Specimens for electrochemical studies were 1 x 1 cm. These samples were prepared by attaching an insulated copper wire to one of their faces using an aluminium conducting tape and cold mounted epoxy resin. The specimen were abraded through 1000-grit silicon carbide metallurgical paper in accordance to ASTM G59-97 degreased in acetone, and washed with distilled water. Electrochemical measurements were conducted using the potentiodynamic polarization technique (PDP) according to ASGM G 3-89 and ASTM 5-94. The conventional three electrode electrochemical cell system was used. The electrochemical cell was made of a 200 ml covered Pyrex glass conical flask suitable for the conventional three electrode system i.e. reference electrode, working electrode and counter electrode. The aluminium was used as the working electrode, platinum rods as the counter electrode and silver/silver chloride 3 M KCl electrode as the reference electrode (SSE). The corrosion inhibition of the specimen was studied in the acid and acid-inhibitor solution using the linear potentiodynamic electrochemical measurement technique. All electrochemical measurements were carried out at room temperature (± 25°C) using the autolab potentiostat (PGSTAT30 computer controlled) with the general purpose electrochemical software (GPES) version 4.9. Before potentiodynamic cyclic polarization was taken, the specimens were immersed in the electrolytes for a suitable time to stabilize at the open circuit potential (OCP). Potentiodynamic polarization curves were measured at a scan rate of 2mV/s starting from -1.0V to 1.2V. After each scan, the electrolytes were replaced with fresh electrolyte. Solutions were replaced after each test run. All the potentials reported were plotted versus the SSE potentials.

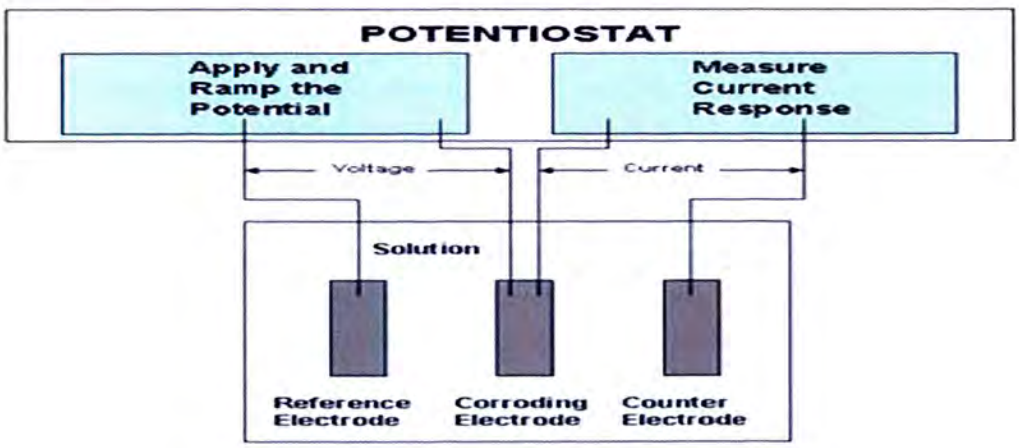

Figure 3.2: Potentiostat set-up

3.2.1 Potentiodynamic polarization measurements:

Polarization curves were recorded potentiodynamically using the Gamry Potentiostat. The assembly consists of a platinum foil as an auxiliary electrode and a saturated calomel electrode (SCE) as a reference electrode. The corrosion potential (E_{corr}), corrosion current density (I_{corr}), percentage inhibition efficiency (%IE) and Tafel constant (b_a and b_c) were

obtained from the cathodic and anodic curves. The measured corrosion current densities values were used to calculate the inhibition efficiency by making use of the equation given below:

$$\mu_{PDP} = \frac{i_{corr}^{0} - i_{corr}^{i}}{i_{corr}^{0}} \times 100 \qquad (24)$$

where i_{corr}^{0} and i_{corr}^{i} are values of corrosion current density in absence and in presence of inhibitor, respectively.

The potentiostatic method of polarization has the advantage that it can follow more closely the behavior of metals during the formation and breakdown of passivating films, where the behavior primarily depends on the potential of the metal, and very large changes in currents can occur at constant potential [75;76].

3.3 Quantum chemical studies

Quantum chemical methods enable the definition of a large number of molecular quantities characterizing the reactivity, shape and binding properties of a complete molecule as well as of molecular fragments and substituents [77-111]. The sketches and calculations were done using Gaussian09 software. The optimized geometrical structures were obtained using the Spartan10 software program [77]. Quantitative structure activity relationship (QSAR) was also performed to assess the relationship between the inhibition effect and the molecular properties.

Quantum chemical calculations derived some parameters namely: dipole moment, highest occupied molecular orbital (HOMO), the lowest unoccupied molecular orbital (LUMO), partial atomic charges, etc. These parameters were used to explain the reactivity tendency and the reactive centres of the phthalocyanine studied. The QSAR (quantitative structure activity relationship) was performed to investigate the possible correlation between the quantum chemical parameters and the experimental inhibition efficiencies reported. The quantum chemical calculation and the geometry optimization were done using density functional theory (DFT) using the 6-31G (d) basis set. The DFT is known to produce a good estimate of molecular properties that are related to the molecular reactivity. Among the molecular properties that are well reproduced by the DFT include the energy of the highest occupied molecular orbital (E_{HOMO}), energy of the lowest unoccupied molecular orbital (E_{LUMO}), electronegativity, global hardness and softness, electron affinity, ionization potential, etc.

These quantities are often defined using the Koopman's theorem:

Electronegativity (χ) is the measure of the power of an electron or group of atoms to attract electrons towards itself and it can be estimated by using the equation:

$$\chi \cong -\tfrac{1}{2}\,(E_{HOMO} + E_{LUMO}) \qquad (25)$$

Global hardness (η) measures the resistance of an atom to a charge transfer and was estimated using the equation:

$$\eta \cong -\tfrac{1}{2} (E_{HOMO} - E_{LUMO}) \quad (26)$$

Global electrophilicity index (ω) was estimated by using the electronegativity and chemical hardness parameters through the equation:

$$\omega = \chi^2/2\eta \quad (27)$$

A high value of electrophilicity describes a good electrophile while a small value of elecrophilicity describes a good nucleophile.
Global softness (σ), describes the capacity of an atom or group of atoms to receive electrons [114], it was estimated by using the equation:

$$\sigma = 1/\eta \cong -2/(E_{HOMO} - E_{LUMO}) \quad (28)$$

Electron affinity (A) is the energy released when an electron is added to a neutral molecule; it is related to E_{LUMO} through the equation:

$$A \cong - E_{LUMO} \quad (29)$$

Ionization potential (I) is the amount of energy required to remove an electron from a molecule; it is related to the energy of the E_{HOMO} through the equation:

$$I \cong - E_{HOMO} \quad (30)$$

CHAPTER 4

RESULTS AND DISCUSSION

4.1 Weight loss method

Weight loss measurements were carried out on aluminium metal sheets. The temperature and concentration of the inhibitor varied, but the concentration of the acid solution remained the same (1M). The metal sheets were immersed in the solution for 12 hours for each inhibitor.

4.1.1 The effect of the inhibitor concentration on the inhibition efficiency for aluminum

Figures 4.1 to 4.5 show the plots of inhibition efficiency versus concentration for each inhibitor at different temperatures before and after addition of potassium iodide (KI). According to the results, there is an increase in inhibition efficiency as the concentration of the inhibitor increases, while the inhibition efficiency decreases with an increase in temperature, in both cases of addition of KI and without KI. This behavior is observed because the acid becomes more aggressive at higher temperatures. Looking at Pc1 for example, at 30°C the inhibition efficiency is 63.7% at 25 ppm and increases to 67.6% at 100 ppm. However, at the same concentration (100 ppm), the inhibition efficiency is 67.6% at 30°C and decreases to 55.5% at 70°C. After adding KI, Pc1 at 30°C goes from an inhibition efficiency of 63.7% for 25 ppm to 81.8% for 25 ppm. However, even with the addition of KI, the inhibition efficiency of Pc1 decreases from 81.8% (25 ppm) to 61.4 (25 ppm) as the temperature increased. The results show that the addition of KI enhances the inhibition efficiency but does not interrupt the trend that is followed by the inhibitors.

The results below indicate that an increase in alkyl chain length also increases the inhibition efficiency. As seen from the results, at 70°C, the phthalocyanine with the most substitution (Pc1) has the highest inhibition efficiency. Pc1 at 100 ppm has an inhibition efficiency of 55.5% and 78.8% with KI. However, with naphthalocyanine, the inhibitor with the least substitution (nPc3) has the highest inhibition efficiency of 44.5% but nPc1 shows the highest inhibition efficiency of 81.5% with K

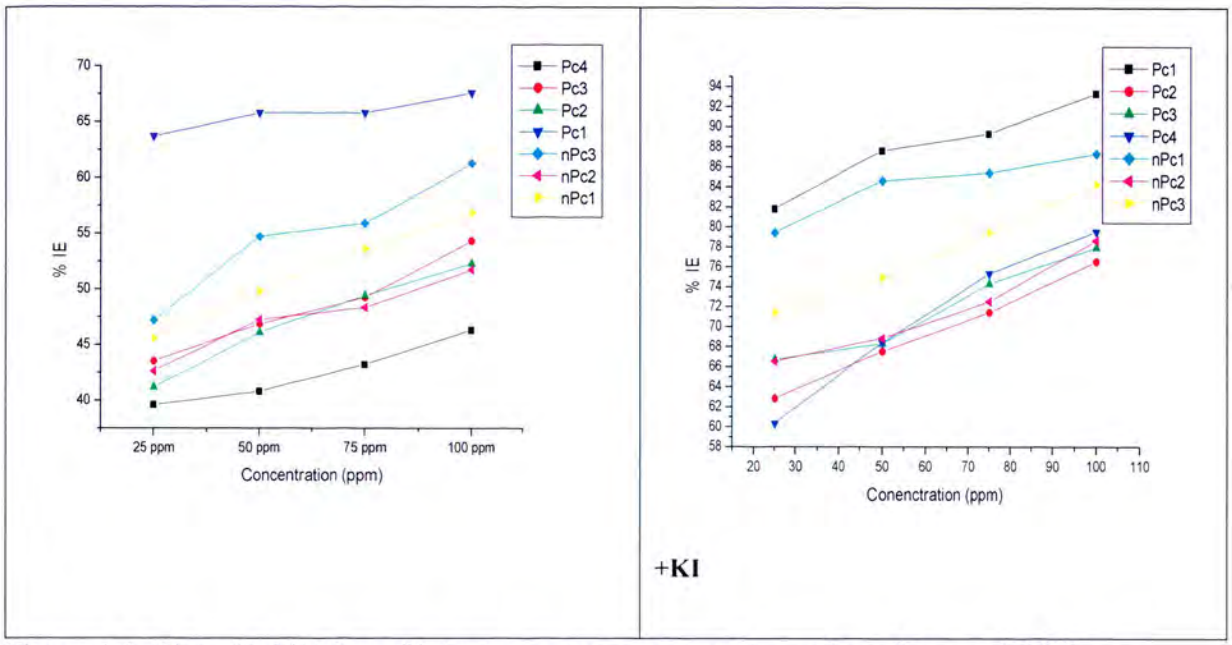

Figure 4.1: Plot of inhibition efficiency against concentration using all seven inhibitors at 30°C with and without KI.

Figure 4.1 clearly shows that the inhibition efficiency for all the inhibitors (Pc1, Pc2, Pc3, Pc4, nPc1, nPc2 and nPc3) increases as the inhibitor concentration increases. The plot shows that Pc1 and nPc3 have the highest inhibition efficiency as previously discussed on the paragraph above. With addition of KI the inhibition efficiency increases for all inhibitors, but follows the same trend as the plot without KI, however, Pc1 and nPc1 have the highest inhibition efficiency in this case.

At 30°C without addition of KI, the order is:- Pc1>nPc3>nPc1>Pc3>Pc2>nPc2>Pc4.

At 30°C with addition of KI, the order is:- Pc1>nPc1>nPc3>Pc4>nPc2>Pc3>Pc2.

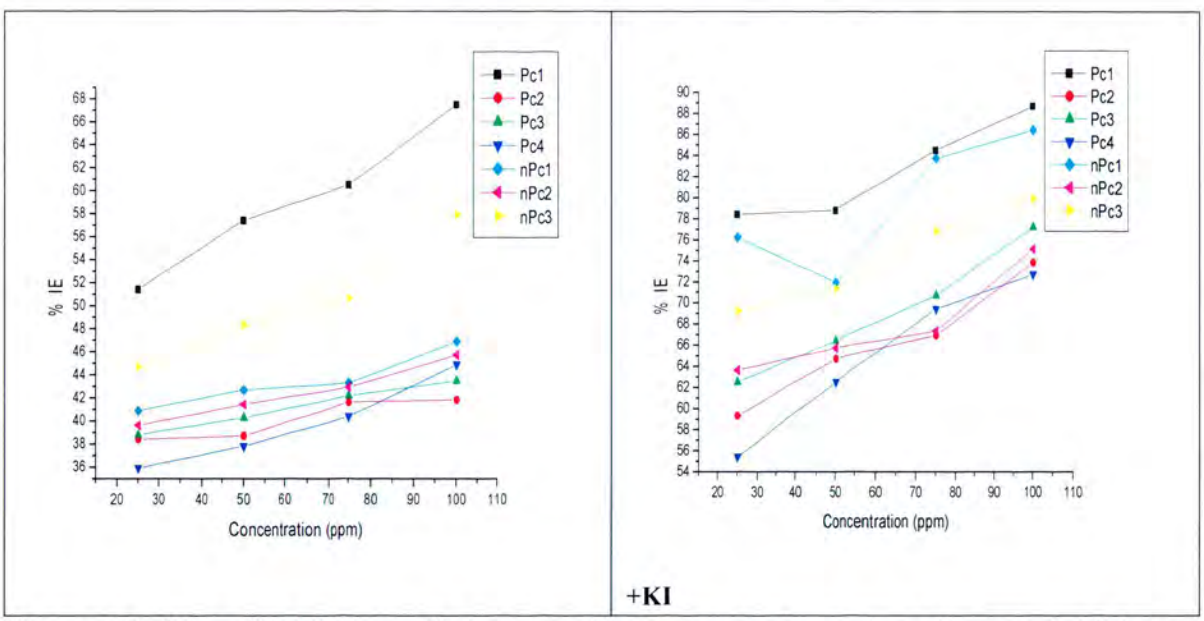

Figure 4.2: Plot of inhibition efficiency against concentration using all seven inhibitors at 40°C with and without KI.

Figures 4.2 shows that the inhibition efficiency increases as the concentration increases at 40^0c. Like 4.1, the plot without KI shows Pc1 and nPc3 to have the highest inhibition efficiency, whereas the plot with KI shows Pc1 and nPc1 to have the highest inhibition efficiency. This could be attributed to the long alkyl chain of the nPc1, which is enhanced by the KI. Nonetheless, the addition of KI still does not change the trend shown by the inhibitor.

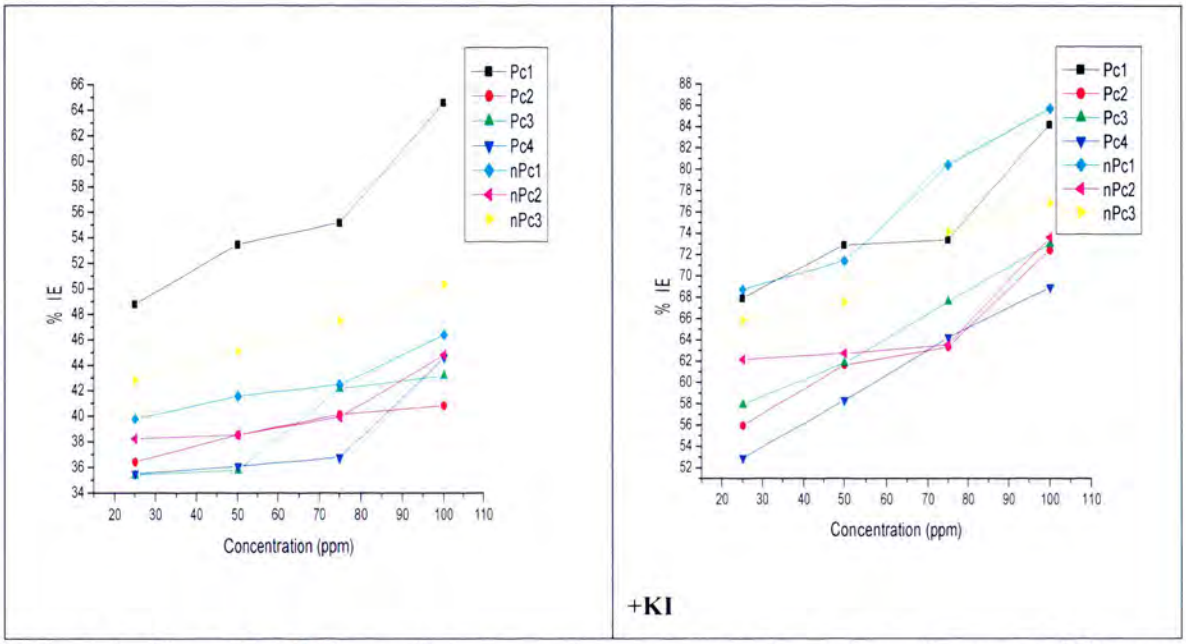

Figure 4.3: Plot of inhibition efficiency against concentration using all seven inhibitors at 50°C with and without KI.

Figure 4.3 also show that the inhibition efficiency for all inhibitors increases with an increase in concentration. Pc1 and nPc3 have the highest inhibition efficiency without the KI and with the KI, Pc1 and nPc1 still have the highest inhibition efficiency.

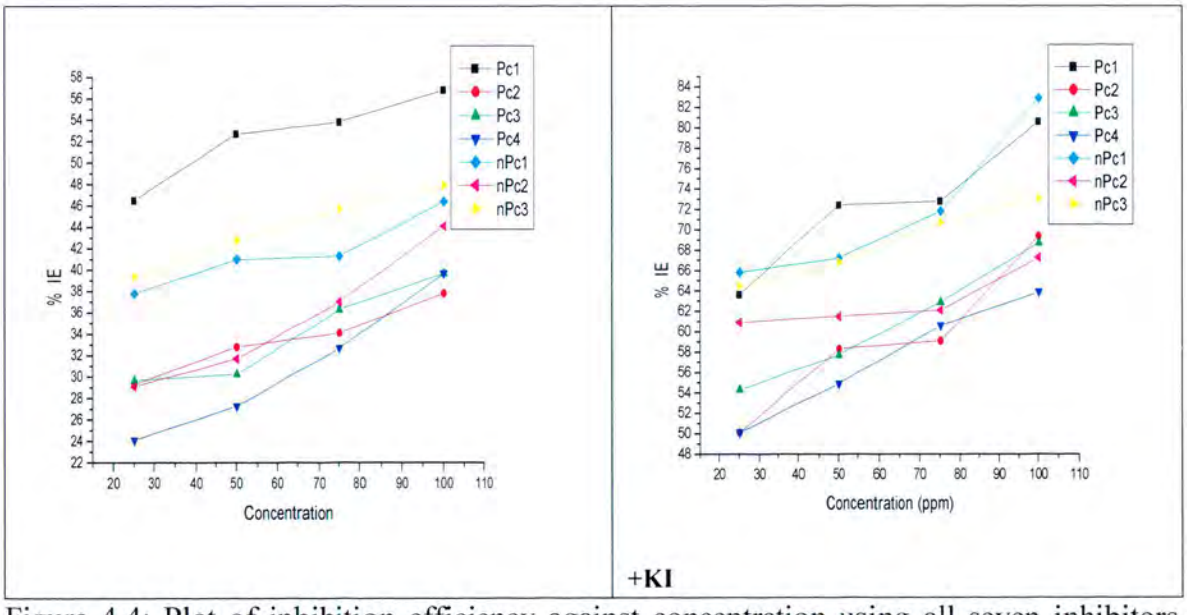

Figure 4.4: Plot of inhibition efficiency against concentration using all seven inhibitors at 60°C with and without KI.

Figure 4.4 also show that the inhibition efficiency for all inhibitors increases with an increase in concentration. Pc1 and nPc3 have the highest inhibition efficiency without the KI and with the KI, Pc1 and nPc1 have the highest inhibition efficiency.

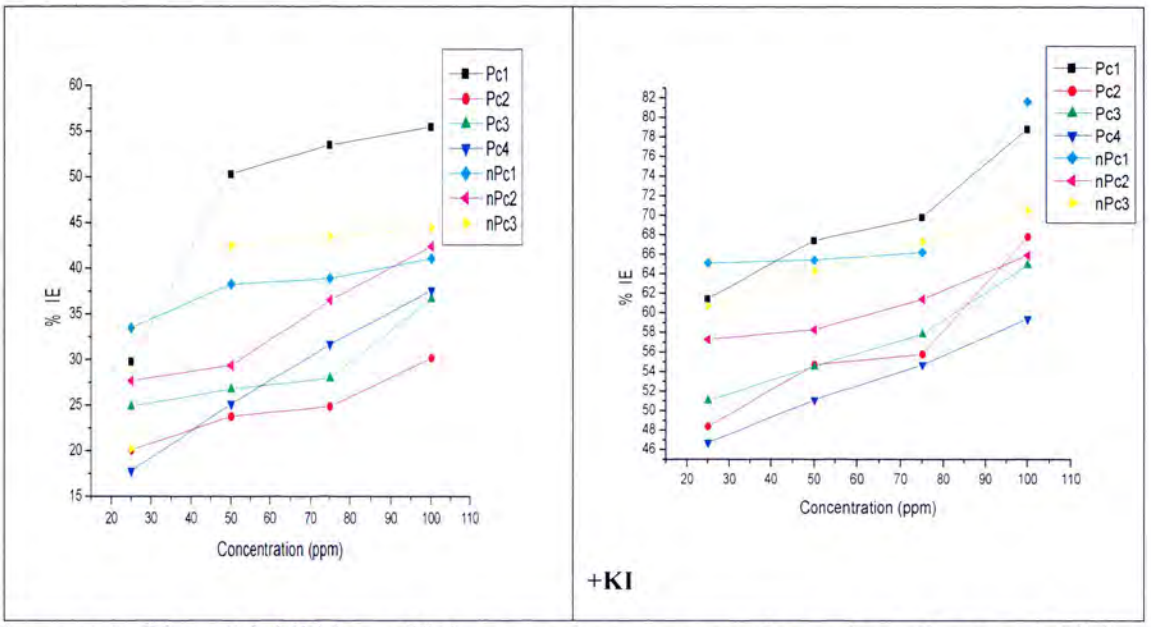

Figure 4.5: Plot of inhibition efficiency against concentration using all seven inhibitors at 70°C with and without KI.

Figure 4.5 also shows that the inhibition efficiency for all inhibitors increases with an increase in concentration. Pc1 and nPc3 have the highest inhibition efficiency without the KI and with the KI, Pc1 and nPc1 have the highest inhibition efficiency. The plots also indicate that the inhibition efficiency decreases with increasing temperature.

4.1.2. The effect of temperature on the inhibition efficiency on aluminium.

Thermodynamic adsorption parameters and kinetics of corrosion parameters are useful for clarifying the adsorption behaviour of an inhibitor. The effect of temperature on the inhibited acid-metal reaction is highly complex because many changes occur on the metal surface, such as rapid etching, desorption of the inhibitor and the inhibitor itself might undergo decomposition or rearrangement [78]. The inhibition efficiency decreases with an increase in temperature. This is due to fact that the adsorption coverage of the inhibitor on aluminium surface increases with the concentration of the inhibitor. It is noted that the inhibition efficiency depends on the temperature and decreases as the temperature increases, which indicates that, dissolution of aluminium predominates on the surface. Therefore, the corrosion rate increases with an increasing temperature. This effect can be explained by the decrease of strength of the adsorption process at high temperature, suggesting physical adsorption [79]. In this work, the effect that temperature has on inhibition efficiency was studied on various concentrations ranging from 25 – 100 ppm for all inhibitors. The temperatures used were from 30-70°C and an immersion time of 12 hours.

The dependence of the corrosion rate on temperature can be expressed by Arrhenius equation and transition state equations as presented in equation 29 and 30 below.

$$\log C_R = \log A - \frac{E_a}{2.303RT} \tag{31}$$

$$C_R = \frac{RT}{Nh}\exp\left(\frac{\Delta S*}{R}\right)\exp\left(-\frac{\Delta H*}{RT}\right) \tag{32}$$

where, C_R is the corrosion rate ($g.cm^{-2}.h^{-1}$), E_a is the apparent activation energy, R is the molar gas constant (8.314 $J.K^{-1}.mol^{-1}$), T is the absolute temperature, A is the frequency factor, ΔH^* is the apparent enthalpy of activation, ΔS^* is the apparent entropy of activation, h is Planck's constant, and N is the Avogadro number.

Figure 4.6- 4.12 show the Arrhenius plot for aluminium corrosion is 1M HCl in the absence and presence of different concentrations of all the seven inhibitors studies with and without KI.

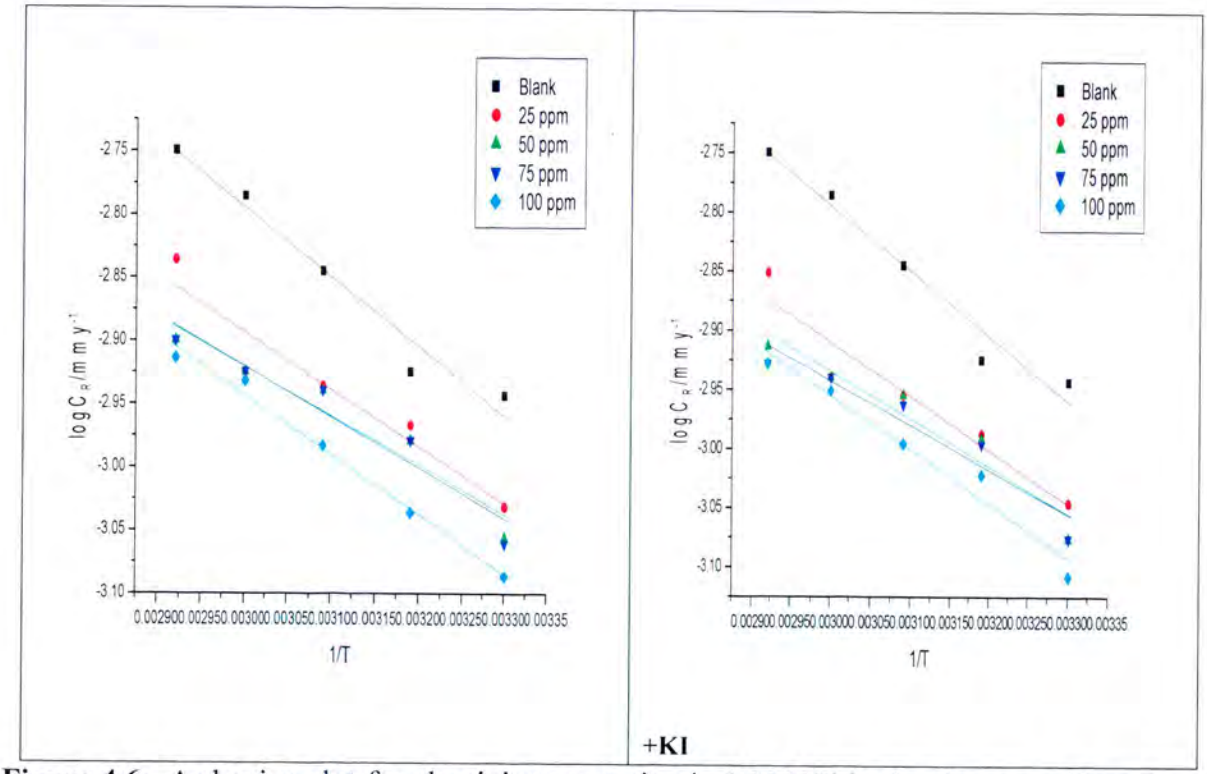

Figure 4.6: Arrhenius plot for aluminium corrosion in 1 M HCl in the absence and presence of different concentrations of Pc1 with and without KI.

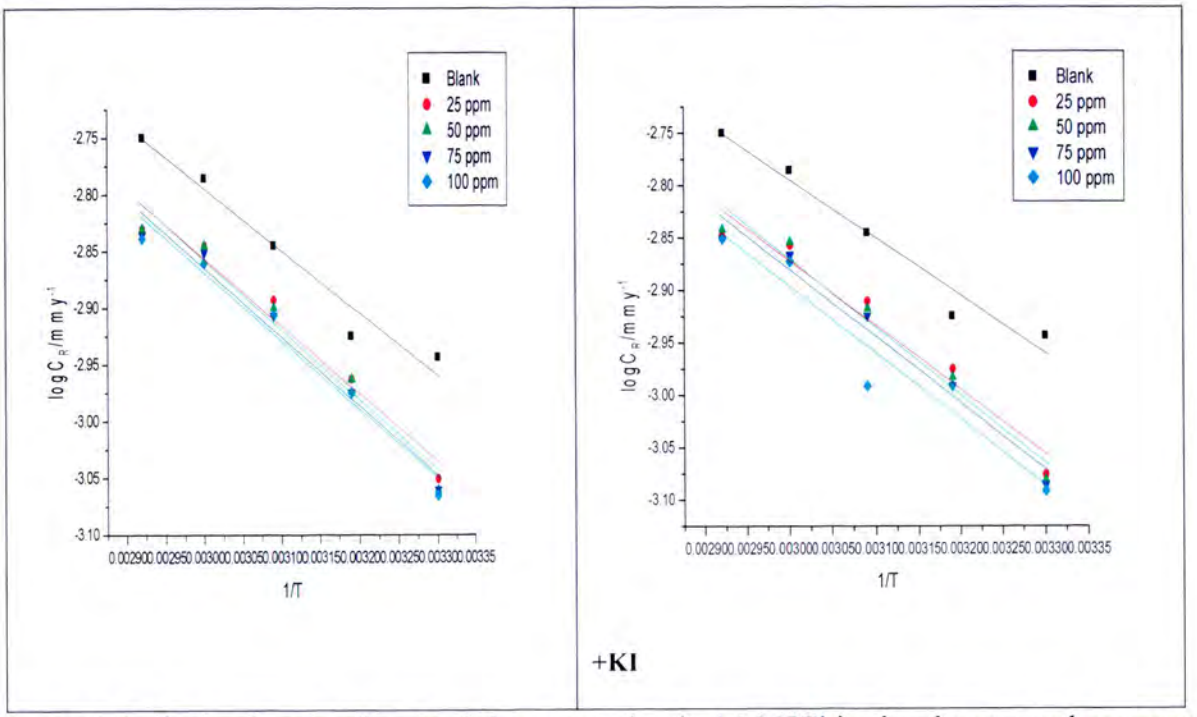

Figure 4.7: Arrhenius plot for aluminium corrosion in 1 M HCl in the absence and presence of different concentrations of Pc2 with and without KI.

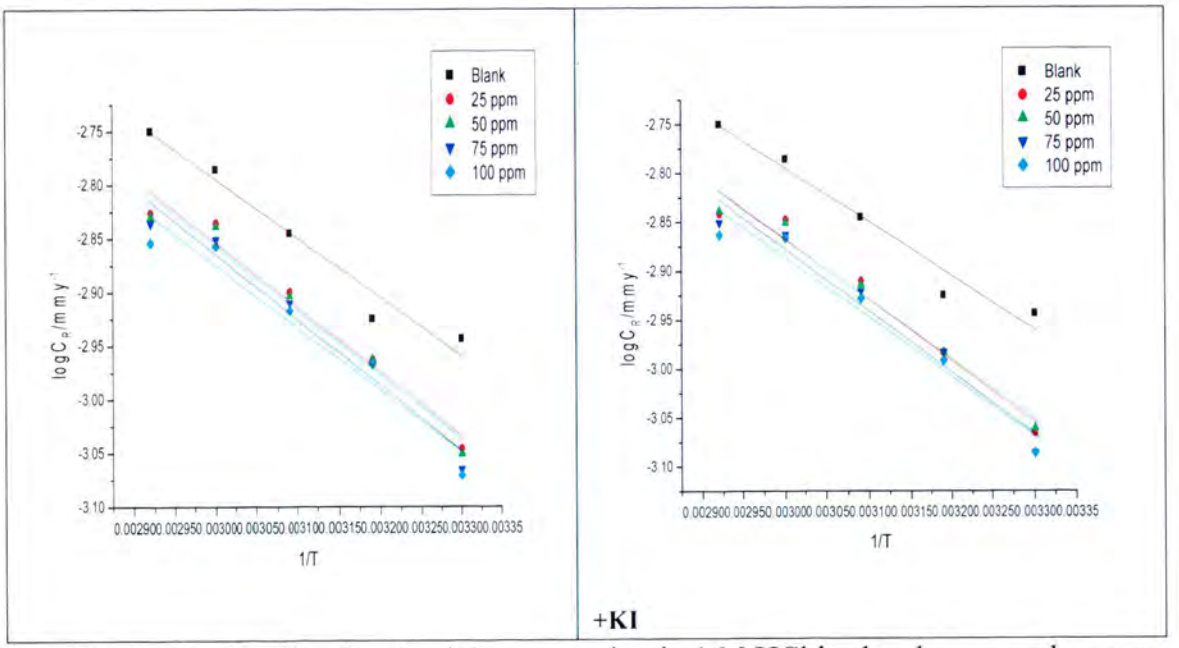

Figure 4.8: Arrhenius plot for aluminium corrosion in 1 M HCl in the absence and presence of different concentrations of Pc3 with and without KI.

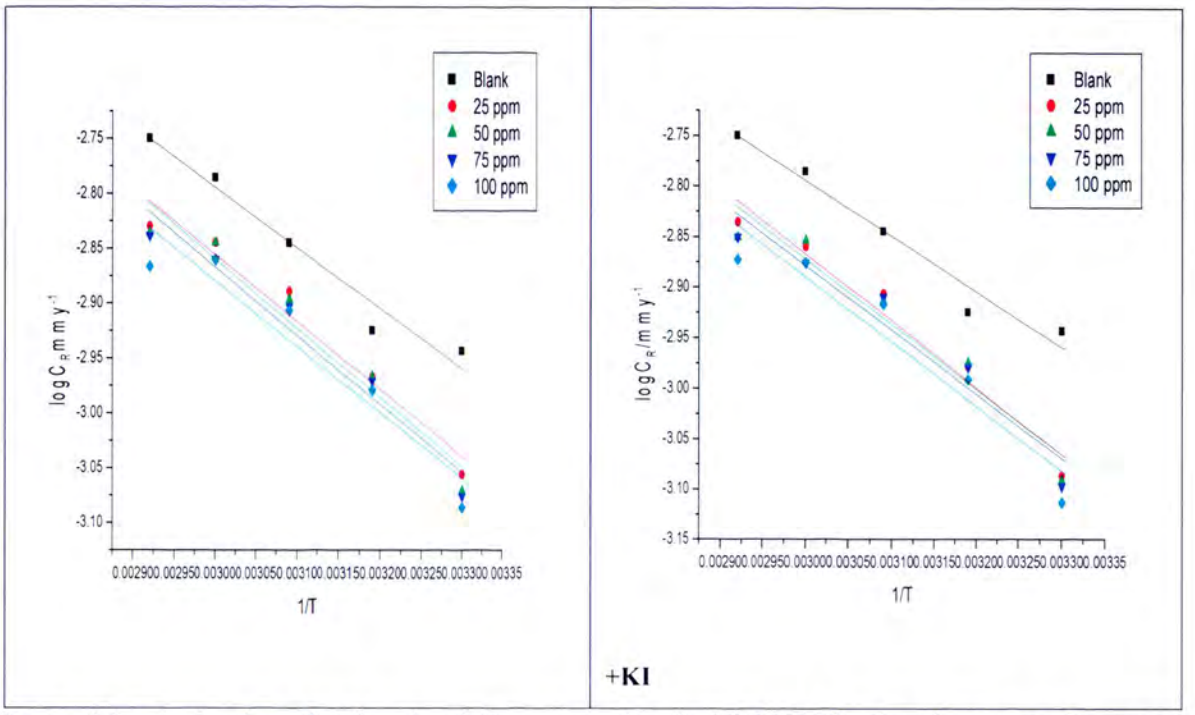

Figure 4.9: Arrhenius plot for aluminium corrosion in 1 M HCl in the absence and presence of different concentrations of Pc4 with and without KI.

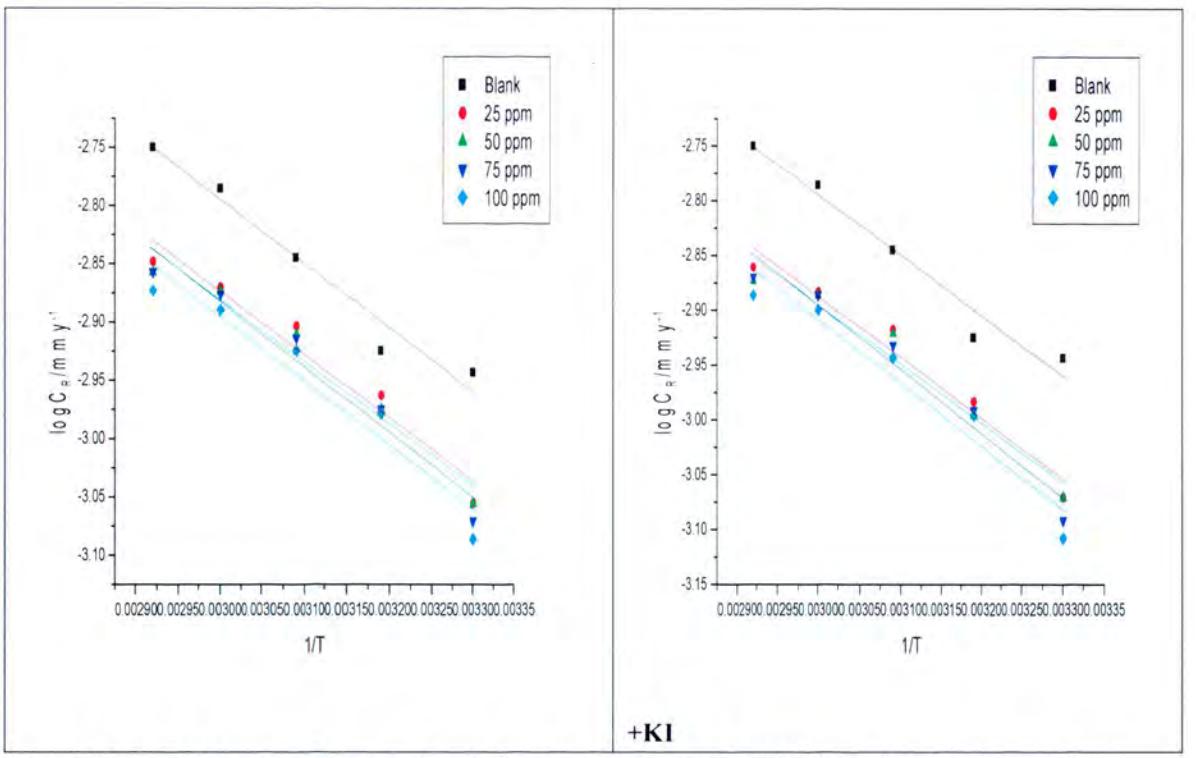

Figure 4.10: Arrhenius plot for aluminium corrosion in 1 M HCl in the absence and presence of different concentrations of nPc1 with and without KI.

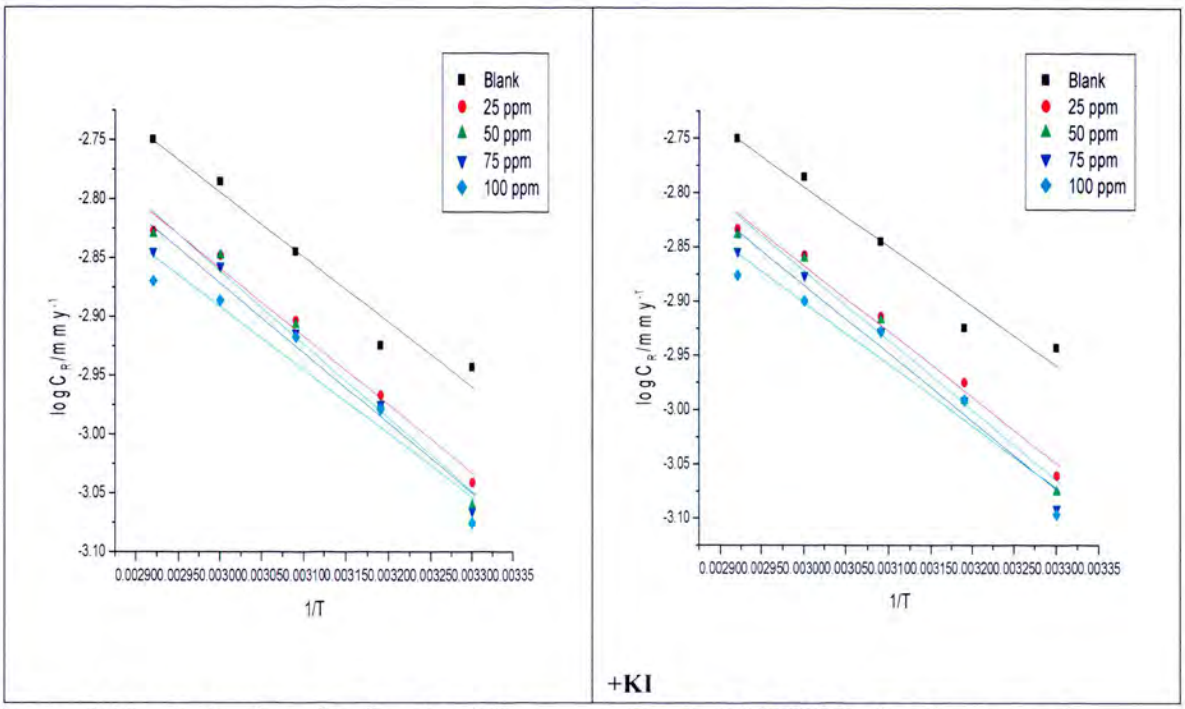

Figure 4.11: Arrhenius plot for aluminium corrosion in 1 M HCl in the absence and presence of different concentrations of nPc2 with and without KI.

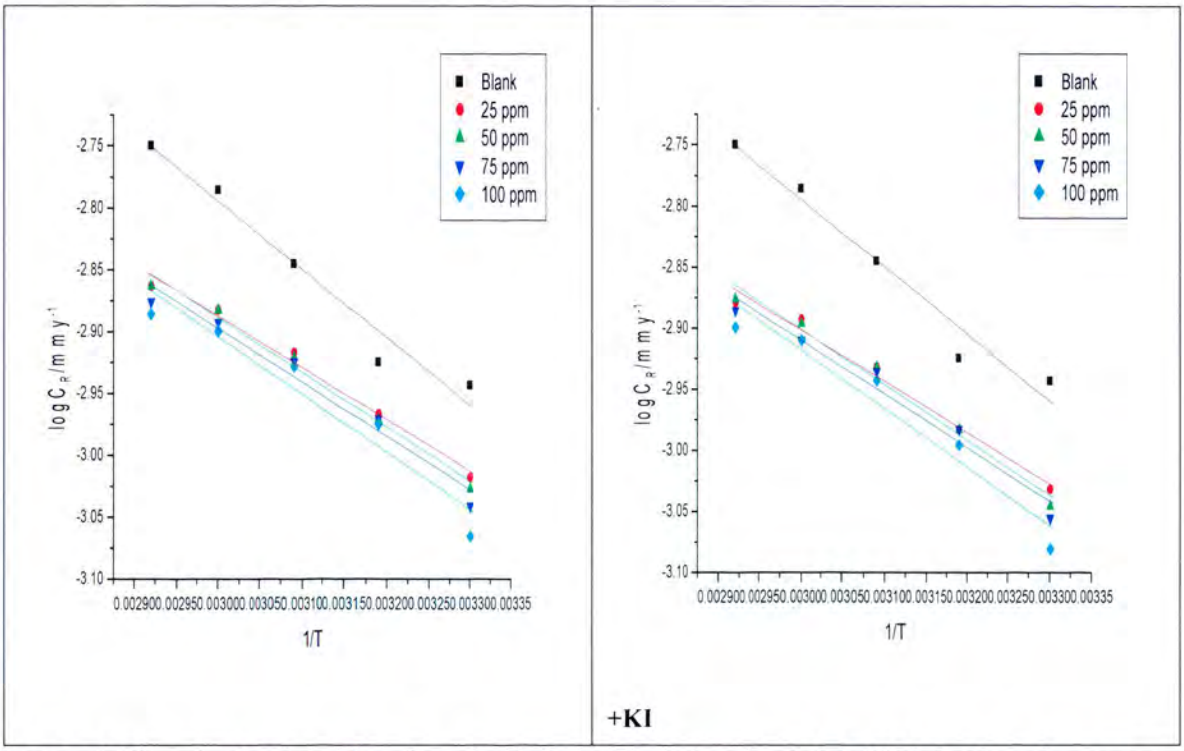

Figure 4.12: Arrhenius plot for aluminium corrosion in 1 M HCl in the absence and presence of different concentrations of nPc3 with and without KI.

4.1.3 Thermodynamic Parameters

Thermodyanamic parameters of corrosion, namely activation energy E_a, entropy ΔS and enthalpy ΔH at different concentrations of the phthalocyanines were calculated from the Arrhenius equation (31) and its alternative formulation called the transition state equation (32). Activation energies were calculated from the Arrhenius plots(figure 4.6-4.12), which represent the relationship between $\log(C_R)$ and the reciprocal absolute temperature (1/T). The values of entropy ΔS and of the enthalpy ΔH were obtained using the transition state equation (32) [80].

Figures 4.13-4.19 shows the transition state plots for all the seven inhibitors at different temperatures with and without KI.

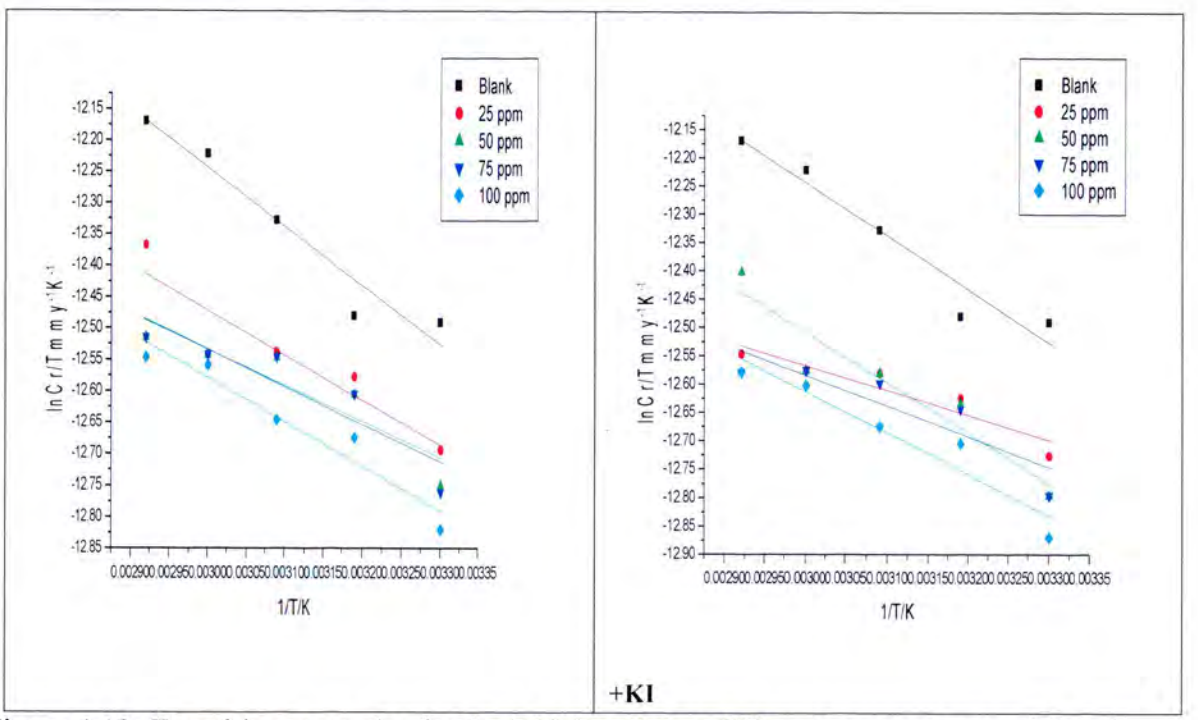

Figure 4.13: Transition state plot for the inhibitor Pc1 at different temperatures with and without KI.

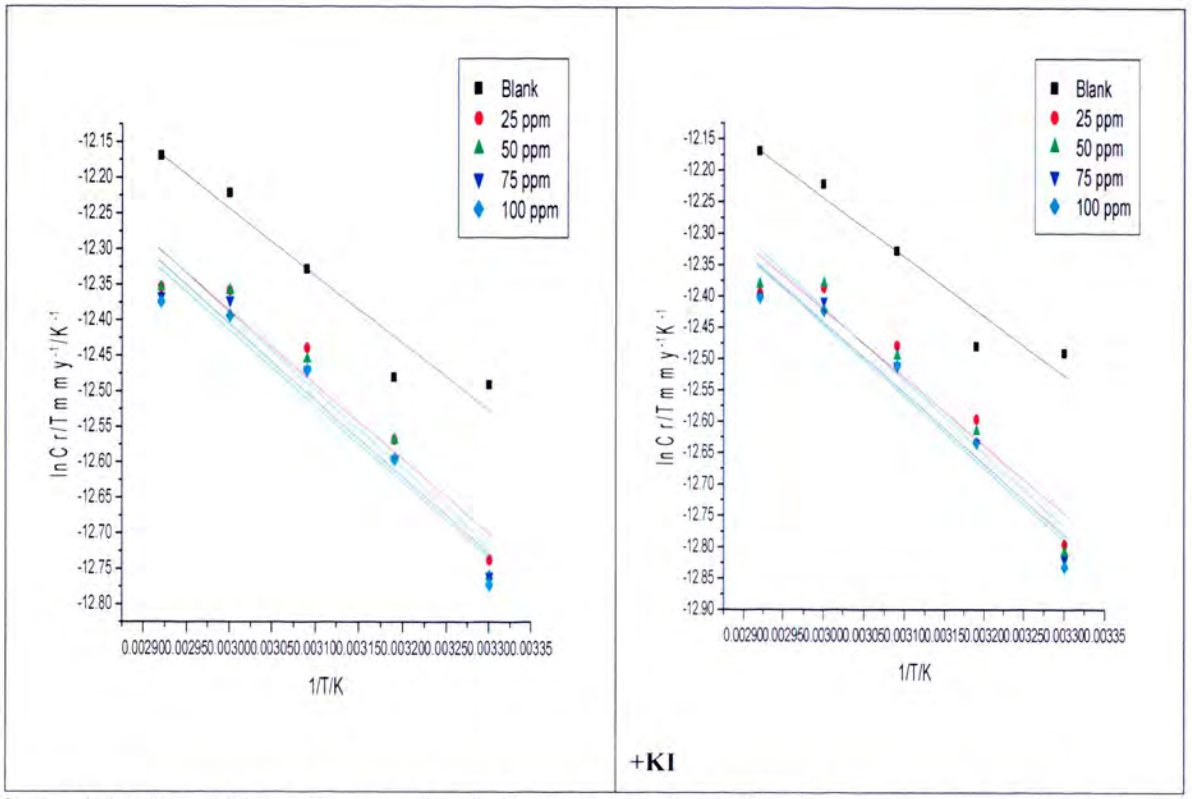

Figure 4.14: Transition state plot for the inhibitor Pc2 at different temperatures with and without KI.

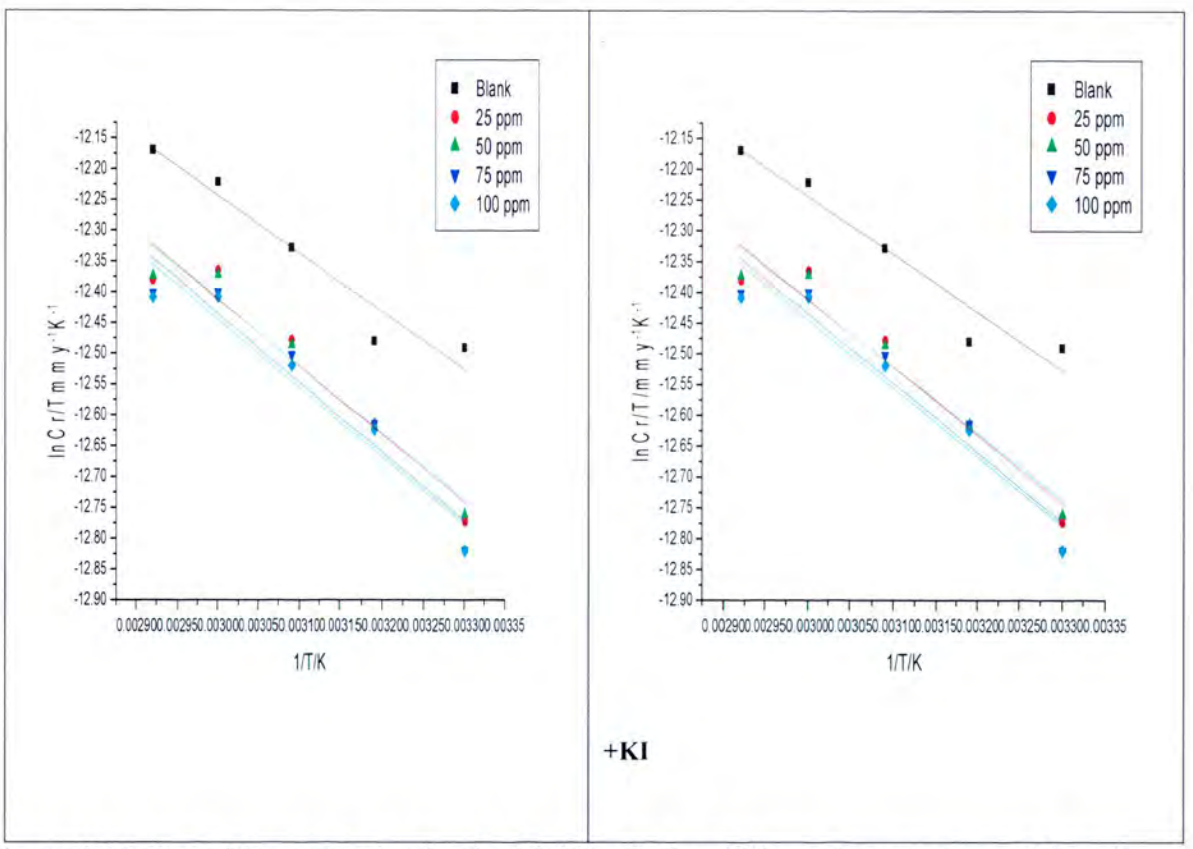

Figure 4.15: Transition state plot for the inhibitor Pc3 at different temperatures with and without KI.

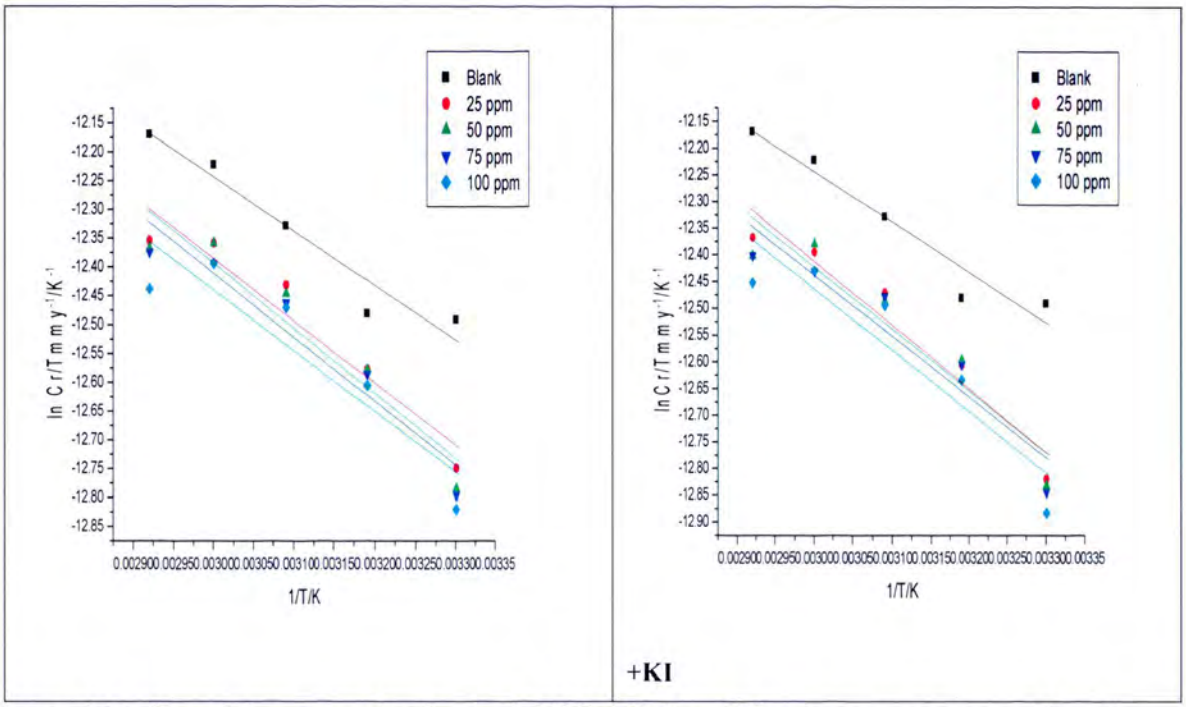

Figure 4.16: Transition state plot for the inhibitor Pc4 at different temperatures with and without KI.

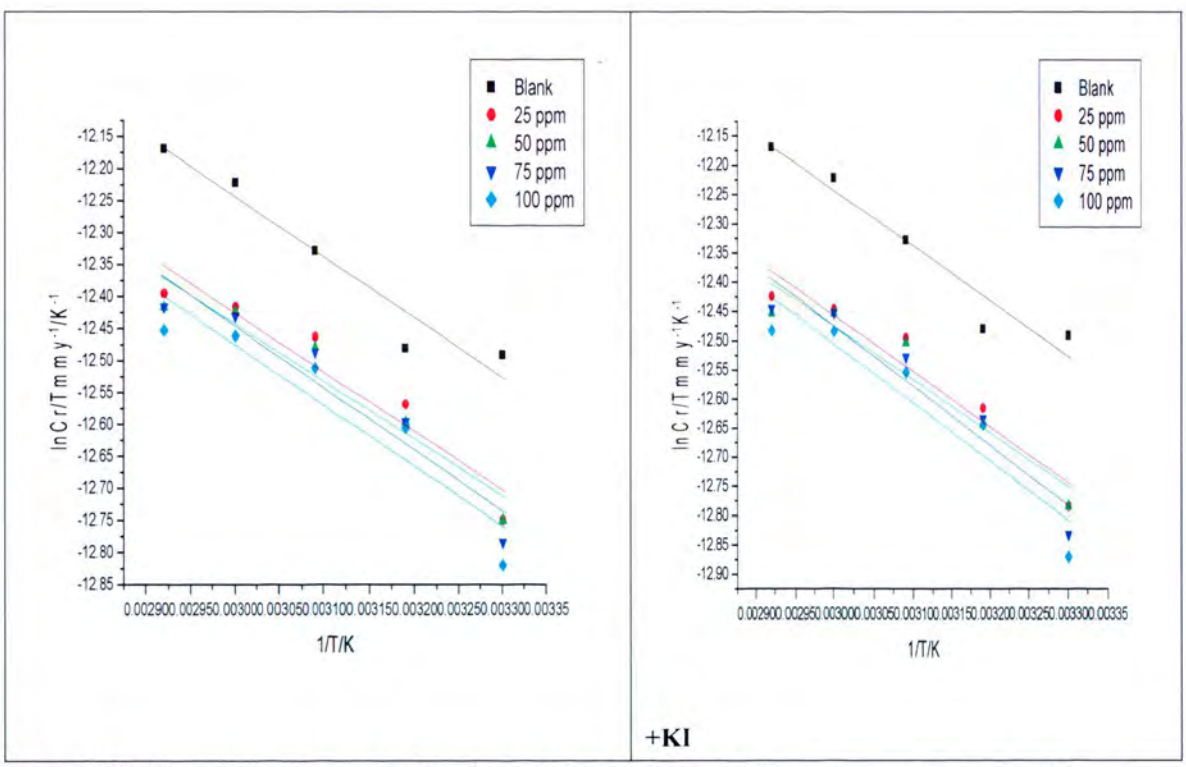

Figure 4.17: Transition state plot for the inhibitor nPc1 at different temperatures with and without KI.

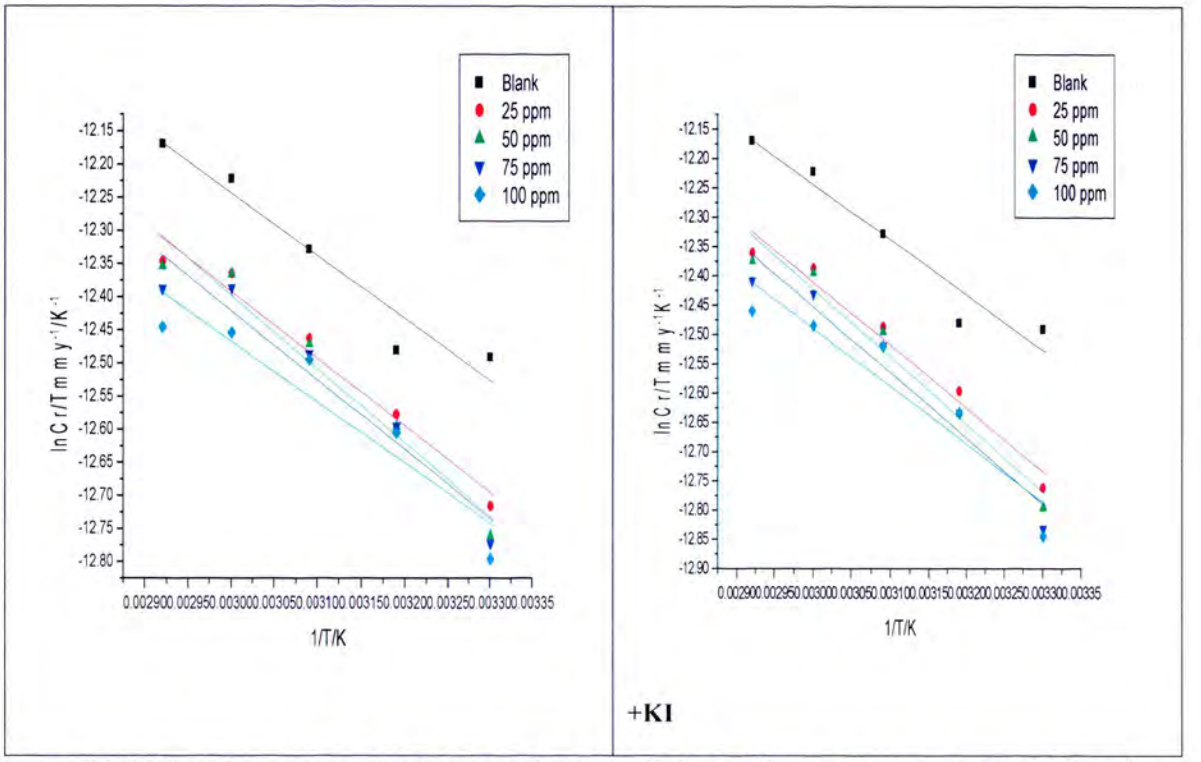

Figure 4.18: Transition state plot for the inhibitor nPc2 at different temperatures with and without KI.

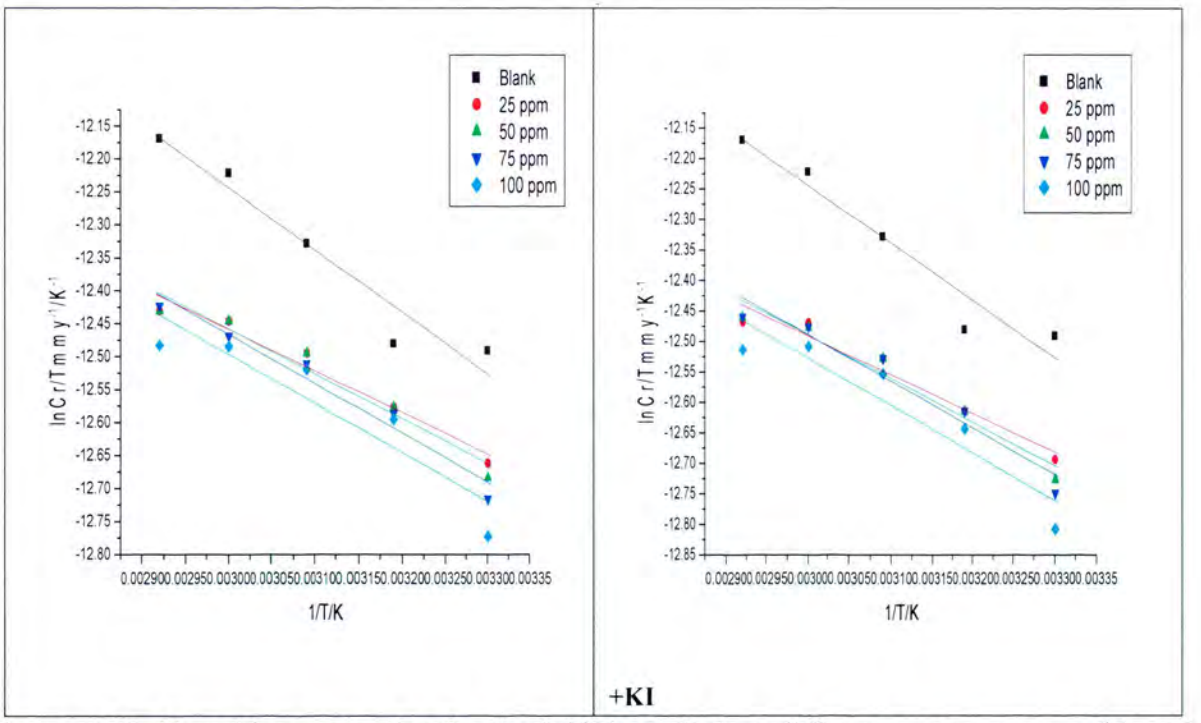

Figure 4.19: Transition state plot for the inhibitor nPc3 at different temperatures with and without KI.

Activation Energy

Activation energy is the least amount of energy required for a chemical reaction to take place; it is usually expressed in terms of joules per mole of reactants. Higher values of E_a in the presence of the inhibitor are a good indication of strong inhibition action by the phthalocyanine compounds by increasing the energy barrier for the corrosion process. Higher values of E_a in the presence of the inhibitor can also be related with the increase in thickness of the double layer that enhances the E_a of the corrosion process. Tables 4.1 and 4.2 show the different parameters from the Arrhenius plots with and without KI.

The positive values of ΔH reflect the endothermic nature of aluminium dissolution process. The negative values of ΔS imply that the disorderness is increased on going from reactant to product.

Table 4.1: Activation parameters derived from the Arrhenius plots without KI.

Name of Inhibitor	Concentration of inhibitor (ppm)	Apparent Activation energy(E_a) (kJ mol^{-1})	Enthalpy of activation (ΔH) (kJ mol^{-1})	Entropy of activation (ΔS) (J K^{-1} mol^{-1})
Blank	-	10.552	166.995	-275.786
Pc1	25 ppm	8.681	137.380	-283.297
	50 ppm	7.486	118.473	-287.398
	75 ppm	7.696	121.793	-286.766
	100 ppm	9.093	143.908	-284.515
Pc2	25 ppm	11.413	180.617	-274.394
	50 ppm	11.816	186.991	-273.21
	75 ppm	11.678	184.804	-273.757
	100 ppm	11.579	183.241	-274.13
Pc3	25 ppm	11.495	181.919	-274.101
	50 ppm	11.519	182.290	-274.083
	75 ppm	11.728	185.601	-273.603
	100 ppm	11.103	175.714	-275.679
Pc4	25 ppm	11.704	185.217	-273.514
	50 ppm	12.101	191.509	-272.388
	75 ppm	11.941	188.966	-273.018
	100 ppm	11.473	181.563	-274.66
nPc1	25 ppm	10.387	164.373	-277.798
	50 ppm	10.181	161.125	-278.556
	75 ppm	10.742	169.994	-276.902
	100 ppm	10.571	167.297	-277.659
nPc2	25 ppm	11.106	175.763	-275.363
	50 ppm	11.967	189.387	-272.825
	75 ppm	11.401	180.423	-274.72
	100 ppm	10.338	163.604	-278.289
nPc3	25 ppm	7.967	126.090	-285.331
	50 ppm	8.423	133.301	-284.168
	75 ppm	8.309	131.490	-282.542
	100 ppm	8.894	140.759	-282.865

Table 4.2: Activation parameters derived from the Arrhenius plots after the addition of KI.

Name of Inhibitor	Concentration of inhibitor	Apparent Activation energy(E_a) (kJ mol^{-1})	Enthalpy of activation (ΔH) (kJ mol^{-1})	Entropy of activation (ΔS) (J K^{-1} mol^{-1})
Blank	-	10.552	166.995	-275.786
Pc1	25 ppm	8.744	138.385	-277.321
	50 ppm	7.700	121.861	-278.444
	75 ppm	7.214	114.170	-275.738
	100 ppm	8.768	138.757	-276.471
Pc2	25 ppm	11.724	185.542	-273.754
	50 ppm	12.383	195.971	-271.755
	75 ppm	12.137	192.074	-272.682
	100 ppm	12.085	191.247	-272.45
Pc3	25 ppm	11.877	187.955	-273.215
	50 ppm	11.707	185.261	-273.738
	75 ppm	12.052	190.721	-272.889
	100 ppm	11.654	184.427	-273.329
Pc4	25 ppm	12.645	200.113	-270.909
	50 ppm	12.333	195.181	-271.94
	75 ppm	12.176	192.698	-272.535
	100 ppm	12.261	194.039	-272.496
nPc1	25 ppm	10.633	168.276	-277.321
	50 ppm	10.311	163.179	-278.444
	75 ppm	11.214	177.469	-275.738
	100 ppm	11.054	174.937	-276.471
nPc2	25 ppm	11.644	184.277	-273.9
	50 ppm	12.306	194.749	-272.019
	75 ppm	12.032	190.415	-273.09
	100 ppm	10.917	172.760	-276.744
nPc3	25 ppm	8.0047	126.673	-285.488
	50 ppm	8.659	133.301	-283.515
	75 ppm	8.393	131.490	-282.273
	100 ppm	9.176	140.759	-282.281

The values of enthalpy and entropy of activation were calculated from the plots of $\log C_R/T$ *vs.* 1/T (Figures 4.6- 4.16).

4.1.4 Adsorption Isotherm Studies

The adsorption process is usually determined through graphs known as adsorption isotherm. In order to gain more information about the mode of adsorption of these compounds on the surface of aluminium, the experimental data was tested with several adsorption isotherms. The values of the surface coverage (θ) for different concentration at 30°C, has been used to explain the best isotherm that determines the adsorption process. The surface coverage values (θ) were evaluated using corrosion rate values obtained from the weight method. Attempts were made to fit these θ values to various isotherms including Langmuir, Frumkin,

Freundlich and Temkin isotherm. The linearity of the Langmuir plot suggests that the experimental data obeys Langmuir isotherm [79].

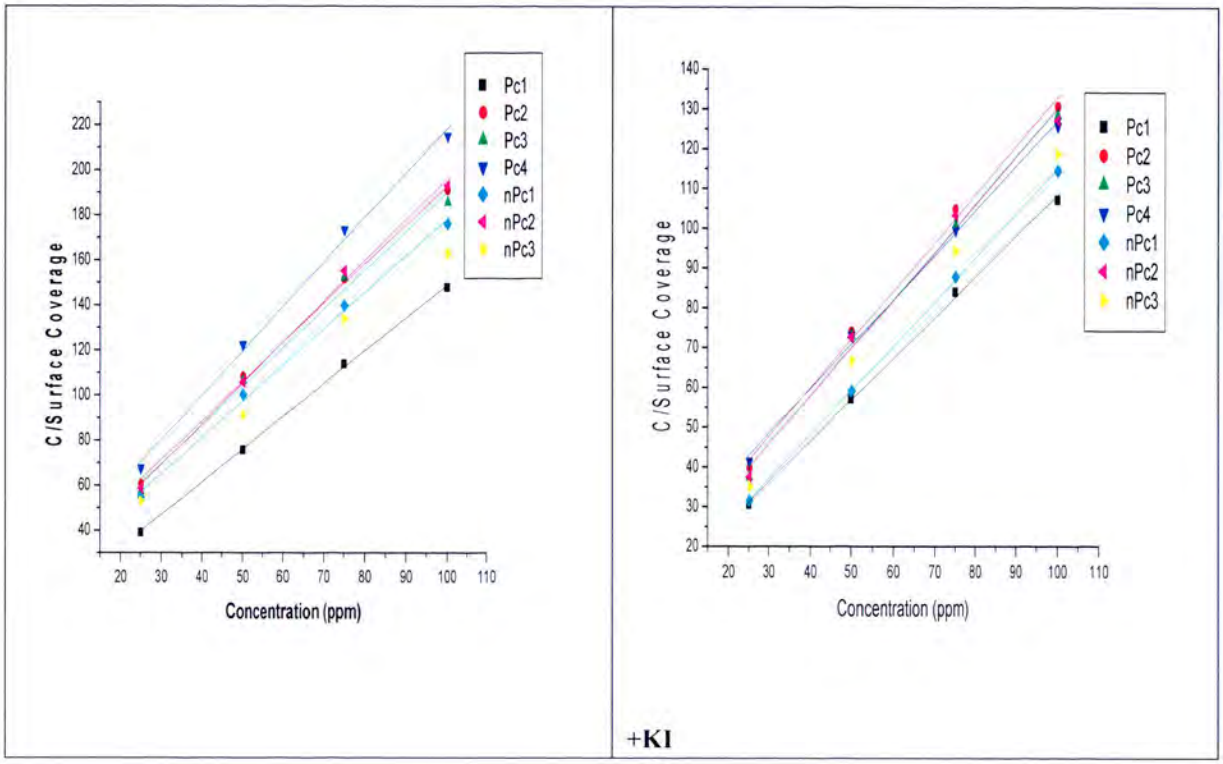

Figure 4.20: Plot of Langmuir adsorption isotherm for the studied phthalocyanine inhibitors.

According to this adsorption isotherm, the surface coverage is related to the equilibrium adsorption constant, K_{ads} and the concentration of the inhibitor:

$$\theta = \frac{K_{ads} C_{inh}}{1 + K_{ads} C_{inh}} \tag{33}$$

This equation can be rearranged to:

$$\frac{C_{inh}}{\theta} = \frac{1}{K_{ads}} + C_{inh} \tag{34}$$

where, θ is the degree of surface coverage, K_{ads} is the equilibrium constant of the adsorption/desorption process and C_{inh} is the concentration of the inhibitor.

Table 4.3 and 4.4 show the thermodynamic parameters derived from the Langmuir adsorption isotherm plots for the inhibitors under study with and without addition of KI.

Table 4.3: Thermodynamic parameters derived from the Langmuir adsorption isotherm for the inhibitors under study.

Inhibitor	Temperature /K	K_{ads} (10^3 x mol^{-1})	$-\Delta G°_{ads}$ (kJ mol^{-1})	$\Delta H°$ (kJ mol^{-1})	$\Delta S°$ (kJ mol^{-1})
Pc1	303	22.98851	-18.0186	18.05598	
	313	76.33588	-21.0425	21.08111	
	323	48.78049	-19.9142	19.95405	0.12336
	333	55.24862	-20.2279	20.26898	
	343	312.5	-24.5937	24.63601	
Pc2	303	15.64945	-17.0496	17.07595	
	313	34.24658	-19.0229	19.05012	
	323	90.09009	-21.4599	21.48798	0.08695
	333	99.0099	-21.6978	21.72675	
	343	51.67959	-20.0596	20.08942	
Pc3	303	17.40644	-17.3177	17.34512	
	313	24.53988	-18.1831	18.21143	
	323	40.56795	-19.4497	19.47893	0.0905
	333	86.95652	-21.3707	21.40084	
	343	55.71031	-20.2489	20.27994	
Pc4	303	9.376465	-15.759	15.79153	
	313	14.41961	-16.8434	16.87701	
	323	35.02627	-19.0796	19.11428	0.10737
	333	40.98361	-19.4754	19.51115	
	343	46.83841	-19.8118	19.84863	
nPc1	303	54.94505	-20.214	20.21809	
	313	51.67959	-20.0596	20.06383	
	323	64.72492	-20.6267	20.63106	0.01351
	333	76.62835	-21.0521	21.0566	
	343	58.99705	-20.3933	20.39793	
nPc2	303	17.40644	-17.3177	17.34817	
	313	19.36108	-17.5859	17.61737	
	323	53.33333	-20.139	20.17148	0.10055
	333	70.92199	-20.8571	20.89058	
	343	66.88963	-20.7096	20.74409	
nPc3	303	47.28132	-19.8355	19.86158	
	313	51.94805	-20.0727	20.09964	
	323	20.40816	-17.7186	17.7464	0.08608
	333	116.9591	-22.1175	22.14616	
	343	173.913	-23.1171	23.14663	

Table 4.4: Thermodynamic parameters derived from the Langmuir adsorption isotherm for the inhibitors under study with the addition of KI.

Inhibitor	Temperature /K	K_{ads} (10^3 x mol^{-1})	$-\Delta G°_{ads}$ (kJ mol^{-1})	$\Delta H°$ (kJ mol^{-1})	$\Delta S°$ (kJ mol^{-1})
Pc1	303	69.68641	-20.8128	21.55915	
	313	84.74576	-21.3058	22.07678	
	323	85.47009	-21.3272	22.12281	2.4632
	333	136.9863	-22.5158	23.33605	
	343	180.1802	-23.2063	24.05118	
Pc2	303	42.2833	-19.554	21.06809	
	313	48.19277	-19.8836	21.44766	
	323	61.53846	-20.4995	22.11353	4.99699
	333	76.27765	-21.0405	22.7045	
	343	86.95652	-21.3707	23.08467	
Pc3	303	17.40644	-20.27	23.07856	
	313	24.53988	-20.4535	23.35475	
	323	40.56795	-20.6762	23.67015	9.26918
	333	86.95652	-21.0812	24.16784	
	343	55.71031	-21.7482	24.92753	
Pc4	303	54.94505	-20.214	25.3283	
	313	58.13953	-20.3564	25.63949	
	323	56.65722	-20.2913	25.74318	16.87887
	333	61.34969	-20.4918	26.11246	
	343	66.44518	-20.6928	26.48225	
nPc1	303	65.14658	-20.6431	19.44708	
	313	67.11409	-20.7181	19.48261	
	323	81.30081	-21.2012	19.92624	-3.94726
	333	101.0101	-21.7482	20.43376	
	343	256.4103	-24.0953	22.74139	
nPc2	303	93.89671	-21.5642	28.91081	
	313	134.2282	-22.4645	30.05357	
	323	82.98755	-21.253	29.08453	24.24623
	333	92.59259	-21.5289	29.60289	
	343	96.61836	-21.6362	29.95266	
nPc3	303	108.6957	-21.9329	28.72286	
	313	128.2051	-22.3489	29.36295	
	323	99.50249	-21.7103	28.94845	22.40912
	333	116.9591	-22.1175	29.57974	
	343	111.1111	-21.9883	29.67463	

The free energy of adsorption (ΔG_{ads}) of the inhibitors on the aluminium surface was calculated using the following equation:

$$K_{ads} = \frac{1}{55.5} \exp\left[\frac{-\Delta G^{o}_{ads}}{RT}\right] \quad (35)$$

where 55.5 is the molar concentration of water in the solution expressed in M ($molL^{-1}$), R is the gas constant (8.314 $kJ^{-1}mol^{-1}$), K_{ads} is the equilibrium constant for the adsorption process and T is the absolute temperature in Kelvin.

Generally, the energy values of -20kJmol^{-1} or less negative are associated with an electrostatic interaction between charged molecules and charged metal surface, physisorption. Those of -40kJmol^{-1} or more negative involve charge sharing or transfer from the inhibitor molecules to the metal surface to form a coordinate covalent bond, chemisorption. From the results shown in table 4.3 and 4.4, the values of ΔG_{ads} range between -15.759 (for Pc4 at 303K) and -23.1171 (for nPc3 at 343K) which suggest that the adsorption involves two types of interaction, physisorption and chemisorption. After the addition of KI, the values of ΔG range between -19.554 (for Pc2 at 303K) and -24.0953 (for nPc1 at 343) this suggests that the adsorption involved here is the mixed type adsorption (physisorption and chemisorption). The negative values of ΔG suggest that the adsorption of the inhibitors on the aluminium surface is a spontaneous process.

The results shown in Table 4.1 and 4.2 represent the values of E_a in the presence of the inhibitor without and with addition of KI. Higher activation energy values symbolize the physical adsorption mechanism and no change or lower values of activation energy in the inhibited system in comparison with the blank activation energy value indicate the chemical adsorption mechanism.

The activation energies obtained do not have any constant pattern or behaviour (increasing or decreasing) across the increase in concentration of the inhibitor. In the absence of KI, Pc1 and nPc3 have activation energy values lower than that of the inhibitor. Activation energy for Pc1 ranges from 7.486 (50 ppm) to 9.093839 (100 ppm) kJ mol^{-1}, and ranges from 7.967 (25 ppm) to 8.894853 (100 ppm) kJ mol^{-1} for nPc3. After adding KI, Pc1 and nPc3 are still the inhibitors that have the lowest activation energy. Pc1 ranges between 7.214 (75 ppm) to 8.768 (100 ppm) kJ mol^{-1} and nPc3 ranges between 8.005 (25 ppm) to 9.176 (100 ppm) kJ mol^{-1}. Table 4.1 and 4.2 show that Pc2, Pc3, Pc4, nPc1 and nPc2 have higher values of E_a than the blank which indicates physisorption. For example, Pc2 has values of E_a ranging from 11.41256 (25 ppm) to 11.816 (50 ppm) kJ mol^{-1} and range between 10.33848 (100 ppm) and 11.96776 (50 ppm) kJ mol^{-1} for nPc2. With KI, the E_a values of Pc2 range from 11.72478 (25 ppm) to 12.38378 (50 ppm) kJ mol^{-1} and range between 10.917 (100 ppm) and 12.30661 (50 ppm) kJ mol^{-1} for nPc2.

From the observations and results obtained for the Gibbs free energy of adsorption (ΔG^{o}_{ads}) and the apparent activation energy (E_a), it can be inferred that the type of mechanism of adsorption for the studied phthalocyanine inhibitors on the aluminium surface is mixed type (i.e., they exhibit both physisorption and chemisorption mechanisms).

4.2 Electrochemical measurements

4.2.1 Potentiodynamic polarization (PDP)

Calculation of corrosion rates requires the determination of corrosion currents using Tafel Slope Analysis. Electrochemical corrosion parameters such as corrosion potential (E_{corr}), anodic and cathodic tafel slopes (b_a and b_c) and corrosion current (i_{corr}) were obtain by the extrapolation of the Tafel lines. The measured i_{corr} values are related to the inhibition efficiency through the following equation:

$$\mu_{PDP} = \frac{i^0_{corr} - i^i_{corr}}{i^0_{corr}} \times 100 \qquad (36)$$

where i^0_{corr} and i^i_{corr} are values of corrosion current density in absence and in presence of inhibitor.

Figures 4.21-4.27 show the potentiodynamic polarization curves for aluminium in 1 M HCl for the seven inhibitors with and without addition of KI.

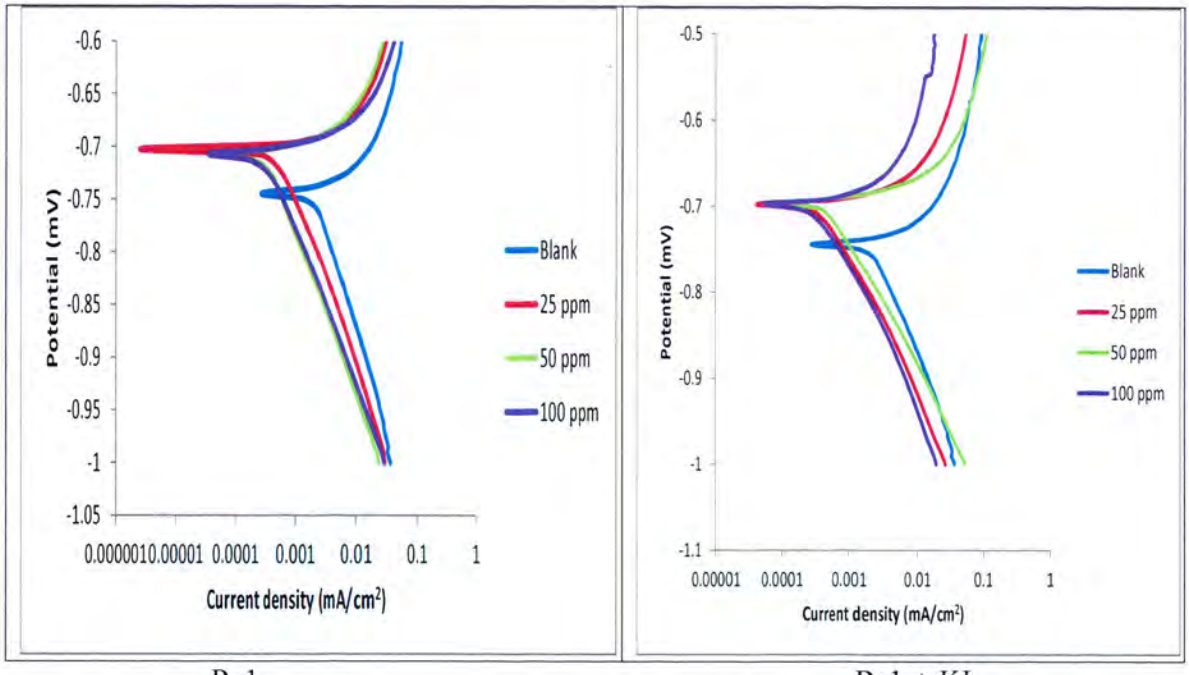

Pc1 Pc1 + KI

Figure 4.21: Potentiodynamic polarization curves for aluminium 1 M HCl and in the absence and presence of Pc1 at different concentrations.

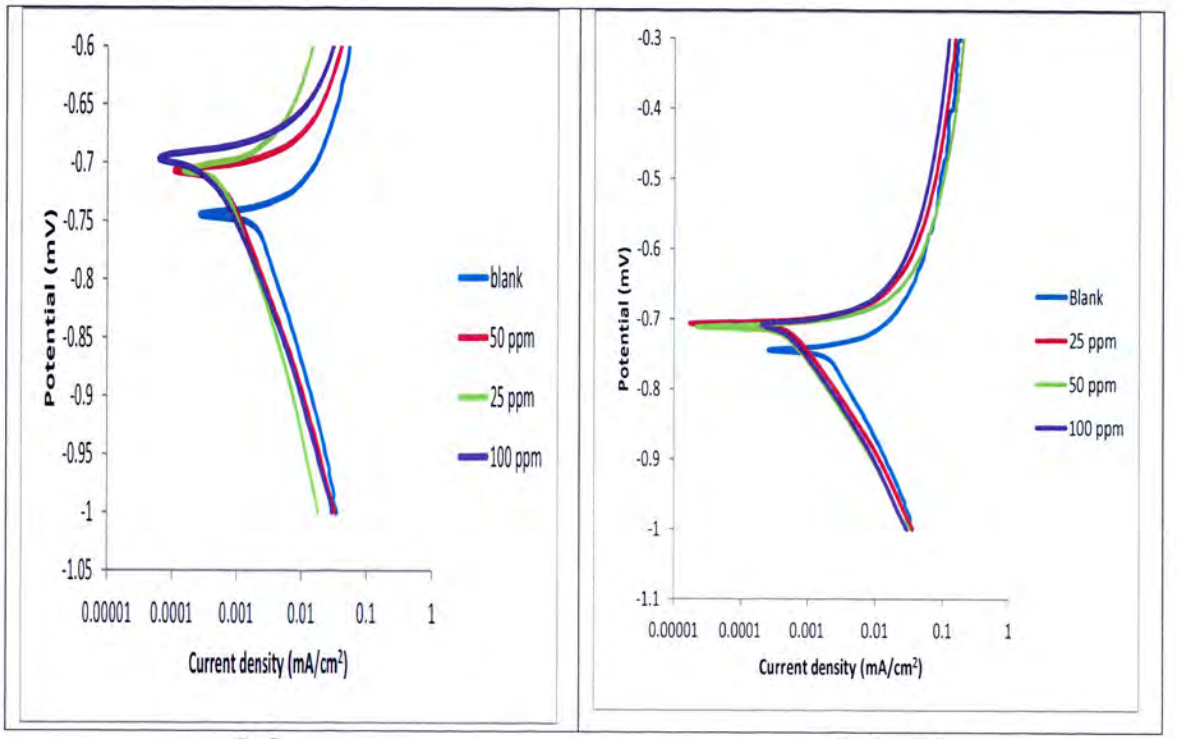

Pc2 Pc2 +KI

Figure 4.22: Potentiodynamic polarization curves for aluminium 1 M HCl and in the absence and presence of Pc2 at different concentrations.

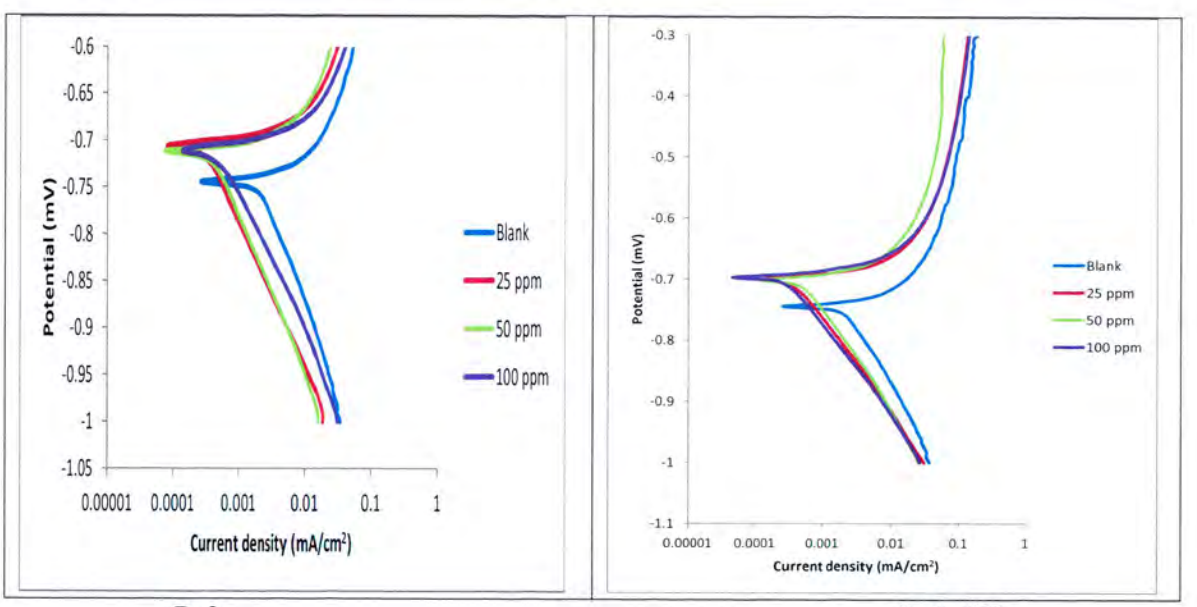

Pc3 Pc3 +KI

Figure 4.23: Potentiodynamic polarization curves for aluminium 1 M HCl and in the absence and presence of Pc3 at different concentrations.

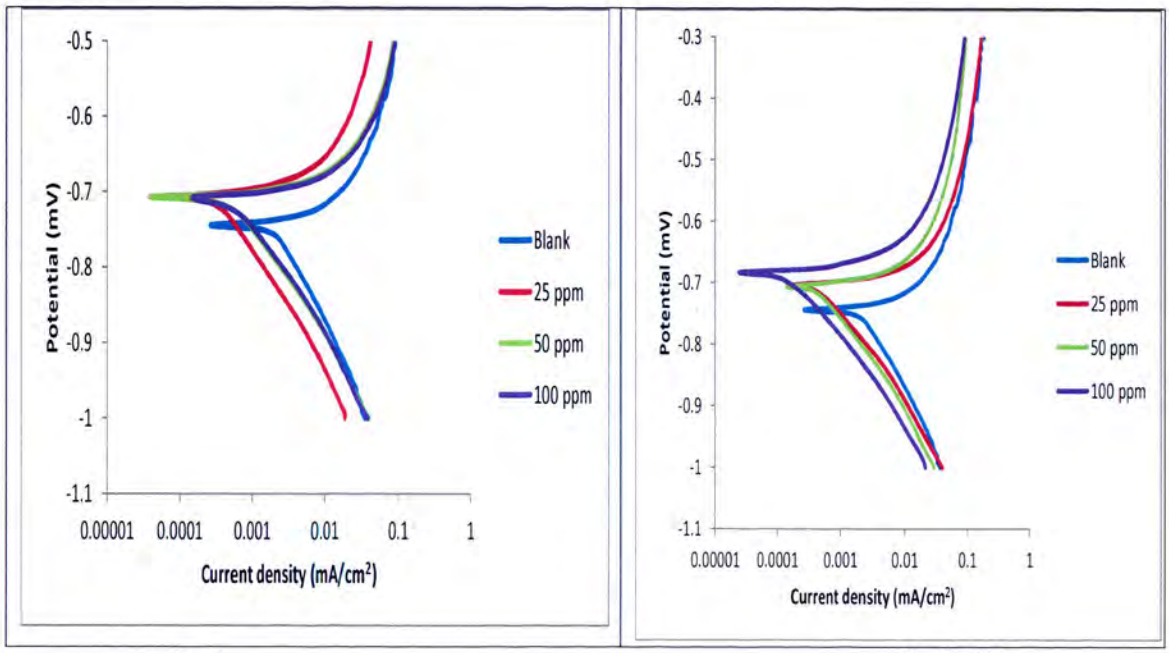

Pc4 Pc4 +KI

Figure 4.24: Potentiodynamic polarization curves for aluminium 1 M HCl and in the absence and presence of Pc4 at different concentrations.

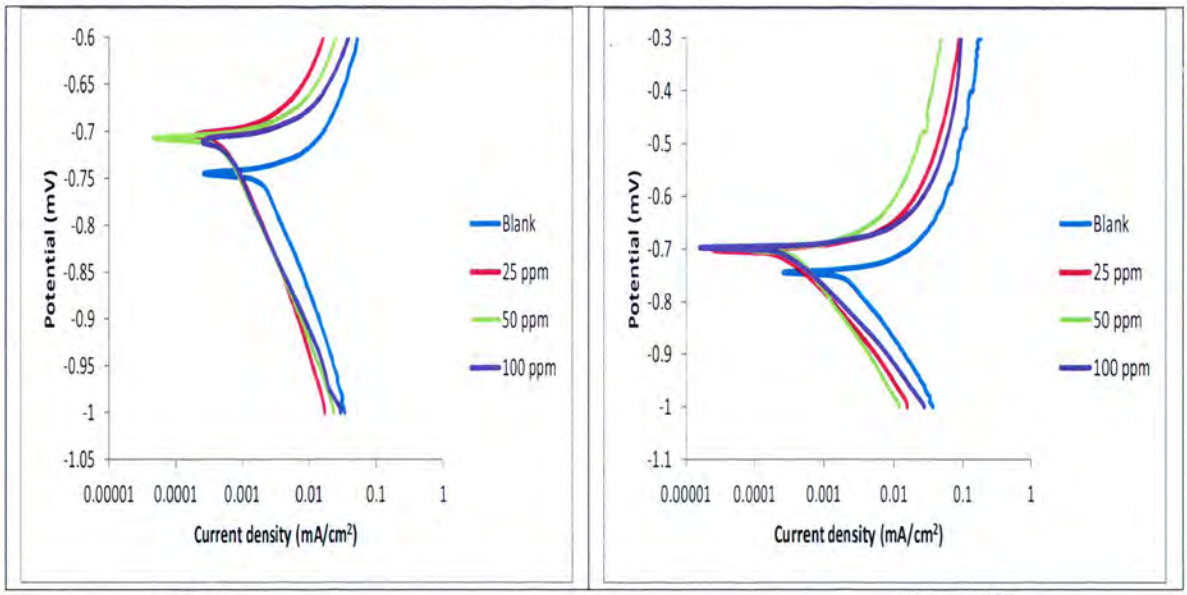

nPc1 nPc1 +KI

Figure 4.25: Potentiodynamic polarization curves for aluminium 1 M HCl and in the absence and presence of nPc1 at different concentrations.

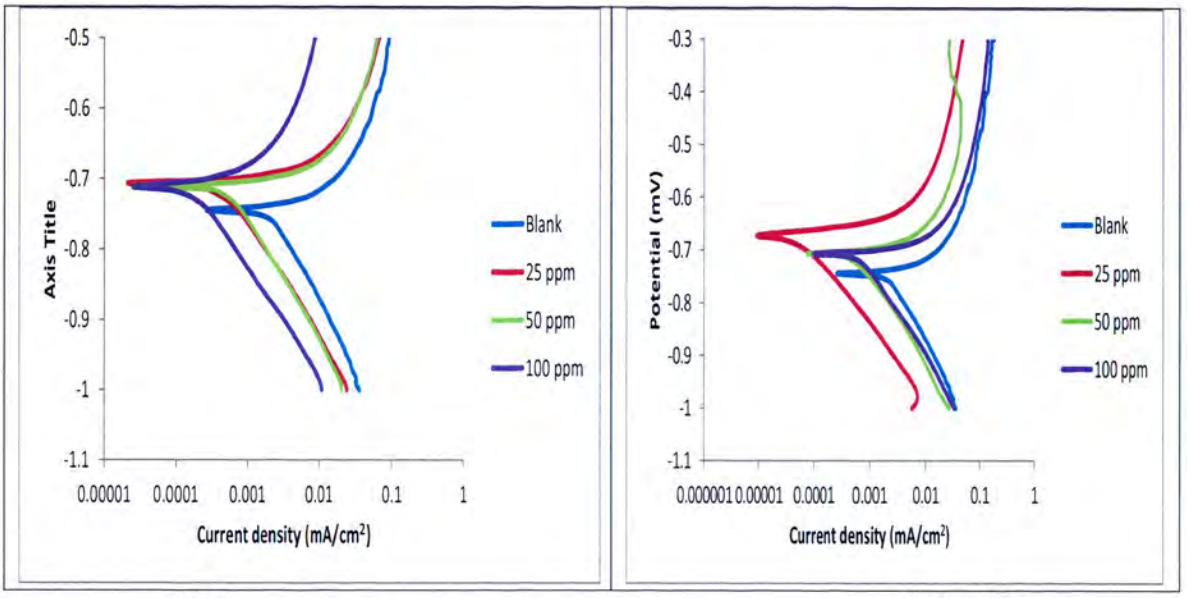

nPc2 nPc2 +KI

Figure 4.26: Potentiodynamic polarization curves for aluminium 1 M HCl and in the absence and presence of nPc2 at different concentrations.

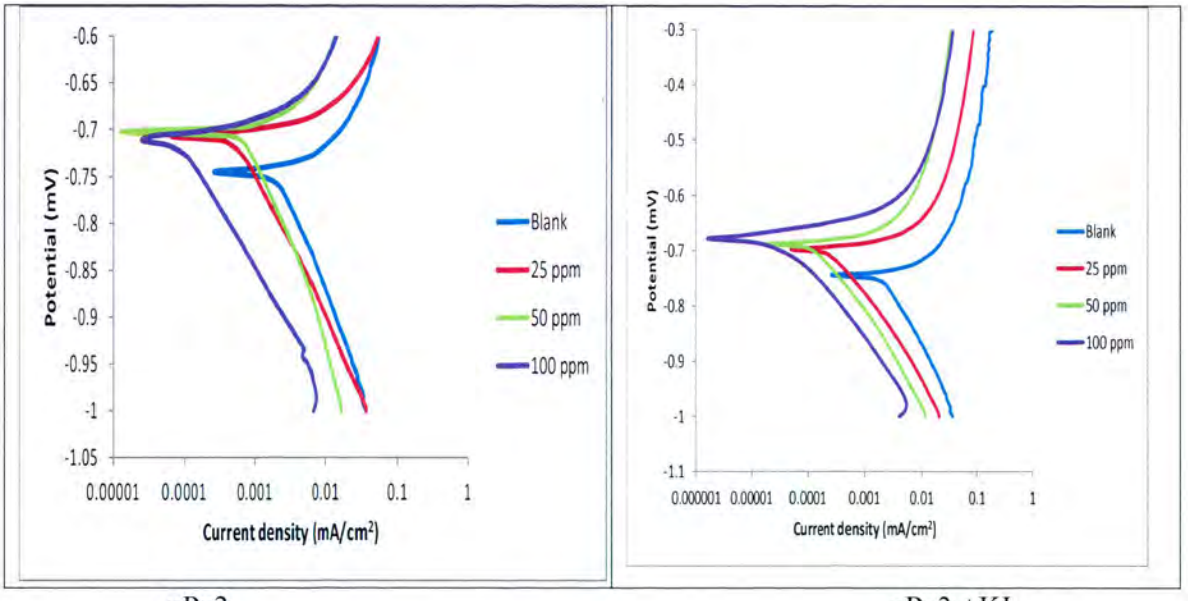

nPc3 nPc3 +KI

Figure 4.27: Potentiodynamic polarization curves for aluminium 1 M HCl and in the absence and presence of nPc3 at different concentrations.

Figure 4.21 – 4.27 shows the potentiodynamic polarization curves for aluminium in 1 M HCl in the absence and presence of different concentrations (25 ppm, 50 ppm, 100 ppm) of the phthalocyanines. It is clear that the different concentrations of the inhibitor reduces the current values at the same potential. The most important trend shown by the plots is that the presence of the inhibitor shifts the current to lower regions. The plots show that higher concentrations of the inhibitor are more shifted to lower currents e.g. Pc1 and nPc1. However

in other instances, the concentrations of the inhibitor does not follow any order e.g. nPc2. This may have occurred because some inhibitors did not completely dissolve in solution. Nonetheless, all the plots clearly show that the addition of the inhibitor shifts the currents to lower regions, this trend confirms that phthalocyanines have the ability to inhibit corrosion. From the polarization curves, one can see that both cathodic current and the anodic current are affected; this implies that it confirms that the inhibitors show a mixed-type mechanism [80].

The values for the corrosion current densities and corrosion potentials were estimated from the intersection of the anodic and cathodic Tafel lines. Table 4.5 and 4.6 show the electrochemical parameters: corrosion potential (E_{corr}), corrosion current density (i_{corr}), Tafel slopes (b_c and b_a), inhibition efficiency ($E\%$) for aluminium in 1 M HCl, with the seven inhibitors and addition/without addition of KI.

Table 4.5: Potentiodynamic polarization parameters such as corrosion potential (E_{corr}), corrosion current density (i_{corr}) and anodic and cathodic Tafel slopes (b_a and b_c) using different inhibitors.

Name of inhibitor	Concentration of inhibitor (ppm)	$-E_{corr}$ (V)	i_{corr} ($x10^{-3}$) (mA)	b_c (V/dec)	b_a (V/dec)	$E_{PDP\%}$
Blank	-	0.742	1.792	0.029	0.165	-
Pc1	25 ppm	0.706	0.4205	0.023	0.121	76.5%
	50 ppm	0.707	0.3338	0.02	0.167	81.4%
	100 ppm	0.705	0.2889	0.015	0.137	83.9%
Pc2	25 ppm	0.707	0.5323	0.034	0.154	70.3%
	50 ppm	0.706	0.3985	0.014	0.091	77.8%
	100 ppm	0.695	0.2687	0.018	0.100	85.0%
Pc3	25 ppm	0.704	0.2904	0.013	0.160	83.8%
	50 ppm	0.710	0.3319	0.012	0.139	81.5%
	100 ppm	0.711	0.4510	0.020	0.136	74.8%
Pc4	25 ppm	0.437	0.8325	0.078	0.079	83.0%
	50 ppm	0.735	1.209	0.024	0.146	76.9%
	100 ppm	0.731	1.031	0.021	0.147	74.2%
nPc1	25 ppm	0.709	0.1010	0.051	0.200	70.0%
	50 ppm	0.705	0.2937	0.011	0.138	86.1%
	100 ppm	0.704	0.3675	0.018	0.136	71.2%
nPc2	25 ppm	0.704	0.2797	0.010	0.104	84.3%
	50 ppm	0.709	0.2663	0.012	0.058	85.1%
	100 ppm	0.707	0.1577	0.029	0.147	91.2%
nPc3	25 ppm	0.704	0.4962	0.015	0.165	72.1%
	50 ppm	0.701	0.6130	0.029	0.105	65.3%
	100 ppm	0.708	0.6807	0.013	0.105	96.2%

Table 4.5 above shows that the values of E_{corr} and i_{corr} with the inhibitor are lower than that of the blank (HCl, without inhibitor) solution. The values of the Tafel slopes of b_c and b_a change after the inhibitors are added, which indicated that the inhibitor molecules are adsorbed on both the cathodic and anodic sites resulting in an inhibition of both anodic dissolution and

cathodic reduction reactions. The inhibition efficiency values do not follow any trend along the increasing inhibition concentrations. However, nPc3 shows the highest inhibition efficiency value of 96.2%.

Table 4.6: Potentiodynamic polarization parameters such as corrosion potential (E_{corr}), corrosion current density (i_{corr}) and anodic and cathodic Tafel slopes (b_a and b_c) using different inhibitors, with the addition of KI.

Name of inhibitor	Concentration of inhibitor (ppm)	$-E_{corr}$ (V)	i_{corr} ($x10^{-3}$) (mA)	b_c (V/dec)	b_a (V/dec)	$E_{PDP\%}$
Blank	-	0.742	1.792	0.029	0.165	
Pc1	25 ppm	0.698	0.2732	0.013	0.111	84.5%
	50 ppm	0.695	0.3929	0.014	0.128	84.8%
	100 ppm	0.680	0.1731	0.014	0.071	90.3%
Pc2	25 ppm	0.705	0.4091	0.011	0.110	77.2%
	50 ppm	0.709	0.2262	0.009	0.063	87.4%
	100 ppm	0.708	0.4054	0.017	0.124	77.4%
Pc3	25 ppm	0.698	0.3014	0.013	0.120	83.2%
	50 ppm	0.700	0.4207	0.002	0.137	76.5%
	100 ppm	0.695	0.2347	0.010	0.128	86.9%
Pc4	25 ppm	0.704	0.3983	0.017	0.115	77.8%
	50 ppm	0.705	0.3726	0.013	0.131	79.2%
	100 ppm	0.684	0.1520	0.024	0.117	91.5%
nPc1	25 ppm	0.700	0.2209	0.017	0.119	87.7%
	50 ppm	0.699	0.3244	0.033	0.142	81.9%
	100 ppm	0.698	0.2533	0.017	0.120	85.9%
nPc2	25 ppm	0.671	0.0169	0.011	0.046	99.1%
	50 ppm	0.705	0.3053	0.012	0.085	82.1%
	100 ppm	0.707	0.5060	0.013	0.125	71.0%
nPc3	25 ppm	0.456	0.7798	0.038	0.085	56.5%
	50 ppm	0.685	0.1161	0.019	0.124	93.5%
	100 ppm	0.676	0.0075	0.016	0.042	99.6%

Table 4.6 above shows the Tafel slope parameters after the addition of KI. The values of E_{corr} and i_{corr} with the inhibitor are lower than that of the blank (HCl, without inhibitor) solution. The values of the Tafel slopes of b_c and b_a change after the inhibitors are added, which indicated that the inhibitor molecules are adsorbed on both the cathodic and anodic sites resulting in an inhibition of both anodic dissolution and cathodic reduction reactions. In the case of b_c, the values are lower and higher than the value without the inhibitor and the values of b_a are all lower than the value without the inhibitor. The inhibition efficiency values do not follow any trend along the increasing inhibition concentrations. However, nPc3 shows the highest inhibition efficiency value of 99.6%.

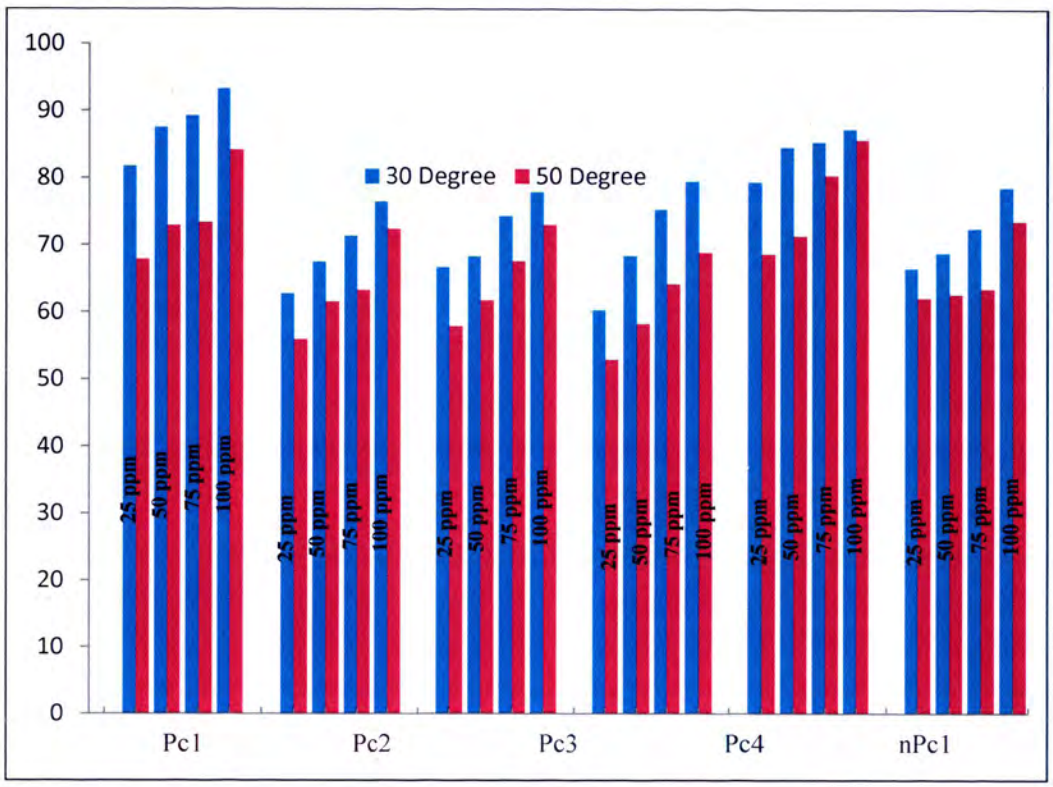

Fig 4.28: Plot of Inhibition Efficiency against Concentration at 30^0C and 50^0C with KI.

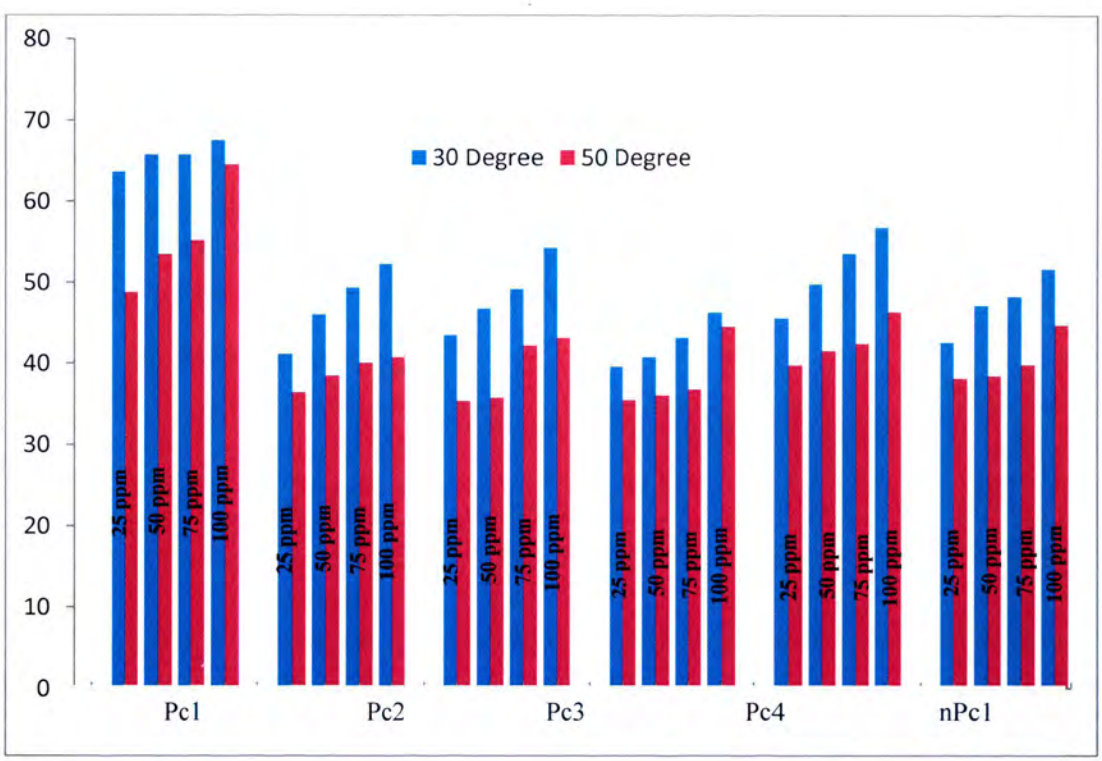

Fig 4.29: Plot of Inhibition Efficiency against Concentration at 30^0C and 50^0C without KI.

4.3 Synergism Consideration

The synergism parameters, S_I was evaluated using the relationship given by Aramaki and Hackerman and also reported elsewhere [Gomma G.K. Mater. Chem. Phys. 54(1994). 241-246; Umoren S.A. Ogbobe O. Ebenso E.E. Bull. Electrochem. 22(4) (2006) 155; Ebenso E.E. Mater. Chem. Phys. 79(2003) 58 and Ebenso E.E. Bull. Electrochem (5)19(2003) 209].

$$S_I = \frac{1-I_{1+2}}{1-I'_{1+2}} \quad (37)$$

Where $I_{1+2} = I_1 + I_2$; I_1 = inhibition efficiency of the KI; I_2 = inhibition efficiency of the naphthalocyanine or phthalocyanine used as inhibitors and I'_{1+2} = measured inhibition efficiency of naphthalocyanine or phthalocyanine in combination with KI.

This parameter was evaluated from the inhibition efficiency values obtained from both the weight loss and electrochemical techniques and the results are presented in Table 47. The S_I values for both methods employed as shown in Table 4.7 for the different concentration and temperatures of the inhibitors studied are greater than unity. This indicates that the improved inhibition efficiency caused by the addition of KI to the naphthalocyanine and phthalocyanine is only due to synergistic effect. Similar results have been reported elsewhere [Labari L., Harek Y. Portugaliae Electrochimica Acta 22(2004) 227; Labari L., Harek Y., Traisnel M., Mansri A. J. Appl. Electrochem. 34(2004) 833].

Strong chemisorption of iodide ions on the aluminium surface are responsible for the synergistic effect of iodide ions in combination with the cation of the inhibitors studies. The cation is the absorbed by columbic attraction on the aluminium surface where iodide ions are already adsorbed by chemisorption. Stabilization of the adsorbed iodide ions with cations leads to a greater surface coverage and therefore greater inhibition. It could therefore be concluded the addition of KI enhances the inhibition efficiency to a considerable extent due to the increase in the surface coverage in the presence of iodide ions (when $S_I>1$, it signifies synergistic effect and when $S_I<1$, it means antagonistic effect.

Table 4.7: Synergistic Parameters

	Concentration of Inhibitor (ppm)			
Inhibitor	25	50	75	100
Pc1	1.42 (1.53)	1.35 (1.58)	1.32	1.28 (1.51)
Pc2	1.49 (1.59)	1.46 (1.49)	1.43	1.37 (1.78)
Pc3	1.44 (1.64)	1.45 (1.75)	1.37	1.37 (1.46)
Pc4	1.53 (1.74)	1.36 (1.64)	1.27	1.24 (1.38)
nPc1	1.23 (1.40)	1.21 (1.70)	1.24	1.25 (1.44)
nPc2	1.43 (1.38)	1.45 (1.68)	1.39	1.32 (2.03)
nPc3	(2.22)	(1.26)		(1.49)

( ) = Synergistic parameters from electrochemical technique

Chapter 5

Quantum chemical studies on naphthalocyanine and phthalocyanines derivatives

5.1. Introduction

The study of corrosion inhibitors using weight loss and electrochemical methods (chapter 3 and chapter 4 respectively) provides information about the extent of damage on the metal surface as a result of corrosion. Electrochemical techniques may also provide information on the type of reactions and the thermochemistry related to the reactions involved in the corrosion process. However, both methods (i.e., weight loss and electrochemical techniques) do not provide sufficient information on the mechanism of action between the corrosion inhibitor and the metal surface. This information is significant in view of the fact that understanding the mechanism of any action provides a possible means to either prevent such a reaction (if it is undesirable) or encourage it (if it is desirable). Since, metal corrosion is an undesirable reaction, especially for the industrial applications, it is of vital importance to understand the interaction mechanism between the metal surface and the inhibitor molecules so as to develop better corrosion inhibitors that could assist in reducing or preventing corrosion. A key point in understanding the mechanism of action of a corrosion inhibitor is obtaining information on the molecular properties of the inhibitor which are related to the reactivity of the inhibitor. Such molecular properties include the energy of the highest occupied molecular orbital (HOMO), the energy of the lowest unoccupied molecular orbital (LUMO), the charges on the atoms, the dipole, etc.

One of the techniques utilized to understand the mechanism involved in the interaction between corrosion inhibitor molecules and metal surface and for obtaining relevant molecular reactivity properties of the inhibitor is the computational chemistry techniques [81]. These techniques include quantum chemical approaches, quantitative structure activity relationship (QSAR) and molecular dynamics. Quantum chemical approaches are utilized for the study of the molecular properties of corrosion inhibitors as well as in determining the interaction strength between a metal surface and the different sites of interaction with the inhibitor molecule. QSAR techniques are utilized in designing new corrosion inhibitors using the concept that the activity exhibited by a molecule is related to the molecular properties of that molecule. Molecular dynamics on the other hand is utilized to study the behaviour of the inhibitor interacting with the metal surface of different temperatures and different solvent media. In the next paragraphs we provide a brief detail of each of these techniques and how they are utilized in the study of corrosion inhibitors as well as the interaction involving the metal surface and the corrosion inhibitor [82].

5.2. Quantum chemical techniques

5.2.1. General description of the techniques

Quantum mechanical methods are all based on solving the time-independent Schrodinger equation for the electrons of a molecular system as a function of the position of the nuclei [82]. Quantum chemical techniques are divided into two categories namely, molecular mechanics and electronic structure methods. Molecular mechanics technique considers a compound as consisting of atoms connected by springs, which are the forces of interaction between atoms. In this way, molecular mechanics does not take into consideration the fact that molecules are stable arrangement of nuclei and electrons. Molecular mechanics are useful for studying large molecular systems (i.e., systems with many atoms) because it does not take into consideration the heavy calculations involving the electron-electron interactions. As a result it is faster and more economic than other electronic structure methods [83]. Despite its economic advantage, molecular mechanics is less accurate than quantum mechanical methods because it cannot provide properties dependant on the electron density, such as HOMO-LUMO energies, dissociation reactions and conjugated π systems [81]. Therefore, for the study of small to medium-sized molecules, electronic structure methods are preferred to molecular mechanics. Since the phthalocyanines have conjugated π systems in their molecular structures, the application of molecular mechanics in the study of these compounds is limited and only electronic structure methods will be utilized.

Electronic structure methods consider the molecule as consisting of electrons in stable arrangement with nuclei [81]. These methods obtain the properties of a given molecule by solving the Schrödinger equation for that system. For a time independent case, the Schrödinger equation for a particle of mass m moving in one dimension with energy E is

$$-\frac{\hbar^2}{2m}\frac{d^2\psi}{dx^2} + V\psi = E\psi \tag{38}$$

where, V is the potential energy of the particle; ħ is a convenient modification of Planck's constant and ψ is the wave function. For a three dimensional system, the Schrödinger equation takes the form:

$$-\frac{\hbar^2}{2m}\nabla^2\psi + V\psi = E\psi \tag{39}$$

where $\nabla^2 = \frac{\partial^2}{\partial x^2} + \frac{\partial^2}{\partial y^2} + \frac{\partial^2}{\partial z^2}$

The solution of the Schrödinger equation provides information such as the wave function and the energy of the system. The molecular properties such as the geometry, dipole moment, Raman spectra, IR spectra, etc., are derived from the information on the geometry and the energy of the molecule.

The electronic structure methods are subdivided into semi-empirical and *ab initio* methods. Semi-empirical methods are simplified versions of Hartree-Fock theory using empirical (derived from experimental data) corrections in order to improve performance [84]. Semi-empirical methods solve the Schrödinger equation by neglecting some of the electron-electron repulsion terms arising from the interactions between electrons in a molecule [85]. In doing so, semi-empirical methods becomes cost-effective, especially for the study of large molecules. The neglect of electron-electron interaction is taken into consideration differently, resulting in different methods under the semi-empirical approach. Some of these methods include the following:

- Modified neglect of differential overlap (MNDO). In this method, the parameterization is based on the one-centre two-electron integrals. The two electron integrals are evaluated using the idea of multipole-multipole interactions from classical electrostatics [86].
- Austin model 1 (AM1). This method solves the two-electron integrals using the modified expression for nuclear-nuclear core repulsion. The advantage for using this expression is that it results in non-physical attractive forces that mimic van der Waals interactions [87].
- Parameterized model number 3 (PM3). This method uses a Hamiltonian that is very similar to the AM1 Hamiltonian but the parameterization strategy (i.e., the process of deciding and defining the parameters necessary for a complete or relevant specification of a model or geometric object) is different. PM3 is parameterized to reproduce a large number of molecular properties [88].

Semi-empirical methods serve as efficient computational tools which can yield fast quantitative estimates for a number of properties. This may be particularly useful for correlating large sets of experimental and theoretical data, for establishing trends in classes of related molecules, and for scanning a computational problem before proceeding with higher level of treatments [82,83]. Semi-empirical calculations are much faster than their *ab initio* counterparts. Their results, however, can be misrepresentative if the molecule being computed is not similar enough to the molecules in the database used to parameterize the method. Semi-empirical approaches neglect many smaller integrals to speed up the calculations.

Ab initio methods solve the Schrödinger equation without introducing any external parameters (e.g., empirical data or experimental data) into the equation. Because these methods solve the Schrödinger equation analytically, they are computationally unaffordable for most large molecules [89]. Various methods that can be considered as *ab initio* include the Hartree-Fock (HF) method, Møller-Plesset perturbation (MP) theory method and the Density Functional Theory (DFT) method. Although there are many *ab initio* methods, the study in this work is performed using the density functional method. The selection of this method for the study is based on the fact that it is computationally affordable as compared to other *ab initio* based method such as Møller-Plesset perturbation. It's accuracy and performance is comparable to most superior *ab initio* methods in most cases [90]. In the next paragraphs, we provide a more detail discussion on the theory behind the DFT methods.

5.2.2. Methods based on Density functional theory

Density functional theory (DFT) is a quantum mechanical modelling method used in chemistry to investigate the electronic structure (principally the ground state) of many-body systems, in particular atoms, molecules, and the condensed phase. The basic idea of density functional theory (DFT) is to describe a system in terms of its electron density [91]. Within this theory, the properties of a molecular system can be determined by using functionals, i.e. functions of another function, which in this case is the spatially dependent electron density. Hence the name density functional theory comes from the use of functionals of the electron density. For instance, it expresses the energy of a system as a functional (i.e., a function of a function) of the electron density ρ, i.e.

$$E = E[\rho(r)] \tag{40}$$

The electron density is the measure of the probability of an electron being present at a specific location, and it is an observable [92]. Like wave function-based methods, DFT methods describe the electronic structure and properties of molecular systems by solving the Schrödinger equation. However, while wave function-based methods focus on the determination of the wave function, ψ, DFT methods focus on the determination of the electron density.

DFT methods are based on the proof by Kohn and Hohenberg that "There exists a universal functional of the density, $F[\rho(r)]$, independent of $v(r)$ [the external potential due to the nuclei], such that the expression $E = \int v(r)\,\rho(r)\,dr + F[\rho(r)]$ has as its minimum the correct ground state energy associated with $v(r)$" [93]. This means that the exact ground state energy of a molecular system is a functional only of the electron density and the fixed positions of the nuclei (for a given set of nuclear coordinates, the electron density uniquely determines the energy and all properties of the ground state). If the mathematical form of the universal functional were known, the exact electron density function of the ground state would provide a reference for the utilization of the variational principle [94]. Regrettably, this form it is not known, nor can it be precisely determined or systematically improved. Therefore, approximate functionals have been proposed, often built in such a way as to fit the correct results for certain well characterised systems. To achieve this, their mathematical form contains external parameters (i.e., parameters that are introduced into the Schrödinger equation), what makes DFT a basically semi-empirical method [95, 96]. In order to build functionals to best fit the energy evaluation, the total energy, E, viewed as a function of ρ, is partitioned into three components: kinetic energy, $T[\rho]$, nuclear-electron interaction, $V_{Ne}[\rho]$, and an electron-electron interaction term $V_{ee}[\rho]$:

$$E[\rho] = T[\rho] + V_{Ne}[\rho] + V_{ee}[\rho] \tag{41}$$

Density functional theory (DFT) is often the most popular and versatile electronic structure method to study moderate to large systems. This preference reflects the efficiency of DFT compared to correlated wavefunction theories such as coupled cluster theory, even though

accuracy and, more importantly, predictability (i.e., systematic convergence to the right answer), are sacrificed [97].

5.3. Molecular properties related to the reactivity of corrosion inhibitors

Electronic properties (such as the electron density, the dipole moment, the partial charges on the atoms, etc.) of a molecule informs about reactivity. The electronic properties are influenced by the type of functional groups present in the molecule. Molecules that have functional groups with high electron density are preferred as corrosion inhibitors, because the adsorption of the corrosion inhibitor on the metal surface requires that electrons are donated from the corrosion inhibitor to the partially filled or vacant d orbitals of the metal to form a coordinating bond between the inhibitor and the metal [87,88].

5.3.1. Electron density

Electric charges in the molecule are obviously responsible for electrostatic interactions. The local densities are important in many chemical reactions and for physiochemical properties of compounds [78]. The electron density can be thought of as a cloud or gas of negative charge that varies/differs in density throughout the molecule [98]. The region with high electron density on a molecule would therefore play an important role in donating electron to the metal surface, assisting in the binding of the inhibitor on the metal surface. Such regions include the lone pair of electron on heteroatoms (N, O, S and P), the π electrons in multiple bonds (double or triple bonds) and π electron cloud in aromatic systems [99, 100].

5.3.2. Atomic charges (partial charges on the atoms)

Charge-based parameters are widely utilized as measure of chemical reactivity and selectivity because the charge on the atoms may indicate the distribution of electron density in a molecule. Unlike many other electronic properties that can be extracted from a quantum mechanical wave function, such as electron density, permanent electrical moments, or the molecular electrostatic potential, the partial atomic charge on an atom in a molecule is not a quantum mechanical observable. As a result, the rules for determining partial atomic charges, which involves assigning quantitative values to the amount of electron density belonging to each atom in a molecule, are ambiguous. Many different methods have been developed with the objective of estimating the partial atomic charges and include the class IV charge model [101], Mulliken atomic charges [102-104] Löwdin charges [105–108] and the concept of a partial atomic charge is some-what illogical, because it depends on the method used to delimit between one atom and the next [85]. In the study of corrosion inhibitors, the interest is to identify the atoms with the highest negative charge because it has been shown that the atom with the highest negative charge tend to have a great capacity to donate electrons to the metal surface [109].

5.3.3. Highest occupied molecular orbital (HOMO) and lowest unoccupied molecular orbital (LUMO) and other parameters derived.

The highest occupied molecular orbital (E_{HOMO}) and the lowest unoccupied molecular orbital energy (E_{LUMO}) are very popular quantum chemical parameters. These orbitals (shown in figure 5.1), also called the frontier orbitals, determine the way the molecules interact with other species. The highest occupied molecular orbital is that orbital, in a molecular orbital diagram of a given system, which is last occupied by electrons. The lowest unoccupied molecular orbital, in a molecular orbital diagram of a given system, is the first orbital unoccupied by electrons, usually occurring just above the HOMO. The HOMO is the orbital that could act as an electron donor since it is the orbital with electron with highest energy. The LUMO, on the other hand, is the orbital that could act as the electron acceptor since it is the orbital with the lowest energy among the unoccupied orbitals. The energy of the HOMO (E_{HOMO}) is directly related to the ionization potential (section 5.1) and the energy of the LUMO (E_{LUMO}) is directly related to the electron affinity (section 5.1). The difference in energy between the HOMO and LUMO (i.e., $E_{HOMO-LUMO}$) is an important parameter for understanding the reactivity/stability of molecules; a large HOMO-LUMO gap implies high stability or the molecule in chemical reactions [81,82].

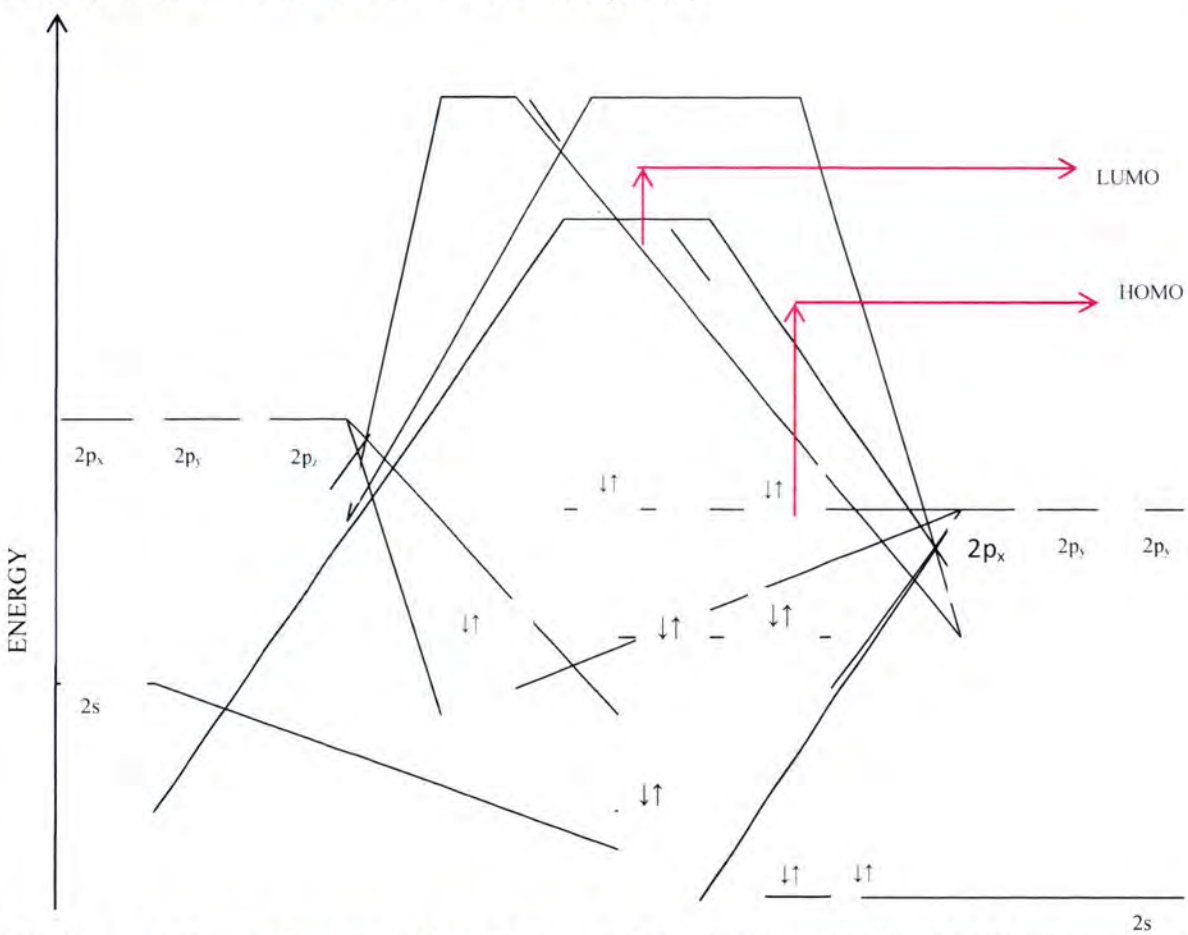

Figure 5.1: The molecular orbital diagram of the Carbon dioxide (CO_2) molecule. The LUMO and HOMO are shown in the diagram.

Other molecular properties derived from the HOMO and the LUMO include the electronegativity, global hardness and global softness. These parameters are briefly defined below following Koopmans' theory [102];

Electronegativity (χ) is the measure of the power of an electron or group of atoms to attract electron towards itself [110]; it is defined through the equation

$$\chi = -\frac{1}{2}(E_{HOMO} + E_{LUMO}) \quad (42)$$

where E_{HOMO} is the energy of the highest occupied molecular orbital and E_{LUMO} is the energy of the lowest unoccupied molecular orbital.

Global hardness (η) measures the resistance of an atom to charge transfer; it is defined using the equation [111, 112]:

$$\eta = -\frac{1}{2}(E_{HOMO} - E_{LUMO}) \quad (43)$$

Global softness (σ) describes the capacity of an atom or group of atoms to receive electrons; it is estimated using the equation [82, 113]:

$$\sigma = \frac{2}{(E_{HOMO} - E_{LUMO})} \quad (44)$$

5.3.4. Dipole Moment

The dipole moment is widely used to describe the polarity. Dipole moment is the measure of polarity of a polar covalent bond. In a polar molecule like HCl, the more electronegative atom, (Cl atom) pulls the shared electrons towards one side, thereby polarising the bonding electrons. This charge polarization effect may be explained using the dipole moment concept, which is better defined as the product of charge on the atoms and the distance between the two bonded atoms [77]. For instance, if we consider that the charge on H is q_1 and the charge on Cl is q_2 and the separation distance is r, then the dipole moment (μ) for the HCl molecule can be written

$$\mu = (q_1 \times q_2)\, r \quad (45)$$

Figure 5.2: Illustration of the partial charges and the dipole moment for the HCl.

In the study of corrosion inhibitors, the dipole moment may have varying influences; in some cases, the inhibition efficiency increases with the increase in the dipole moment of the inhibitors [113]; in other cases it decreases with the increase in the dipole moment; there are also situations in which the dipole moment may not have any influence on the inhibition efficiency of the compounds [114].

5.3.5. Number of electrons transferred

The number of electrons transferred from the inhibitor molecule to the metal surface also may indicate the tendency of the inhibitor to bind on the metal surface. The higher the number of electrons transferred by the inhibitor, the greater is the possibility of strong bonding between the inhibitor and the metal surface. When studying the homologous series of compounds, it is interesting to determine which compound has the greatest tendency to transfer electrons. The change in the number of electrons transferred is estimated through the equation:

$$\Delta N = \chi_m - \frac{\chi_{inh}}{2(\eta_m - \eta_{inh})} \qquad (46)$$

where χ_m and χ_{inh} denote the absolute electronegativity for the metal surface of interest and the inhibitor molecule respectively; η_m and η_{inh} denote the absolute hardness of metal surface of interest and the inhibitor molecule respectively [90].

In real situations, the number of electrons transferred may not be exactly as that predicted by eqn. 5.9. However, this equation provides a reasonable estimation necessary to select the molecules that has a greater tendency to donate electrons.

5.3.6. Fukui Functions

The Fukui function is a reactivity index which measures the tendency of a region in a molecule to accept or donate electrons in a chemical reaction [112]. It generalizes the concept of a frontier orbital by including the relaxation of the orbital upon an electron transfer. In the framework of the Density Functional Theory (DFT), the Fukui function *f(r)* is defined as the derivative of the density ρ(r) relative to the total number of electrons N at constant external potential v_{ext} [115, 116]:

$$f(\mathbf{r}) = [\partial\rho(\mathbf{r})/\partial N]v_{ext}. \qquad (47)$$

The reactivity of a molecule is more easily discussed by using a discrete index, the condensed Fukui function f_k, which is obtained by partitioning the density of electrons between fragments:

$$f_k = [\partial N_k/\partial N]v_{ext} \qquad (48)$$

where N_k is the number of electrons in fragment k of the molecule [1117].

In the simpler version, the Fukui functions are estimated and interpreted from the computation of a change of the electronic density due to the removal (resulting in an cation) or addition (resulting in an anion) of one electron from (or to) the whole molecule. The Fukui function estimated through the removal of an electron has the form

$$f^+ = q_{(N+1)} - q_N \qquad \text{for a nucleophilic attack} \qquad (49)$$

where, $q_{(N+1)}$ is the charge of the cation and q_N is the charge of the corresponding neutral molecule. The Fukui function estimated through the addition of an electron has the form

$$f^- = q_N - q_{(N-1)} \qquad \text{for an electrophilic attack} \qquad (50)$$

where $q_{(N-1)}$ is the charge of the atom upon the formation of an anion. The preferred site for nucleophilic attack is the atom or region in the molecule where the value of f^+ is the highest and the preferred site for an electrophilic attack is the atom/region in the molecule where the value of f^- is the highest.

In summary, all the parameters mentioned in this section are considered important in the discussion of the inhibition ability of corrosion inhibitors. In the next section, the results of the DFT study will be discussed for the different phthalocyanine compounds. The molecular properties are compared across compounds and with respect to the inhibition efficiency of the compounds (obtained in chapter 3).

5.4 Results and discussion

5.4.1. Geometry of phthalocyanines and naphthalocyanines

The geometries of the studied phthalocyanine (Pc) and naphthalocyanines (nPc) are shown respectively. As discussed in chapter 2, four phthalocyanine and three naphthalocyanines were selected for comparison purposes with specific objectives. Pc1 is a phthalocyanine substituted with the octabutoxy functional groups; Pc2 is a phthalocyanine substituted with the octakis(octyloxy) groups; Pc3 is a phthalocyanine substituted with the tetra-*tert*-butyl groups and Pc4 is a phthalocyanine. nPc1 is a naphthalocyanine substituted with octabuxy functional groups; nPc2 is a naphthalocyanine substituted with the tetra-*tert*-butyl groups. A comparison of Pc1, Pc2 and Pc3 provides information on the role of the substituent group (i.e., tetra-*tert*-butyl) in determining the corrosion inhibition. A comparison of Pc1 and either Pc3 or Pc4 provides information on the role of the ether group (-OR) in influencing the inhibition performance of phthalocyanines. Finally a comparison of Pc3 and Pc4 provides information on the influence of the size of the alkyl chain in determining the inhibition performance of phthalocyanines. Likewise, for naphthalocyanines, a comparison between nPc1 and nPc2 will give information on the role of the substituent group on the inhibitor. A comparison between nPc2 and nPc3 will provide information on the effect of the size of the alkyl chain on the inhibition efficiency.

A comparison of Pc1 and nPc1 provides information on the role of the aromatic ring, present in the naphthalocyanines, in influencing the corrosion inhibition of these macrocycles.

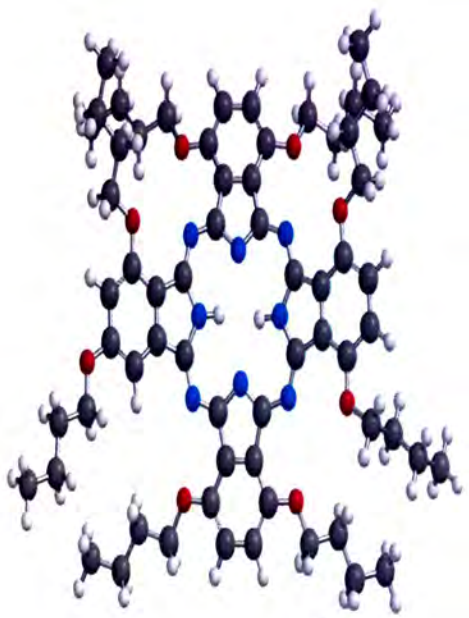

Pc1

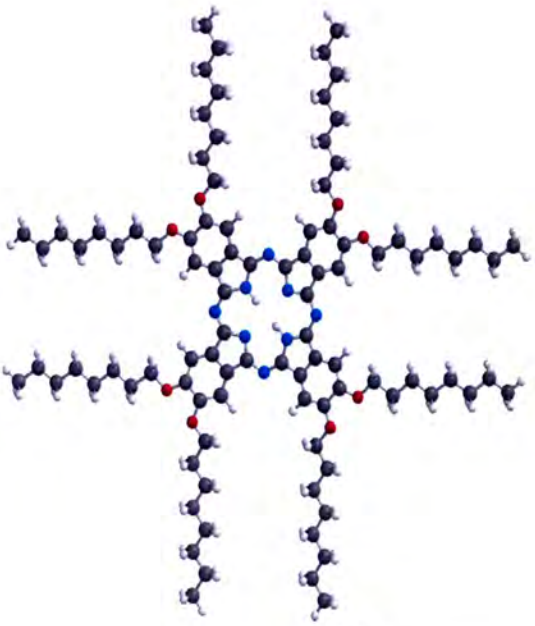

Pc2

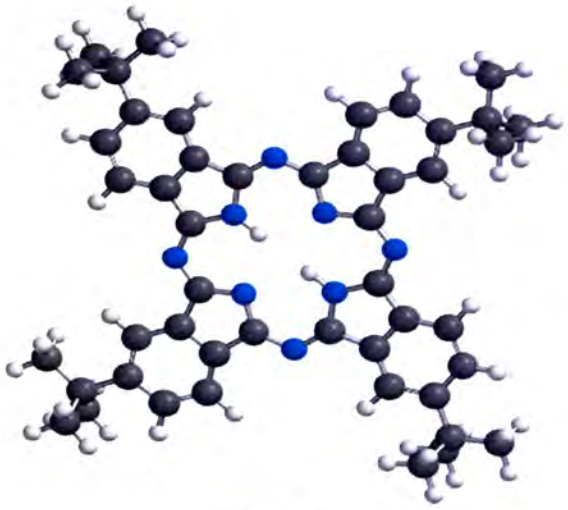

Pc3

Pc4

Figure 5.2. Optimized geometric representation of the structures of phthalocyanines studied in this work. Pc1 denotes 1,4,8,11,15,18,22,25-Octabutoxy-29*H*,31*H*-phthalocyanine, Pc2 denotes 2,3,9,10,16,17,23,24-Octakis(octyloxy)-29*H*,31*H*-phthalocyanine, Pc3 represent 2,9,16,23-Tetra-*tert*-butyl-29*H*,31*H*-phthalocyanine and Pc4 denotes 29*H*,31*H*-phthalocyanine. The nitrogen atoms are indicated with the blue colour; the O atoms are indicated with the red colour, H atoms are indicated with blue colour and C atoms are indicated with grey colour.

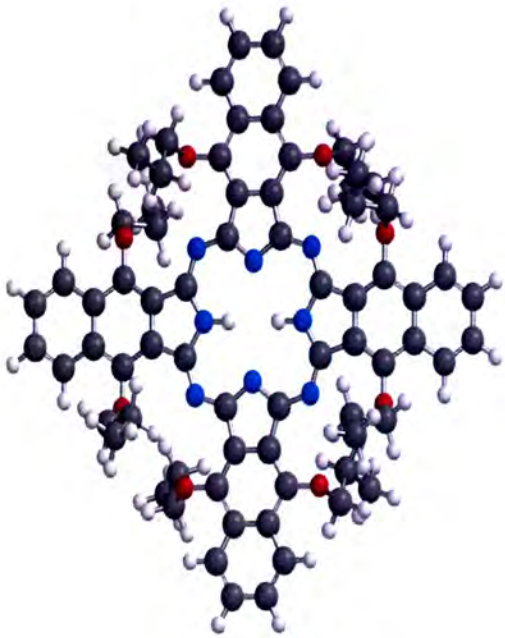

nPc1

nPc2

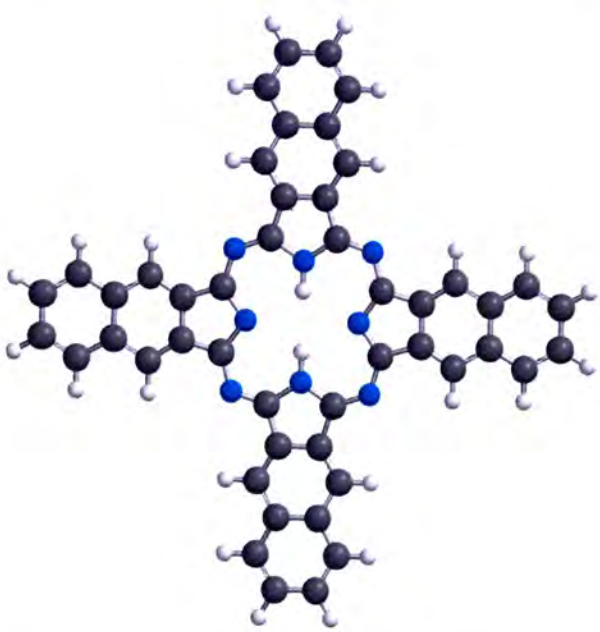

nPc3

Figure 5.3. Optimized geometric representation of the structures of naphthalocyanines studied in this work. nPc1 denotes 5,9,14,18,23,27,32,36-Octabutoxy-2,3-naphthalocyanine, nPc2 denotes 2,11,20,29-Tetra-*tert*-butyl-2.3-naphthalocyanine and nPc3 represents 2,3-naphthalocyanine. The nitrogen atoms are indicated with the blue colour; the O atoms are indicated with the red colour, H atoms are indicated with blue colour and C atoms are indicated with grey colour.

5.4.2. Molecular orbitals and Reactivity parameters

The frontier molecular orbitals play important role in informing the reactive sites of the inhibitors. In order to obtain more details, the molecular orbital density distribution is calculated [118,119]. Figures 5.4–5.7 show the HOMO and the LUMO for the phthalocyanine and naphthalocyanines. In Pc1, the HOMO is delocalized on the pyrrole ring and the nearby meso nitrogen atoms. The HOMO location in Pc2 is mostly distributed near the nitrogen and the oxygen atoms. In Pc3 and Pc4, the HOMO is localized near the nitrogen atom.

The HOMO density in nPc1, nPc2, nPc3 is mostly distributed near the nitrogen atoms. Pc1, the LUMO is delocalized on the nitrogen atoms of the pyridine ring and near the nitrogen atoms on the pyrrole ring. For Pc2, Pc3, and Pc4, the LUMO is delocalized on the nitrogen atoms of the pyrrole ring and nearby the nitrogen atoms on the pyridine ring. With nPc1, nPc2 and nPc3, the LUMO distribution is on the nitrogen atoms of the pyrrole ring and near the nitrogen atoms on pyridine.

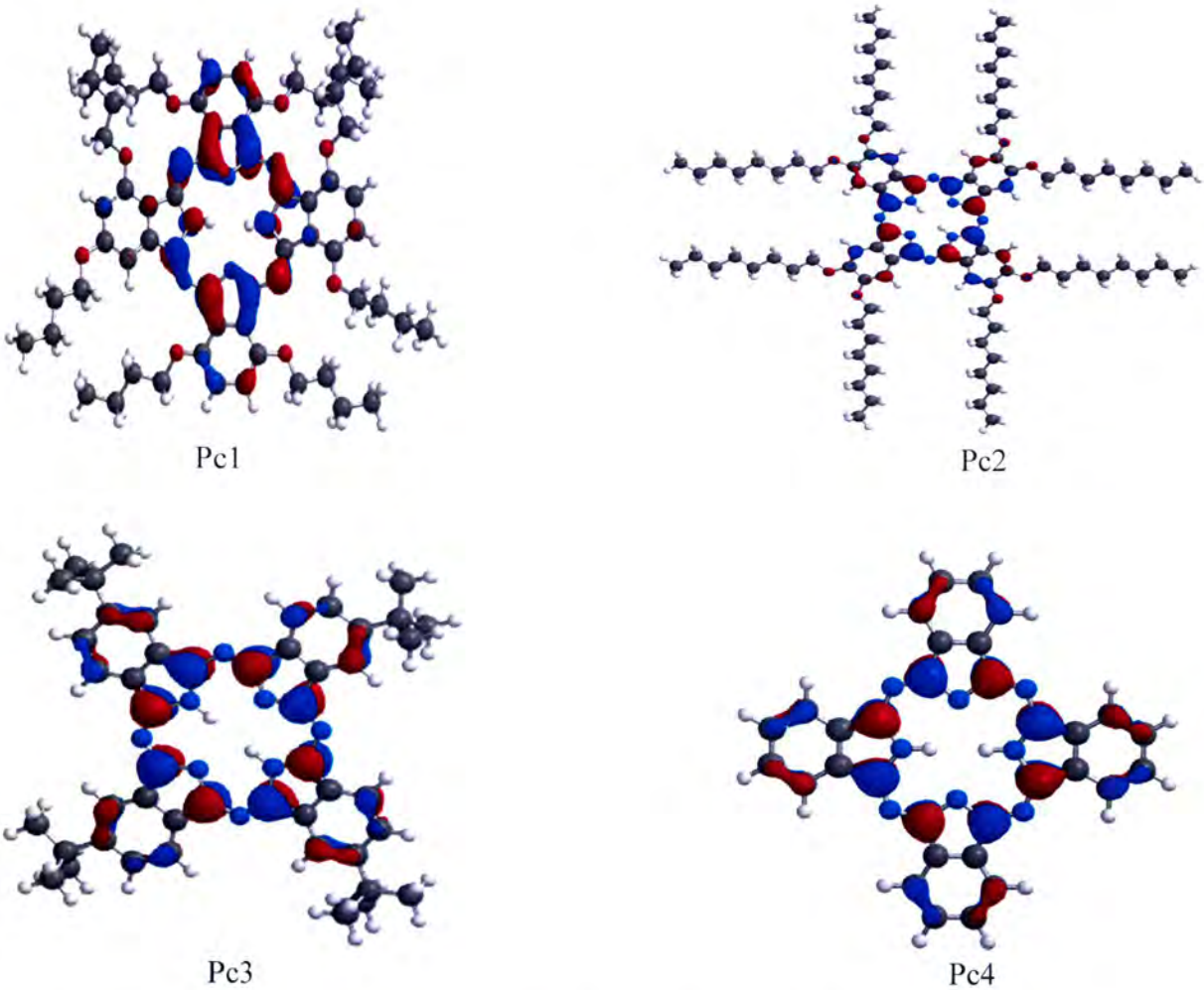

Figure 5.4. Highest occupied molecular orbital (HOMO) for each of the studied phthalocyanine macrocycles.

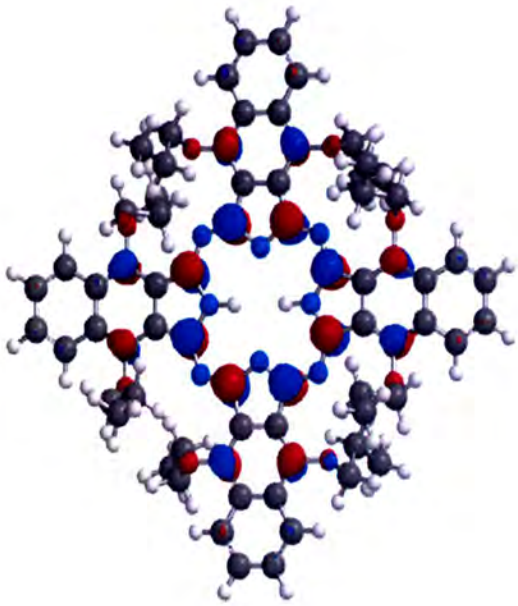

nPc1

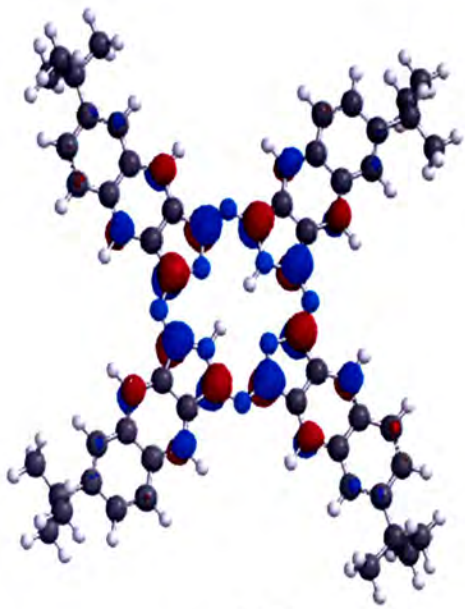

nPc2

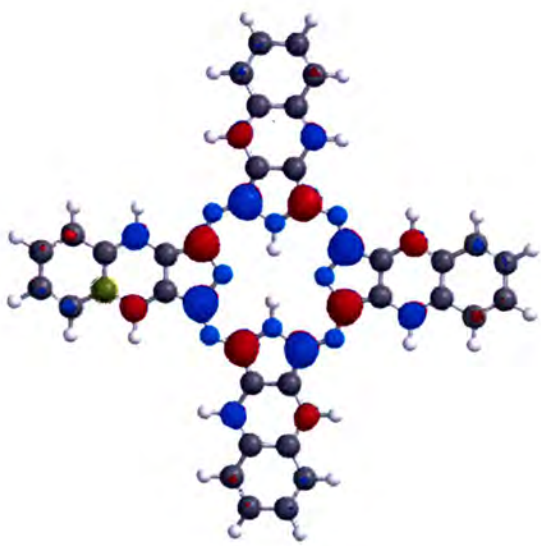

nPc3

Figure 5.5. Highest occupied molecular orbital (HOMO) for each of the studied naphthalocyanine macrocycles.

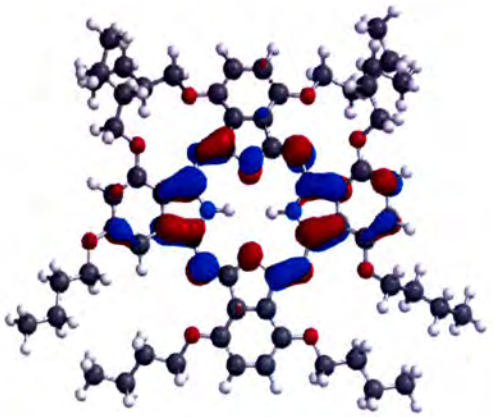

Pc1

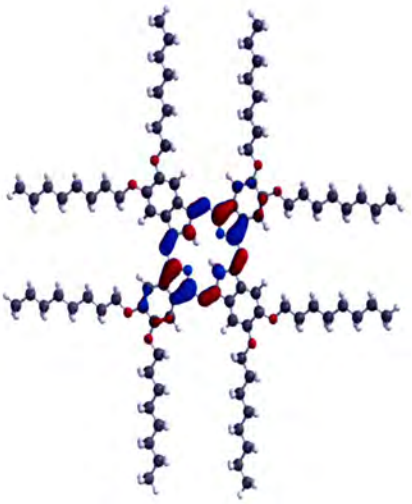

Pc2

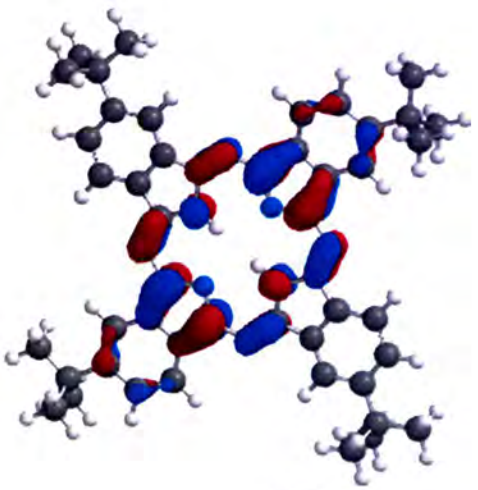

Pc3

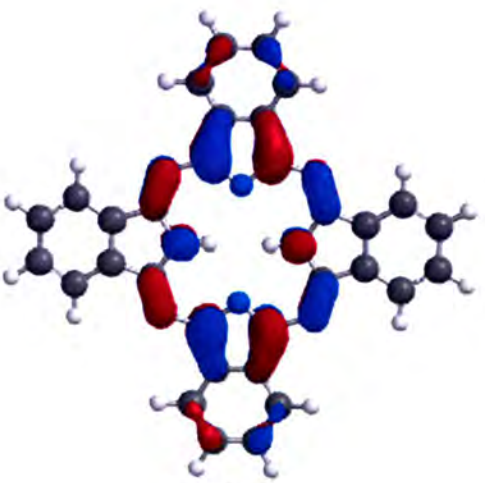

Pc4

Figure 5.6. Lowest unoccupied molecular orbital (LUMO) for each of the studied phthalocyanine macrocycles.

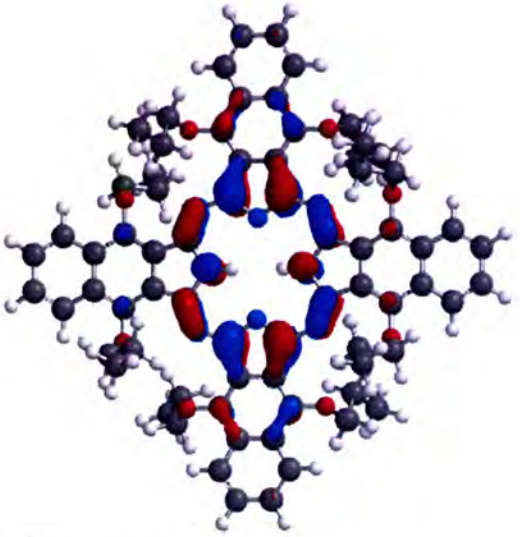

nPc1

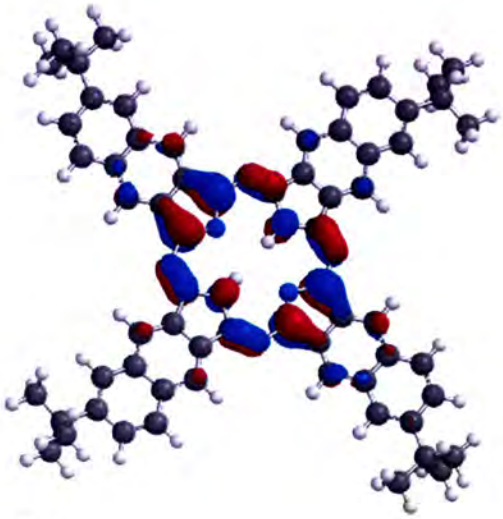

nPc2

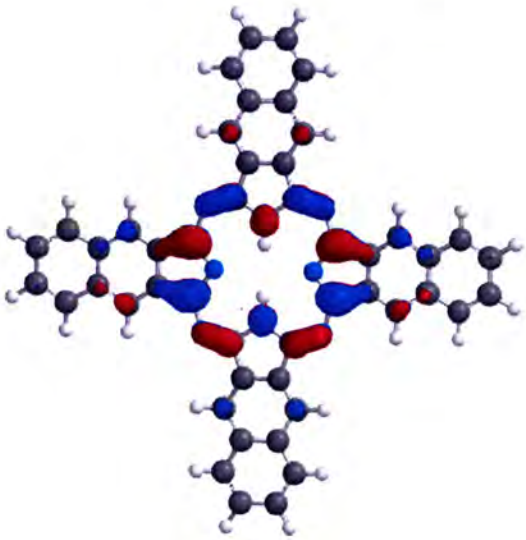

nPc3

Figure 5.7. Lowest unoccupied molecular orbital (LUMO) for each of the studied naphthalocyanine macrocycles.

The investigated molecular reactivity parameters are reported in Table 5.1 and they include the energy of the HOMO (E_{HOMO}), energy of the LUMO (E_{LUMO}), absolute hardness (η), absolute softness (σ) and dipole moment. The inhibition efficiency parameter, obtained from experimental data is also included in the table for comparison purpose. In the discussion, the parameters are described across structures to obtain a comparison of the reactivity for the different compounds, which is related to the tendency of the compounds to bind on the metal surface.

E_{HOMO}, E_{LUMO} and ΔE. Among the studied phthalocyanines, E_{HOMO} has a trend of Pc1 > Pc2 > Pc3 > Pc4. These results suggest that Pc1 has the highest tendency to donate electrons to an electron poor species while Pc4 has the least tendency to donate electrons to the metal surface (as discussed in section 5.1). The results also indicate the role of the substituent groups in

influencing the ability of the compounds to donate electrons. The structures with the substituent groups, either alkyl chain or ether-alkyl chain after the central unit, are better electron donor than the main phthalocyanine unit (Pc1). The alkyl chain and the ether groups are known as electron-donor groups. In this case, they would donate electrons to the central phthalocyanine moiety. Their electron donating ability accounts for the high E_{HOMO} energy for the substituted phthalocyanines than the unsubstituted phthalocyanine. Pc1 has a shorter alkyl chain ($-(CH_2)_3CH_3$) after the ether O atom than Pc2, which has a ($-(CH_2)_7CH_3$). Since Pc1 has higher E_{HOMO} than Pc2, it can be inferred that the ability of electron donating is influenced by the length of the alkyl chain (i.e., the longer the chain the lower the inhibition efficiency).

E_{LUMO} decreases in the order Pc1>Pc2 >Pc3>Pc4, suggesting that Pc4 has the highest tendency to accept electrons from an electron rich species. Therefore, for cases in which the filled *d* orbitals of the metal donate electrons to the inhibitor molecule (in what is known as back-donation mechanism), these electrons would be accommodated in the LUMO of the inhibitor molecules. The molecule with the highest tendency to accept these electrons is the Pc4.

The values of ΔE show the following trend Pc2 > Pc4 > Pc3 > Pc1. In this way, Pc1 is the most reactive species and Pc2 is the least reactive species, suggesting that Pc1 has the highest tendency to interact with the metal surface. Since it has the highest tendency to interact with them metal surface and also the highest tendency to donate electrons, it would preferably have the highest tendency towards inhibition of metal corrosion, which confirm the experimental findings (chapter 3).

Table 5.1: Calculated quantum chemical parameters for the studied macrocycles.

structures	Reactivity parameters[a]								
	E_{HOMO}	E_{LUMO}	ΔE	η	σ	ΔN	ω	μ	%IE
Phthalocyanines									
Pc1	-4.11	-2.20	1.91	0.955	1.05	-2.01	5.21	1.09	67.6
Pc2	-4.44	-2.27	2.17	1.085	0.92	-1.68	5.19	0.03	52.3
Pc3	-4.80	-2.67	2.13	1.065	0.94	-1.53	6.55	0.16	54.3
Pc4	-4.98	-2.83	2.15	1.075	0.93	-1.44	7.09	0.01	46.2
Naphthalocyanines									
nPc1	-4.25	-2.58	1.67	0.835	1.2	-2.15	6.98	0.09	56.8
nPc2	-4.43	-2.46	1.97	0.985	1.02	-1.8	6.02	0.00	51.7
nPc3	-4.55	-2.76	1.79	0.895	1.12	-1.87	7.46	0.00	61.3

[a] η is hardness, σ is softness, ΔN is fraction of electrons transferred, ω is Electrophilicity, μ is dipole moment.

Among the studied naphthalocyanines, the trend in the E_{HOMO} is nPc1>nPc2 >nPc3. These results suggest that nPc1 has the highest tendency to donate electrons to an electron poor species while nPc3 has the least tendency to donate electrons to the metal surface. As, with the phthalocyanines, the results are also suggestive of the role of the substituent groups in influencing the electron donating ability of the compounds; nPc1, which has an ether-alkyl

substituent group, has higher electron donating ability than nPc2, which has only an alkyl-branched substituent.

E_{LUMO} decreases following the order nPc3> nPc1 > nPc2, suggesting that nPc3 has the highest tendency to accept electrons from an electron reach species. Therefore, in a possible back-donation mechanism, the d orbitals on the metal atoms would donate electrons to the LUMO of the inhibitor molecule. The molecule with the highest tendency to accept these electrons is the Pc3.

The values of ΔE has the following trend nPc2 > nPc3 > nPc1. In this way, nPc1 has the lowest value of ΔE, suggesting that nPc1 has the highest tendency to interact with the metal surface. Since it has the highest tendency to interact with the metal surface and also the highest tendency to donate electrons, it would preferably have the highest tendency towards inhibition of metal corrosion, what is also confirmed by the experimental findings (chapter 3).

A comparison of the results of phthalocyanines and naphthalocyanines provides information on which of these macrocycles has greater tendency to donate electrons and to also interact with the metal surface, thereby to have a greater tendency to inhibit metal corrosion. Pc1 can be compared with nPc1 because they have the same substituent at similar positions; Pc3 can be compared with nPc2 because they have the same substituent at similar positions and Pc4 can be compared with nPc3 because they have the same substituent at similar positions. The E_{HOMO} results show that, with the exception of the Pc1 and nPc1 pair, the trend is such that $E_{HOMO\ nPc} > E_{HOMO\ Pc}$, suggesting that naphthalocyanines are better electron donor than phthalocyanines. A comparison of the ΔE values show that naphthalocyanines have lower ΔE than phthalocyanines, suggesting that naphthalocyanines would have greater tendency to interact with the metal surface than phthalocyanines. These comparison results are therefore suggestive of the fact that naphthalocyanines have greater tendency to be better corrosion inhibitors than phthalocyanines, what has also been confirmed by experimental findings (chapter 3).

Hardness and Softness. The global softness and hardness principle has been used to explain many experimentally observed reactivity patterns. The local hardness and softness indicates hardest and softest regions of the molecule, respectively, suggesting that the largest values of the local softness need to correspond to the smallest values of the local hardness [120,121]. The principle of hard and soft acids and bases states that hard acids prefer to react with hard bases and soft acids with soft bases [122]. Absolute hardness and softness are important properties to measure the molecular stability and reactivity. Chemical hardness fundamentally signifies the resistance towards the deformation or polarization of the electron cloud of the atoms, ions or molecules under small perturbation of chemical reactions. A hard molecule has a large energy gap and a soft molecule has a small energy gap. Normally, the inhibitor with the least value of global hardness (hence the highest value of global softness) is expected to have the highest efficiency [126]. The results recorded in table 5.1 show that the global hardness follows the trend: Pc1 < Pc3 < Pc4 < Pc2 for phthalocyanine and: nPc1 < nPc3 < nPc2 for naphthalocyanine. In the same way for global softness: Pc1 > Pc3 > Pc4 >

Pc2 for phthalocyanine and: nPc1 > nPc3 > nPc2. This therefore means that Pc1 and nPc1 have the highest inhibition efficiency, which is in agreement with ΔE results/data.

Fraction of electrons transferred. In literature it has been reported that the values of ΔN show the inhibition effect resulted from electron donation. According to Lukovits's study [44], if the value of ΔN < 3.6, the inhibition efficiency increased with increasing electron donating ability of inhibitor at the metal surface. The fraction of electrons transferred was also calculated in table 5.1. It was also observed that inhibition efficiency increased with increase in the values of ΔN. The resulting values of ΔN follow the order: Pc1 < Pc2 < Pc3 < Pc4 for phthalocyanine and: nPc1 < nPc3 < nPc2 for naphthalocyanine. All the values are below 3.6, which indicate good inhibition efficiencies, however, there is no regular trend in the inhibition efficiency by increasing value of ΔN and the order here does not correlate/agree with the order observed from other parameters.

Mulliken atomic charges. The Mulliken atomic charges on the atoms of interest in each of the studied macrocycle are reported in table 5.2. In Pc1, the highest negative charge is on the N atoms followed by the O atoms. This implies that the atoms that are most likely to donate electrons to the empty/partially filled *d* orbitals of the metal are the N atoms and the O atoms. The negative charge on these atoms is likely a result of the presence of lone pair of electrons on these atoms. Of the two atoms, the N atom has the highest negative charge, which may be attributed to the fact that it has lower electronegativity value (3.04) as compared to the O atom (3.44). Therefore, the N atom has fewer tendencies to hold onto its lone pair of electrons than the O atom. Among the different N atoms, N1, N5 and N7, it is noted that the charges on the atoms follow the order N1>N5>N7. This implies that the preferred site for the interaction with the metal surface is the N1 atom (as discussed in section 5.3.2.). However, N1 is a saturated N atom and because of that it is less likely that the metal would interact with this center preferably. It is therefore likely that N5 and N7 atoms are the preferred centers for interaction with the metal surface because they are unsaturated in nature.

Phthalocyanines. Like in Pc1, the highest negative charge in Pc2 is on the N atoms followed by the O atoms. However, among the different N atoms (i.e., N1, N3 and N5), the order of the magnitude of the negative charge is such that N3 > N1 > N5, indicating that N3 would have the highest tendency to donate lone pair of electrons to the metal surface. Although the results suggest that N1 would have a greater tendency to donate lone pair of electrons than N5, it is possible that in practice, N5, which has an unsaturated double bond, donate its electrons better than N1, which is saturated in nature.
In both Pc3 and Pc4 the highest negative charge is on the N atoms and among the different N atoms, the trend in the charges is such that N1 > N5 > N3, suggesting that the preferred site for interaction with the metal atom is the N1 atom. However, as discussed in the previous structures, N1 is a saturated N atom and would have fewer tendencies to form chemical bonds with the metal ions. Therefore, the metal atom is likely to interact with N3 and N5.

Naphthalocyanines. The highest negative charge in nPc1 is on the N atoms followed by the O atoms. The order of the magnitude of the negative charge in nPc1, nP2 and nPc1 is such that

N1>N5>N3, indicating that N1 would have the highest tendency to donate lone pair of electrons to the metal surface. However, N1 is a saturated N atom and because of that it is less likely that the metal would interact with this center preferably. It is therefore likely that N5 and N3 atoms are the preferred centers for interaction with the metal surface because they are unsaturated in nature.

Overall, the charges on the atoms of phthalocyanines and naphthalocyanines suggest that the N atoms are the preferred centers for interaction with the metal atoms on the metal surface. Furthermore, the results suggest that the interaction of the metal atoms with the phthalocyanines and naphthalocyanines also depends on the nature of the N atoms. A comparison of Pc1 and nPc1 suggests that the negative charge on the N atoms is higher on nPc1 than Pc1. This means that nPc1 would have greater tendency to donate electrons to the metal surface. The high negative charge on the N atoms of the nPc1 is mainly due to the electrons delocalization on the naphthalocyanine as a result of the resonance nature of the ring. The presence of extra aromatic rings in the nPc1, as compared to Pc1, increases the electron density in the naphthalocyanine ring, which in turn increases the negative charge on the N atoms. These results suggest that naphthalocyanine are preferably better corrosion inhibitors than phthalocyanine. This conclusion is in agreement also with the experimental findings reported in chapter 3.

Table 5.2. The Mulliken atomic charges on the atoms of interest in each of the studied macrocycle. The numbering of the atoms in the first column refers to the numbering shown in figure 1.2 Only the charges on the non-hydrogen atoms, considered necessary for the discussion, are reported in the table.

a) Mulliken atomic charges on selected atoms for 1,4,8,11,15,18,22,25-Octabutoxy-29*H*,31*H*-phthalocyanine (Pc1).

Atom	Charge (*e*)	Atom	Charge (*e*)
N_1	-0.736	N_9	-0.746
C_{1a}	0.010	C_{9a}	0.012
C_{1b}	0.331	C_{9b}	0.332
O_{1b}	-0.503	C_{9c}	-0.504
C_{1c}	-0.210	O_{9c}	-0.270
C_{1d}	-0.204	C_{9d}	0.393
C_{1e}	0.322	C_{9e}	-0.530
O_{1e}	-0.507	O_{9e}	-0.274
C_{1f}	0.012	C_{9f}	0.043
C_2	0.519	C_{10}	0.511
N_3	-0.522	N_{11}	-0.545
C_4	0.444	C_{12}	0.448
N_5	-0.652	N_{13}	-0.658
C_{5a}	0.021	C_{13a}	0.180
C_{5b}	0.310	C_{13b}	0.315
O_{5b}	-0.506	O_{13b}	-0.511
C_{5c}	-0.204	C_{13c}	-0.208
C_{5d}	-0.205	C_{13d}	-0.207

C_{5e}	0.310	C_{13e}	0.310
O_{5e}	-0.505	O_{13e}	-0.505
C_{5f}	0.026	C_{13f}	0.027
C_6	0.449	C_{14}	0.445
N_7	-0.531	N_{15}	-0.528
C_8	0.518	C_{16}	0.511

b) Mulliken atomic charges on selected atoms for 2,3,9,10,16,17,23,24-Octakis(octyloxy)-29H,31H-phthalocyanine

Atom	Charge (*e*)	Atom	Charge (*e*)
N_1	-0.757	N_9	-0.757
C_{1a}	0.061	C_{9a}	0.059
C_{1b}	-0.276	C_{9b}	-0.276
C_{1c}	0.346	C_{9c}	0.348
O_{1c}	-0.515	O_{9c}	-0.516
C_{1d}	0.348	C_{9d}	0.346
O_{1d}	-0.516	O_{9d}	-0.515
C_{1e}	-0.276	C_{9e}	-0.276
C_{1f}	0.059	C_{9f}	0.061
C_2	0.509	C_{10}	0.509
N_3	-0.573	N_{11}	-0.573
C_4	-0.454	C_{12}	0.454
N_5	-0.675	N_{13}	-0.675
C_{5a}	0.075	C_{13a}	0.075
C_{5b}	-0.284	C_{13b}	-0.284
C_{5c}	0.344	C_{13c}	0.344
O_{5c}	-0.519	O_{13c}	-0.519
C_{5d}	0.342	C_{13d}	0.342
O_{5d}	-0.518	O_{13d}	-0.518
C_{5e}	-0.283	C_{13e}	-0.283
C_{5f}	-0.075	C_{13f}	0.075
C_6	0.455	C_{14}	0.455
N_7	-0.573	N_{15}	-0.573
C_8	0.510	C_{16}	0.510

c) Mulliken atomic charges on selected atoms for 2,2,16,23-Tetra-tert-butyl-29H,31H-phthalocyanine

atom	Charges (*e*)	atom	Charges (*e*)
N_1	-0.746	N_9	-0.746
C_{1a}	0.064	C_{9a}	0.065
C_{1b}	-0.182	C_{9b}	-0.182
C_{1c}	-0.134	C_{9c}	-0.134
C_{1d}	-0.134	C_{9d}	-0.134
C_{1e}	0.182	C_{9e}	-0.182
C_{1f}	-0.065	C_{9f}	0.064
C_2	0.511	C_{10}	0.511

N_3	-0.560	N_{11}	-0.560
C_4	0.456	C_{12}	0.456
N_5	-0.662	N_{13}	-0.662
C_{5a}	0.082	C_{13a}	0.082
C_{5b}	-0.194	C_{13b}	-0.194
C_{5c}	-0.134	C_{13c}	-0.134
C_{5d}	-0.134	C_{13d}	-0.134
C_{5e}	-0.194	C_{13e}	-0.194
C_{5f}	0.082	C_{13f}	0.082
C_6	0.456	C_{14}	0.456
N_7	-0.560	N_{15}	-0.560
C_8	0.511	C_{16}	0.511

d) Mulliken atomic charges on selected atoms for 29H,31H-phthalocyanine

atom	Charges (*e*)	atom	Charges (*e*)
N_1	-0.746	N_9	-0.746
C_{1a}	0.064	C_{9a}	0.065
C_{1b}	-0.182	C_{9b}	-0.182
C_{1c}	-0.134	C_{9c}	-0.134
C_{1d}	-0.134	C_{9d}	-0.134
C_{1e}	0.182	C_{9e}	-0.182
C_{1f}	-0.065	C_{9f}	0.064
C_2	0.511	C_{10}	0.511
N_3	-0.560	N_{11}	-0.560
C_4	0.456	C_{12}	0.456
N_5	-0.662	N_{13}	-0.662
C_{5a}	0.082	C_{13a}	0.082
C_{5b}	-0.194	C_{13b}	-0.194
C_{5c}	-0.134	C_{13c}	-0.134
C_{5d}	-0.134	C_{13d}	-0.134
C_{5e}	-0.194	C_{13e}	-0.194
C_{5f}	0.082	C_{13f}	0.082
C_6	0.456	C_{14}	0.456
N_7	-0.560	N_{15}	-0.560
C_8	0.511	C_{16}	0.511

e) Mulliken atomic charges on selected atoms for 5,9,14,18,23,32,36-Octabutoxy-2,3-naphthacyanine.

Atom	Charge (*e*)	Atom	Charge (*e*)
N_1	-0.754	N_9	-0.754
C_{1a}	0.031	C_{9a}	0.027
C_{1b}	0.208	C_{9b}	0.210
O_{1b}	-0.548	O_{9b}	-0.548
C_{1c}	0.108	C_{9c}	0.107
C_{1d}	-0.193	C_{9d}	-0.190
C_{1e}	-0.136	C_{9e}	-0.136

C_{1f}	-0.136	C_{9f}	-0.136
C_{1g}	-0.193	C_{9g}	-0.190
C_{1h}	0.108	C_{9h}	0.106
C_{1i}	0.209	C_{9i}	0.207
O_{1i}	-0.548	O_{9i}	-0.548
C_{1j}	0.027	C_{9j}	0.031
C_2	0.526	C_{10}	0.527
N_3	-0.544	N_{11}	-0.544
C_4	0.461	C_{12}	0.462
N_5	-0.660	N_{13}	-0.660
C_{5a}	0.048	C_{13a}	0.048
C_{5b}	0.196	C_{13b}	0.196
O_{5b}	-0.549	O_{13b}	-0.547
C_{5c}	0.111	C_{13c}	0.108
C_{5d}	-0.196	C_{13d}	-0.193
C_{5e}	-0.136	C_{13e}	-0.137
C_{5f}	-0.136	C_{13f}	-0.136
C_{5g}	-0.196	C_{13g}	-0.193
C_{5h}	0.110	C_{13h}	0.107
C_{5i}	0.195	C_{13i}	0.197
O_{5i}	-0.549	O_{13i}	-0.548
C_{5j}	0.050	C_{13j}	0.049
C_6	0.461	C_{14}	0.462
N_7	-0.544	N_{15}	-0.545
C_8	0.527	C_{16}	0.527

f) Mulliken atomic charges on selected atoms for 2,11,20,29-Tetra-*tert*-butyl-2,3-naphthalocyanine.

Atom	Charge (*e*)	Atom	Charge (*e*)
N_1	-0.754	N_9	-0.754
C_{1a}	0.074	C_{9a}	0.073
C_{1b}	-0.277	C_{9b}	-0.27
C_{1c}	0.153	C_{9c}	0.141
C_{1d}	-0.280	C_{9d}	-0.19
C_{1e}	0.183	C_{9e}	-0.189
C_{1f}	-0.189	C_{9f}	0.183
C_{1g}	-0.190	C_{9g}	-0.280
C_{1h}	0.141	C_{9h}	0.153
C_{1i}	-0.277	C_{9i}	-0.277
C_{1j}	0.073	C_{9j}	0.074
C_2	0.515	C_{10}	0.515
N_3	-0.564	N_{11}	-0.564
C_4	0.455	C_{12}	0.455
N_5	-0.666	N_{13}	-0.666
C_{5a}	0.093	C_{13a}	0.093
C_{5b}	-0.286	C_{13b}	-0.286
C_{5c}	0.141	C_{13c}	0.141
C_{5d}	-0.192	C_{13d}	-0.192
C_{5e}	-0.190	C_{13e}	-0.190

C_{5f}	0.182	C_{13f}	-0.182
C_{5g}	-0.281	C_{13g}	-0.281
C_{5h}	0.152	C_{13h}	0.152
C_{5i}	-0.286	C_{13i}	-0.286
C_{5j}	0.093	C_{13j}	0.097
C_6	0.455	C_{14}	0.455
N_7	-0.564	N_{15}	-0.564
C_8	0.516	C_{16}	0.516

g) Mulliken atomic charges on selected atoms for 2,3-naphthalocyanine

Atoms	Charge (*e*)	Atom	Charge (*e*)
N_1	-0.754	N_9	-0.754
C_{1a}	0.075	C_{9a}	0.075
C_{1b}	-0.274	C_{9b}	0.274
C_{1c}	0.138	C_{9c}	0.138
C_{1d}	-0.184	C_{9d}	-0.184
C_{1e}	-0.137	C_{9e}	-0.137
C_{1f}	-0.137	C_{9f}	-0.137
C_{1g}	-0.184	C_{9g}	-0.184
C_{1h}	0.138	C_{9h}	0.138
C_{1i}	-0.274	C_{9i}	-0.274
C_{1j}	0.075	C_{9j}	0.075
C_2	0.516	C_{10}	0.516
N_3	-0.563	N_{11}	-0.563
C_4	0.456	C_{12}	0.456
N_5	-0.665	N_{13}	-0.665
C_{5a}	0.095	C_{13a}	0.095
C_{5b}	-0.284	C_{13b}	-0.284
C_{5c}	0.138	C_{13c}	0.138
C_{5d}	-0.186	C_{13d}	-0.186
C_{5e}	-0.137	C_{13e}	-0.137
C_{5f}	-0.137	C_{13f}	-0.137
C_{5g}	-0.187	C_{13g}	-0.187
C_{5h}	0.138	C_{13h}	0.138
C_{5i}	-0.283	C_{13i}	-0.283
C_{5j}	0.093	C_{13j}	0.093
C_6	0.456	C_{14}	0.456
N_7	-0.563	N_{15}	-0.563
C_8	0.517	C_{16}	0.517

The Fukui functions

The condensed Fukui function allows one to distinguish each part of the molecule on the basis of its distinct chemical behaviour due to the different substituted functional group. The f+ measures the changes of density when the molecules gains electrons and it corresponds to reactivity with respect to nucleophilic attack. On the other hand, f^- corresponds to reactivity with respect to electrophilic attack or when the molecule loses electrons [123,124]. The results of the study on are reported in Tables 5.3a-d for phthalocynines and table 5.3e-g for naphthalocynines. From the obtained results, C_{1a} (Pc1), C_4 (Pc2), N5 (Pc3), N_5+N_3 (Pc4), N_5 (nPc1), C_{13a} (nPc2) and N_5+N_{13} have the highest value of f^+, therefore having the strongest nucleophilic attack, while, N1 (Pc1), N3 (Pc2), N5 (Pc3), C1e (Pc4), C1a (nPc1), C13j (nPc2) and C13a have the highest value of f^-, which indicates a strong electrophilic attack.

Table 5.3. The condensed Fukui functions on the studied macrocycles

a) The condensed Fukui functions (both f^+ and f^-) for 1,4,8,11,15,18,22,25-Octabutoxy-29*H*,31*H*-phthalocyanine.

atom	charge on the anion species	charge on the neutral species	f^+	charge on the neutral species	charge on the cation species	f^-
N_1	-0.746	-0.736	-0.010	-0.736	-0.741	0.005
C_{1a}	-0.005	-0.010	0.005	-0.010	-0.011	0.001
C_{1b}	0.315	0.331	-0.016	0.331	0.348	-0.017
O_{1b}	-0.500	-0.503	0.003	-0.503	-0.497	-0.006
C_{1c}	-0.217	-0.210	-0.007	-0.210	-0.197	-0.013
C_{1d}	-0.215	-0.204	-0.011	-0.204	-0.191	-0.013
C_{1e}	0.310	0.322	-0.012	0.322	0.340	-0.018
O_{1e}	-0.504	-0.507	0.003	-0.507	-0.500	-0.007
C_{1f}	0.004	0.012	-0.008	0.012	0.011	0.001
C_2	0.486	0.519	-0.033	0.519	0.549	-0.030
N_3	-0.529	-0.522	-0.007	-0.522	-0.518	-0.004
C_4	0.403	0.444	-0.041	0.444	0.474	-0.030
N_5	-0.648	-0.652	0.004	-0.652	-0.656	0.004
C_{5a}	0.021	0.021	0.000	0.021	0.020	0.001
C_{5b}	0.293	0.310	-0.017	0.310	0.328	-0.018
O_{5b}	-0.506	-0.506	0.000	-0.506	-0.500	-0.006
C_{5c}	-0.217	-0.204	-0.013	-0.204	-0.192	-0.012
C_{5d}	-0.220	-0.205	-0.015	-0.205	-0.192	-0.013
C_{5e}	0.295	0.310	-0.015	0.310	0.328	-0.018
O_{5e}	-0.505	-0.505	0.000	-0.505	-0.497	-0.008
C_{5f}	0.018	0.026	-0.008	0.026	0.025	0.001
C_6	0.420	0.449	-0.029	0.449	0.479	-0.030
N_7	-0.599	-0.531	-0.068	-0.531	-0.525	-0.006
C_8	0.505	0.518	-0.013	0.518	0.548	-0.030
N_9	-0.755	-0.746	-0.009	-0.746	-0.751	0.005
C_{9a}	0.006	0.012	-0.006	0.012	0.012	0.000
C_{9b}	0.319	0.332	-0.013	0.332	0.346	-0.014
C_{9c}	-0.501	-0.504	0.003	-0.504	-0.501	-0.003

O_{9c}	-0.281	-0.270	-0.011	-0.270	-0.258	-0.012
C_{9d}	0.383	0.393	-0.010	0.393	0.404	-0.011
C_{9e}	-0.540	-0.530	-0.010	-0.530	-0.516	-0.014
O_{9e}	-0.286	-0.274	-0.012	-0.274	-0.255	-0.019
C_{9f}	0.044	0.043	0.001	0.043	0.042	0.001
C_{10}	0.481	0.511	-0.030	0.511	0.542	-0.031
N_{11}	-0.552	-0.545	-0.007	-0.545	-0.542	-0.003
C_{12}	0.408	0.448	-0.04	0.448	0.497	-0.049
N_{13}	-0.655	-0.658	0.003	-0.658	-0.661	0.003
C_{13a}	0.018	0.180	-0.162	0.180	0.017	0.163
C_{13b}	0.297	0.315	-0.018	0.315	0.334	-0.019
O_{13b}	-0.511	-0.511	0.000	-0.511	-0.504	-0.007
C_{13c}	-0.220	-0.208	-0.012	-0.208	-0.194	-0.014
C_{13d}	-0.222	-0.207	-0.015	-0.207	-0.194	-0.013
C_{13e}	0.295	0.310	-0.015	0.310	0.328	-0.018
O_{13e}	-0.505	-0.505	0.000	-0.505	-0.497	-0.008
C_{13f}	0.019	0.027	-0.008	0.027	0.026	0.001
C_{14}	0.417	0.445	-0.028	0.445	0.476	-0.031
N_{15}	-0.556	-0.528	-0.028	-0.528	-0.525	-0.003
C_{16}	0.497	0.511	-0.014	0.511	0.541	-0.030

b) The condensed Fukui functions (both f^+ and f^-) for 2,3,9,10,16,17,23,24-Octakis(octyloxy)-29H,31H-phthalocyanine.

atom	charge on the anion species	charge on the neutral species	f^+	charge on the neutral species	charge on the cation species	f^-
N_1	-0.769	-0.757	-0.012	-0.757	-0.763	0.006
C_{1a}	0.055	0.061	-0.006	0.061	0.060	0.001
C_{1b}	-0.285	-0.276	-0.009	-0.276	-0.259	-0.017
C_{1c}	0.334	0.346	-0.012	0.346	0.361	-0.015
O_{1c}	-0.527	-0.515	-0.012	-0.515	-0.501	-0.014
C_{1d}	0.333	0.348	-0.015	0.348	0.363	-0.015
O_{1d}	-0.526	-0.516	-0.01	-0.516	-0.501	-0.015
C_{1e}	-0.285	-0.276	-0.009	-0.276	-0.259	-0.017
C_{1f}	0.059	0.059	0.000	0.059	0.058	0.001
C_2	0.491	0.509	-0.018	0.509	0.545	-0.036
N_3	-0.590	-0.513	-0.077	-0.513	-0.567	0.054
C_4	0.415	-0.454	0.869	-0.454	0.490	-0.944
N_5	-0.667	-0.675	0.008	-0.675	-0.681	0.006
C_{5a}	0.072	0.075	-0.003	0.075	0.073	0.002
C_{5b}	-0.296	-0.284	-0.012	-0.284	-0.267	-0.017
C_{5c}	0.324	0.344	-0.020	0.344	0.353	-0.009
O_{5c}	-0.530	-0.519	-0.011	-0.519	-0.504	-0.015
C_{5d}	0.326	0.342	-0.016	0.342	0.356	-0.014
O_{5d}	-0.531	-0.518	-0.013	-0.518	-0.504	-0.014
C_{5e}	-0.297	-0.283	-0.014	-0.283	0.266	-0.549
C_{5f}	0.072	-0.075	0.147	-0.075	0.073	-0.148
C_6	0.414	0.455	-0.041	0.455	0.490	-0.035
N_7	-0.588	-0.573	-0.015	-0.573	-0.568	-0.005

C_8	0.488	0.510	-0.022	0.510	0.546	-0.036
N_9	-0.769	-0.757	-0.012	-0.757	-0.763	0.006
C_{9a}	0.059	0.059	0.000	0.059	0.058	0.001
C_{9b}	-0.285	-0.276	-0.009	-0.276	-0.259	-0.017
C_{9c}	0.333	0.348	-0.015	0.348	0.363	-0.015
O_{9c}	-0.526	-0.516	-0.01	-0.516	-0.501	-0.015
C_{9d}	0.334	0.346	-0.012	0.346	0.361	-0.015
O_{9d}	-0.527	-0.515	-0.012	-0.515	-0.501	-0.014
C_{9e}	-0.258	-0.276	0.018	-0.276	-0.259	-0.017
C_{9f}	0.055	0.061	-0.006	0.061	0.060	0.001
C_{10}	0.491	0.509	-0.018	0.509	0.545	-0.036
N_{11}	-0.590	-0.573	-0.017	-0.573	-0.567	-0.006
C_{12}	0.415	0.454	-0.039	0.454	0.490	-0.036
N_{13}	-0.667	-0.675	0.008	-0.675	-0.681	0.006
C_{13a}	0.072	0.075	-0.003	0.075	0.073	0.002
C_{13b}	-0.296	-0.284	-0.012	-0.284	-0.267	-0.017
C_{13c}	0.324	0.344	-0.02	0.344	0.358	-0.014
O_{13c}	-0.530	-0.519	-0.011	-0.519	-0.504	-0.015
C_{13d}	0.326	0.342	-0.016	0.342	0.356	-0.014
O_{13d}	-0.531	-0.518	-0.013	-0.518	-0.504	-0.014
C_{13e}	-0.297	-0.283	-0.014	-0.283	-0.266	-0.017
C_{13f}	0.072	0.075	-0.003	0.075	0.073	0.002
C_{14}	0.414	0.455	-0.041	0.455	0.490	-0.035
N_{15}	-0.588	-0.573	-0.015	-0.573	-0.568	-0.005
C_{16}	0.488	0.510	-0.022	0.510	0.546	-0.036

c) The condensed Fukui functions for 2,9,16,23-Tetra-*tert*-butyl 29H,31H-phthalocyanine.

atom	charge on the anion species	charge on the neutral species	f^+	charge on the neutral species	charge on the cation species	f^-
N_1	-0.768	-0.754	-0.014	-0.754	-0.759	0.005
C_{1a}	0.077	0.075	0.002	0.075	0.070	0.005
C_{1b}	-0.290	-0.274	-0.016	-0.274	-0.254	-0.020
C_{1c}	0.138	0.138	0.000	0.138	0.138	0.000
C_{1d}	-0.189	-0.184	-0.005	-0.184	-0.179	-0.005
C_{1e}	-0.143	-0.137	-0.006	-0.137	-0.129	-0.008
C_{1f}	-0.143	-0.137	-0.006	-0.137	-0.129	-0.008
C_{1g}	-0.189	-0.184	-0.005	-0.184	-0.179	-0.005
C_{1h}	0.138	0.138	0.000	0.138	0.138	0.000
C_{1i}	-0.290	-0.274	-0.016	-0.274	-0.254	-0.02
C_{1j}	0.077	0.075	0.002	0.075	0.070	0.005
C_2	0.496	0.516	-0.020	0.516	0.549	-0.033
N_3	-0.574	-0.563	-0.011	-0.563	-0.561	-0.002
C_4	0.419	0.456	-0.037	0.456	0.488	-0.032
N_5	-0.654	-0.665	0.011	-0.665	-0.699	0.034
C_{5a}	0.096	0.095	0.001	0.095	0.088	0.007
C_{5b}	-0.300	-0.284	-0.016	-0.284	-0.262	-0.022
C_{5c}	0.136	0.138	-0.002	0.138	0.137	0.001
C_{5d}	-0.190	-0.186	-0.004	-0.186	-0.180	-0.006

C_{5e}	-0.144	-0.137	-0.007	-0.137	-0.129	-0.008
C_{5f}	-0.145	-0.137	-0.008	-0.137	-0.129	-0.008
C_{5g}	-0.190	-0.187	-0.003	-0.187	-0.180	-0.007
C_{5h}	0.136	0.138	-0.002	0.138	0.137	0.001
C_{5i}	-0.300	-0.283	-0.017	-0.283	-0.262	-0.021
C_{5j}	0.097	0.093	0.004	0.093	0.090	0.003
C_6	0.419	0.456	-0.037	0.456	0.487	-0.031
N_7	-0.574	-0.563	-0.011	-0.563	-0.561	-0.002
C_8	0.495	0.517	-0.022	0.517	0.548	-0.031
N_9	-0.768	-0.754	-0.014	-0.754	-0.795	0.041
C_{9a}	0.077	0.075	0.002	0.075	0.070	0.005
C_{9b}	-0.290	-0.274	-0.016	-0.274	-0.254	-0.020
C_{9c}	0.138	0.138	0.000	0.138	0.138	0.000
C_{9d}	-0.189	-0.184	-0.005	-0.184	-0.179	-0.005
C_{9e}	-0.143	-0.137	-0.006	-0.137	-0.129	-0.008
C_{9f}	-0.143	-0.137	-0.006	-0.137	-0.129	-0.008
C_{9g}	-0.189	-0.184	-0.005	-0.184	-0.179	-0.005
C_{9h}	0.138	0.138	0.000	0.138	0.138	0.000
C_{9i}	-0.290	-0.274	-0.016	-0.274	-0.254	-0.02
C_{9j}	0.077	0.075	0.002	0.075	0.070	0.005
C_{10}	0.496	0.516	-0.02	0.516	0.549	-0.033
N_{11}	-0.574	-0.563	-0.011	-0.563	-0.561	-0.002
C_{12}	0.419	0.456	-0.037	0.456	0.488	-0.032
N_{13}	-0.654	-0.665	0.011	-0.665	-0.669	0.004
C_{13a}	0.096	0.095	0.001	0.095	0.088	0.007
C_{13b}	-0.300	-0.284	-0.016	-0.284	-0.262	-0.022
C_{13c}	0.136	0.138	-0.002	0.138	0.137	0.001
C_{13d}	-0.190	-0.186	-0.004	-0.186	-0.180	-0.006
C_{13e}	-0.144	-0.137	-0.007	-0.137	-0.129	-0.008
C_{13f}	-0.145	-0.137	-0.008	-0.137	-0.129	-0.008
C_{13g}	-0.190	-0.187	-0.003	-0.187	-0.180	-0.007
C_{13h}	0.136	0.138	-0.002	0.138	0.137	0.001
C_{13i}	-0.300	-0.283	-0.017	-0.283	-0.262	-0.021
C_{13j}	0.097	0.093	0.004	0.093	0.090	0.003
C_{14}	0.419	0.456	-0.037	0.456	0.487	-0.031
N_{15}	-0.574	-0.563	-0.011	-0.563	-0.561	-0.002
C_{16}	0.495	0.517	-0.022	0.517	0.548	-0.031

d) The condensed Fukui functions (both f^+ and f^-) for 29H,31H-phthalocyanine.

atom	charge on the anion species	charge on the neutral species	f^+	charge on the neutral species	charge on the cation species	f^-
N_1	-0.759	-0.746	-0.013	-0.746	-0.751	0.005
C_{1a}	0.063	0.064	-0.001	0.064	0.064	0
C_{1b}	-0.192	-0.182	-0.01	-0.182	-0.167	-0.015
C_{1c}	-0.141	-0.134	-0.007	-0.134	-0.125	-0.009
C_{1d}	-0.140	-0.134	-0.006	-0.134	-0.125	-0.009
C_{1e}	-0.193	0.182	-0.375	0.182	-0.168	0.35

C_{1f}	0.063	-0.065	0.128	-0.065	0.064	-0.129
C_2	0.488	0.511	-0.023	0.511	0.551	-0.04
N_3	-0.578	-0.560	-0.018	-0.560	-0.554	-0.006
C_4	0.414	0.456	-0.042	0.456	0.495	-0.039
N_5	-0.655	-0.662	0.007	-0.662	-0.667	0.005
C_{5a}	0.079	0.082	-0.003	0.082	0.080	0.002
C_{5b}	-0.206	-0.194	-0.012	-0.194	-0.178	-0.016
C_{5c}	-0.144	-0.134	-0.01	-0.134	-0.125	-0.009
C_{5d}	-0.144	-0.134	-0.01	-0.134	-0.125	-0.009
C_{5e}	-0.206	-0.194	-0.012	-0.194	-0.179	-0.015
C_{5f}	0.079	0.082	-0.003	0.082	0.080	0.002
C_6	0.414	0.456	-0.042	0.456	0.495	-0.039
N_7	-0.577	-0.560	-0.017	-0.560	-0.553	-0.007
C_8	0.488	0.511	-0.023	0.511	0.551	-0.04
N_9	-0.759	-0.746	-0.013	-0.746	-0.751	0.005
C_{9a}	0.063	0.065	-0.002	0.065	0.063	0.002
C_{9b}	-0.193	-0.182	-0.011	-0.182	-0.168	-0.014
C_{9c}	-0.140	-0.134	-0.006	-0.134	-0.125	-0.009
C_{9d}	-0.141	-0.134	-0.007	-0.134	-0.125	-0.015
C_{9e}	-0.192	-0.182	-0.01	-0.182	-0.167	0
C_{9f}	0.063	0.064	-0.001	0.064	0.064	-0.04
C_{10}	0.488	0.511	-0.023	0.511	0.551	-0.006
N_{11}	-0.578	-0.560	-0.018	-0.560	-0.554	-0.039
C_{12}	0.414	0.456	-0.042	0.456	0.495	0.005
N_{13}	-0.655	-0.662	0.007	-0.662	-0.667	0.002
C_{13a}	0.079	0.082	-0.003	0.082	0.080	-0.016
C_{13b}	-0.206	-0.194	-0.012	-0.194	-0.178	-0.009
C_{13c}	-0.144	-0.134	-0.01	-0.134	-0.125	-0.009
C_{13d}	-0.144	-0.134	-0.01	-0.134	-0.125	-0.015
C_{13e}	-0.206	-0.194	-0.012	-0.194	-0.179	0.002
C_{13f}	0.079	0.082	-0.003	0.082	0.080	-0.039
C_{14}	0.414	0.456	-0.042	0.456	0.495	-0.007
N_{15}	-0.577	-0.560	-0.017	-0.560	-0.553	-0.04
C_{16}	0.488	0.511	-0.023	0.511	0.551	0.005

e) The condensed Fukui functions (both f^+ and f^-) for 5,9,14,18,23,27,32,36-Octabutoxy-2,3-naphthalocyanine.

atom	charge on the anion species	charge on the neutral species	f^+	charge on the neutral species	charge on the cation species	f^-
N_1	-0.768	-0.754	-0.014	-0.754	-0.759	0.005
C_{1a}	0.029	0.031	-0.002	0.031	0.024	0.007
C_{1b}	0.193	0.208	-0.015	0.208	0.230	-0.022
O_{1b}	-0.548	-0.548	0.000	-0.548	-0.544	-0.004
C_{1c}	0.105	0.108	-0.003	0.108	0.110	-0.002
C_{1d}	-0.195	-0.193	-0.002	-0.193	-0.186	-0.007
C_{1e}	-0.141	-0.136	-0.005	-0.136	-0.129	-0.007
C_{1f}	-0.141	-0.136	-0.005	-0.136	-0.129	-0.007
C_{1g}	-0.195	-0.193	-0.002	-0.193	-0.186	-0.007

C_{1h}	0.104	0.108	-0.004	0.108	0.109	-0.001
C_{1i}	0.191	0.209	-0.018	0.209	0.228	-0.019
O_{1i}	-0.547	-0.548	0.001	-0.548	-0.543	-0.005
C_{1j}	0.033	0.027	0.006	0.027	0.028	-0.001
C_2	0.508	0.526	-0.018	0.526	0.555	-0.029
N_3	-0.555	-0.544	-0.011	-0.544	-0.542	-0.002
C_4	0.426	0.461	-0.035	0.461	0.488	-0.027
N_5	-0.560	-0.660	0.1	-0.660	-0.664	0.004
C_{5a}	0.051	0.048	0.003	0.048	0.047	0.001
C_{5b}	0.176	0.196	-0.02	0.196	0.217	-0.021
O_{5b}	-0.551	-0.549	-0.002	-0.549	-0.544	-0.005
C_{5c}	0.104	0.111	-0.007	0.111	0.112	-0.001
C_{5d}	-0.198	-0.196	-0.002	-0.196	-0.191	-0.005
C_{5e}	-0.143	-0.136	-0.007	-0.136	-0.130	-0.006
C_{5f}	-0.143	-0.136	-0.007	-0.136	-0.130	-0.006
C_{5g}	-0.199	-0.196	-0.003	-0.196	-0.191	-0.005
C_{5h}	0.105	0.110	-0.005	0.110	0.114	-0.004
C_{5i}	0.177	0.195	-0.018	0.195	0.217	-0.022
O_{5i}	-0.551	-0.549	-0.002	-0.549	-0.544	-0.005
C_{5j}	0.049	0.050	-0.001	0.050	0.045	0.005
C_6	0.426	0.461	-0.035	0.461	0.489	-0.028
N_7	-0.555	-0.544	-0.011	-0.544	-0.542	-0.002
C_8	0.507	0.527	-0.02	0.527	0.554	-0.027
N_9	-0.769	-0.754	-0.015	-0.754	-0.759	0.005
C_{9a}	0.033	0.027	0.006	0.027	0.029	-0.002
C_{9b}	0.191	0.210	-0.019	0.210	0.228	-0.018
O_{9b}	-0.549	-0.548	-0.001	-0.548	-0.544	-0.004
C_{9c}	0.106	0.107	-0.001	0.107	0.112	-0.005
C_{9d}	-0.197	-0.190	-0.007	-0.190	-0.189	-0.001
C_{9e}	-0.141	-0.136	-0.005	-0.136	-0.129	-0.007
C_{9f}	-0.142	-0.136	-0.006	-0.136	-0.130	-0.006
C_{9g}	-0.197	-0.190	-0.007	-0.190	-0.188	-0.002
C_{9h}	0.106	0.106	0.000	0.106	0.112	-0.006
C_{9i}	0.192	0.207	-0.015	0.207	0.230	-0.023
O_{9i}	-0.549	-0.548	-0.001	-0.548	-0.544	-0.004
C_{9j}	0.029	0.031	-0.002	0.031	0.024	0.007
C_{10}	0.508	0.527	-0.019	0.527	0.555	-0.028
N_{11}	-0.555	-0.544	-0.011	-0.544	-0.543	-0.001
C_{12}	0.427	0.462	-0.035	0.462	0.490	-0.028
N_{13}	-0.650	-0.660	0.010	-0.660	-0.664	0.004
C_{13a}	0.050	0.048	0.002	0.048	0.046	0.002
C_{13b}	0.178	0.196	-0.018	0.196	0.219	-0.023
O_{13b}	-0.550	-0.547	-0.003	-0.547	-0.544	-0.003
C_{13c}	0.101	0.108	-0.007	0.108	0.109	-0.001
C_{13d}	-0.196	-0.193	-0.003	-0.193	-0.188	-0.005
C_{13e}	-0.143	-0.137	-0.006	-0.137	-0.130	-0.007
C_{13f}	-0.143	-0.136	-0.007	-0.136	-0.130	-0.006
C_{13g}	-0.196	-0.193	-0.003	-0.193	-0.188	-0.005
C_{13h}	0.103	0.107	-0.004	0.107	0.111	-0.004
C_{13i}	0.177	0.197	-0.02	0.197	0.218	-0.021

O_{13i}	-0.549	-0.548	-0.001	-0.548	-0.543	-0.005
C_{13j}	0.049	0.049	0.000	0.049	0.046	0.003
C_{14}	0.427	0.462	-0.035	0.462	0.489	-0.027
N_{15}	-0.555	-0.545	-0.01	-0.545	-0.542	-0.003
C_{16}	0.507	0.527	-0.02	0.527	0.554	-0.027

f) The condensed Fukui functions (both f^+ and f^-) for 2,11,20,29-Tetra-*tert*-butyl-2,3-naphthalocyanine

atom	charge on the anion species	charge on the neutral species	f^+	charge on the neutral species	charge on the cation species	f^-
N_1	-0.769	-0.754	-0.015	-0.754	-0.760	0.006
C_{1a}	0.077	0.074	0.003	0.074	0.070	0.004
C_{1b}	-0.292	-0.277	-0.015	-0.277	-0.258	-0.019
C_{1c}	0.153	0.153	0.000	0.153	0.154	-0.001
C_{1d}	-0.287	-0.280	-0.007	-0.280	-0.272	-0.008
C_{1e}	0.179	0.183	-0.004	0.183	0.188	-0.005
C_{1f}	-0.198	-0.189	-0.009	-0.189	-0.179	-0.01
C_{1g}	-0.194	-0.190	-0.004	-0.190	-0.185	-0.005
C_{1h}	0.142	0.141	0.001	0.141	0.140	0.001
C_{1i}	-0.292	-0.277	-0.015	-0.277	-0.258	-0.019
C_{1j}	0.076	0.073	0.003	0.073	0.069	0.004
C_2	0.495	0.515	-0.02	0.515	0.546	-0.031
N_3	-0.574	-0.564	-0.01	-0.564	-0.562	-0.002
C_4	0.418	0.455	-0.037	0.455	0.486	-0.031
N_5	-0.655	-0.666	0.011	-0.666	-0.671	0.005
C_{5a}	0.096	0.093	0.003	0.093	0.088	0.005
C_{5b}	-0.302	-0.286	-0.016	-0.286	-0.266	-0.02
C_{5c}	0.140	0.141	-0.001	0.141	0.140	0.001
C_{5d}	-0.195	-0.192	-0.003	-0.192	-0.187	-0.005
C_{5e}	-0.201	-0.190	-0.011	-0.190	-0.180	-0.010
C_{5f}	0.176	0.182	-0.006	0.182	0.186	-0.004
C_{5g}	-0.287	-0.281	-0.006	-0.281	-0.272	-0.009
C_{5h}	0.149	0.152	-0.003	0.152	0.152	0.000
C_{5i}	-0.301	-0.286	-0.015	-0.286	-0.266	-0.020
C_{5j}	0.095	0.093	0.002	0.093	0.089	0.004
C_6	0.419	0.455	-0.036	0.455	0.486	-0.031
N_7	-0.574	-0.564	-0.010	-0.564	-0.562	-0.002
C_8	0.496	0.516	-0.020	0.516	0.547	-0.031
N_9	-0.769	-0.754	-0.015	-0.754	-0.760	0.006
C_{9a}	0.076	0.073	0.003	0.073	0.069	0.004
C_{9b}	-0.292	-0.27	-0.022	-0.27	-0.258	-0.012
C_{9c}	0.142	0.141	0.001	0.141	0.140	0.001
C_{9d}	-0.194	-0.19	-0.004	-0.19	-0.185	-0.005
C_{9e}	-0.198	-0.189	-0.009	-0.189	-0.179	-0.01
C_{9f}	0.179	0.183	-0.004	0.183	0.188	-0.005
C_{9g}	-0.287	-0.280	-0.007	-0.280	-0.272	-0.008
C_{9h}	0.153	0.153	0	0.153	0.154	-0.001
C_{9i}	-0.292	-0.277	-0.015	-0.277	-0.258	-0.019

C_{9j}	0.077	0.074	0.003	0.074	0.070	0.004
C_{10}	0.459	0.515	-0.056	0.515	0.546	-0.031
N_{11}	-0.574	-0.564	-0.01	-0.564	-0.562	-0.002
C_{12}	0.418	0.455	-0.037	0.455	0.486	-0.031
N_{13}	-0.655	-0.666	0.011	-0.666	-0.671	0.005
C_{13a}	0.096	0.093	0.003	0.093	0.088	0.005
C_{13b}	-0.302	-0.286	-0.016	-0.286	-0.266	-0.02
C_{13c}	0.140	0.141	-0.001	0.141	0.140	0.001
C_{13d}	-0.195	-0.192	-0.003	-0.192	-0.187	-0.005
C_{13e}	-0.201	-0.190	-0.011	-0.190	-0.180	-0.01
C_{13f}	0.176	-0.182	0.358	-0.182	0.186	-0.368
C_{13g}	-0.287	-0.281	-0.006	-0.281	-0.272	-0.009
C_{13h}	0.149	0.152	-0.003	0.152	0.152	0.000
C_{13i}	-0.301	-0.286	-0.015	-0.286	-0.265	-0.021
C_{13j}	0.095	0.097	-0.002	0.097	0.088	0.009
C_{14}	0.419	0.455	-0.036	0.455	0.486	-0.031
N_{15}	-0.574	-0.564	-0.01	-0.564	-0.562	-0.002
C_{16}	0.496	0.516	-0.02	0.516	0.547	-0.031

g) The condensed Fukui functions (both f^+ and f^-) for 2,3 naphthalocyanine.

atom	charge on the anion species	charge on the neutral species	f^+	charge on the neutral species	charge on the cation species	f^-
N_1	-0.768	-0.754	-0.014	-0.754	-0.759	0.005
C_{1a}	0.077	0.075	0.002	0.075	0.070	0.005
C_{1b}	-0.290	-0.274	-0.016	-0.274	-0.254	-0.02
C_{1c}	0.138	0.138	0.000	0.138	0.138	0.000
C_{1d}	-0.189	-0.184	-0.005	-0.184	-0.179	-0.005
C_{1e}	-0.143	-0.137	-0.006	-0.137	-0.129	-0.008
C_{1f}	-0.143	-0.137	-0.006	-0.137	-0.129	-0.008
C_{1g}	-0.189	-0.184	-0.005	-0.184	-0.179	-0.005
C_{1h}	0.138	0.138	0.000	0.138	0.138	0.000
C_{1i}	-0.290	-0.274	-0.016	-0.274	-0.254	-0.020
C_{1j}	0.077	0.075	0.002	0.075	0.070	0.005
C_2	0.496	0.516	-0.020	0.516	0.549	-0.033
N_3	-0.574	-0.563	-0.011	-0.563	-0.561	-0.002
C_4	0.419	0.456	-0.037	0.456	0.488	-0.032
N_5	-0.654	-0.665	0.011	-0.665	-0.699	0.034
C_{5a}	0.096	0.095	0.001	0.095	0.088	0.007
C_{5b}	-0.300	-0.284	-0.016	-0.284	-0.262	-0.022
C_{5c}	0.136	0.138	-0.002	0.138	0.137	0.001
C_{5d}	-0.190	-0.186	-0.004	-0.186	-0.180	-0.006
C_{5e}	-0.144	-0.137	-0.007	-0.137	-0.129	-0.008
C_{5f}	-0.145	-0.137	-0.008	-0.137	-0.129	-0.008
C_{5g}	-0.190	-0.187	-0.003	-0.187	-0.180	-0.007
C_{5h}	0.136	0.138	-0.002	0.138	0.137	0.001
C_{5i}	-0.300	-0.283	-0.017	-0.283	-0.262	-0.021
C_{5j}	0.097	0.093	0.004	0.093	0.090	0.003
C_6	0.419	0.456	-0.037	0.456	0.487	-0.031

N_7	-0.574	-0.563	-0.011	-0.563	-0.561	-0.002
C_8	0.495	0.517	-0.022	0.517	0.548	-0.031
N_9	-0.768	-0.754	-0.014	-0.754	-0.795	0.041
C_{9a}	0.077	0.075	0.002	0.075	0.070	0.005
C_{9b}	-0.290	-0.274	-0.016	-0.274	-0.254	-0.020
C_{9c}	0.138	0.138	0.000	0.138	0.138	0.000
C_{9d}	-0.189	-0.184	-0.005	-0.184	-0.179	-0.005
C_{9e}	-0.143	-0.137	-0.006	-0.137	-0.129	-0.008
C_{9f}	-0.143	-0.137	-0.006	-0.137	-0.129	-0.008
C_{9g}	-0.189	-0.184	-0.005	-0.184	-0.179	-0.005
C_{9h}	0.138	0.138	0.000	0.138	0.138	0.000
C_{9i}	-0.290	-0.274	-0.016	-0.274	-0.254	-0.02
C_{9j}	0.077	0.075	0.002	0.075	0.070	0.005
C_{10}	0.496	0.516	-0.02	0.516	0.549	-0.033
N_{11}	-0.574	-0.563	-0.011	-0.563	-0.561	-0.002
C_{12}	0.419	0.456	-0.037	0.456	0.488	-0.032
N_{13}	-0.654	-0.665	0.011	-0.665	-0.669	0.004
C_{13a}	0.096	0.095	0.001	0.095	0.088	0.007
C_{13b}	-0.300	-0.284	-0.016	-0.284	-0.262	-0.022
C_{13c}	0.136	0.138	-0.002	0.138	0.137	0.001
C_{13d}	-0.190	-0.186	-0.004	-0.186	-0.180	-0.006
C_{13e}	-0.144	-0.137	-0.007	-0.137	-0.129	-0.008
C_{13f}	-0.145	-0.137	-0.008	-0.137	-0.129	-0.008
C_{13g}	-0.190	-0.187	-0.003	-0.187	-0.180	-0.007
C_{13h}	0.136	0.138	-0.002	0.138	0.137	0.001
C_{13i}	-0.300	-0.283	-0.017	-0.283	-0.262	-0.021
C_{13j}	0.097	0.093	0.004	0.093	0.090	0.003
C_{14}	0.419	0.456	-0.037	0.456	0.487	-0.031
N_{15}	-0.574	-0.563	-0.011	-0.563	-0.561	-0.002
C_{16}	0.495	0.517	-0.022	0.517	0.548	-0.031

Electrophilicity. According to the definition, this index measures the propensity of chemical species to accept electrons [121]. A high value of electrophilicity describes a good electrophile, while a low value of electrophilicity describes a good nucleophile [86]. For the overall electrophilicity and according to the computed values follows this pattern: Pc4 > Pc3 > Pc2 > Pc1 for phthalocyanine and nPc3 > nPc1 > nPc2 for naphthalocyanine.

Dipole moment. The dipole moment determines the electron-density distribution in a molecule [125,126]. A good, more reactive, nucleophile is characterized by lower value of μ and conversely a good electrophile is characterized by a high value of μ [131]. According to the results reported in Table 5.1 the value of μ is high at Pc1 and nPc1 following the trend: Pc1 > Pc3 > Pc2 > Pc4 for phthalocyanine and nPc1 > nPc2 = nPc3 for naphthalocyanine. Pc3, Pc2 and Pc4 have very low μ valued, while nP2 and nPc3 are at zero. This suggests that Pc1 and nPc1 have the most electron density. Higher values of dipole moment (μ) probably increase the adsorption between the inhibitor and the metal surface [119] (as also reported for some organic compounds [section 5.3.4].

5.4.3 Statistical analysis of the data using quantitative structure activity relationship (QSAR) approach

The correlation of individual quantum chemical parameters with the inhibition efficiency of the inhibitor is usually less informative because of the complexity of the adsorption process. It is therefore essential to combine several quantum chemical parameters to form a composite index that could be correlated to the experimental inhibition efficiency. A correlation between quantum chemical parameters and the observed inhibition efficiency is studied by means of quantitative structure activity relationship (QSAR) approach in which relevant mathematical equations are used to relate the quantum chemical parameter to the observed inhibition efficiency of an inhibitor. The derived equations are used to predict %IE from the concentrations of the inhibitors and to provide theoretical explanations for the effects of different variables studied [127,81]. In the present work, two models were tested; the linear model and the non-linear model proposed by Lukovits *et al* for the study of interaction of corrosion with metal surface in acidic solutions [127,81]. However, the linear model alone produced the best correlation results between experimental and theoretical data. This equation has the form;

$$IE_{theor} = Ax_i C_i + B \qquad (51)$$

where A and B are the regression coefficients determined through regression analysis, x_i is a quantum chemical index characteristic of the molecule i, C_i is the experimental concentration of the inhibitor.

QSAR was performed using the quantum chemical parameters obtained using the B3LYP/6-31G (d,p) method and those obtained using the AM1 and PM3 methods in an attempt to correlate more than one quantum chemical parameter to the observed inhibition efficiency. The results of the QSAR analysis on the quantum chemical parameters obtained with B3LYP/6-31G(d,p) method show that a combination of two quantum chemical parameters to form a composite index provides the best correlation with the experimental data and the best three equations obtained are of the form;

$IE = 0.553*E_{HOMO}* C_i -0.457*E_{LUMO}* C_i + 194.786$ $\quad R^2 = 0.938$ and SSE = 15.06

$IE = -0.332*\Delta E* C_i -0.197*\Delta N* C_i + 91.578$ $\quad R^2 = 0.934$ and SSE = 16.06

where R^2 is the coefficient of determination, and SSE is the sum of squared errors defined as:

$$SSE = \sum \left(I\%_{experimental} - I\%_{theoretical}\right)^2 \qquad (52)$$

The first equation suggests that a higher E_{HOMO} and lower E_{LUMO} results in greater inhibition efficiency; the second equation suggests that the smaller ΔE and ΔN of an inhibitor, the greater the inhibition efficiency of the inhibitor. Figure 5.8 shows the corresponding representative plots of the correlation between experimental inhibition efficiency and theoretically estimated inhibition efficiency.

a) Quantum chemical parameters considered are E_{HOMO} and E_{LUMO} energies

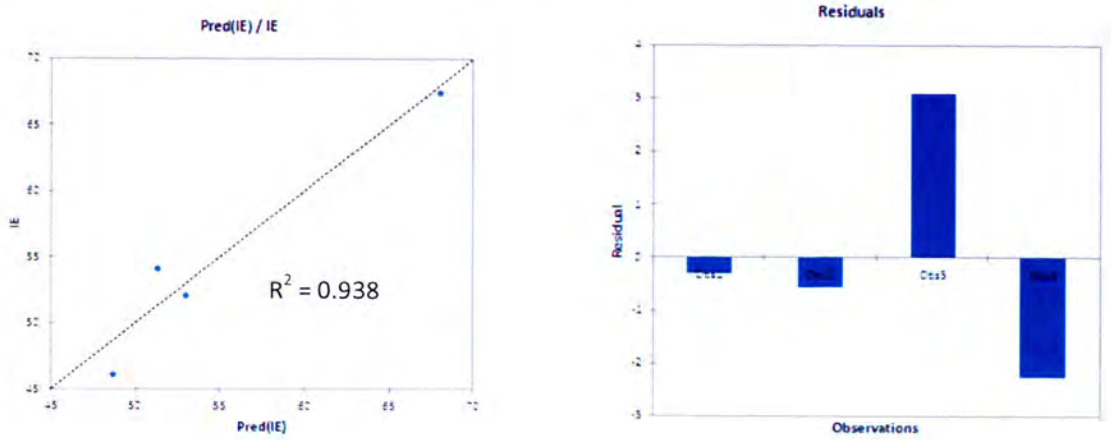

b) Quantum chemical parameters considered are ΔE and ΔN

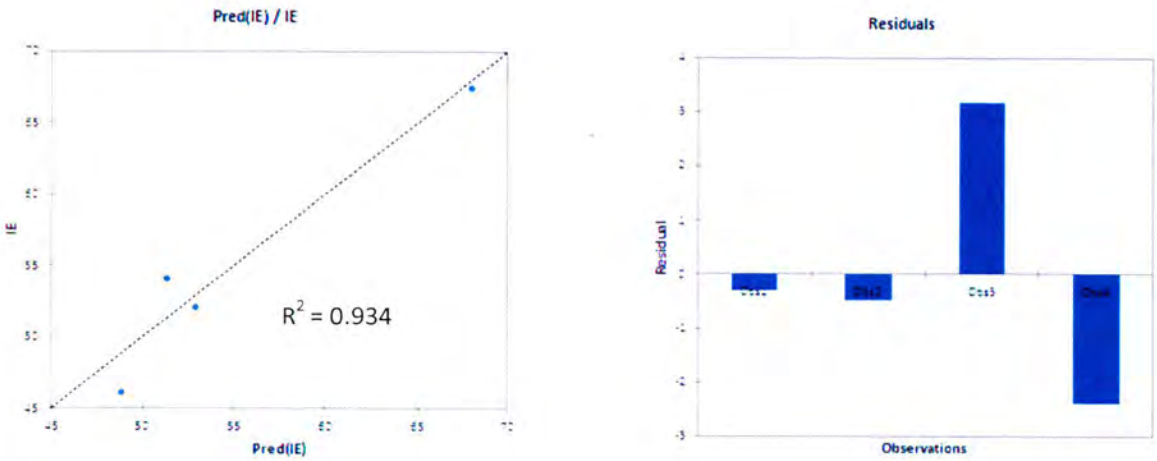

Figure 5.8: Representative plots of correlation between the theoretically estimated %IE and experimentally obtained %IE

CHAPTER 6

CONCLUSIONS

From the results obtained in this study, the following conclusions were reached:

- All the examined phthalocyanine compounds act as excellent corrosion inhibitors for aluminium in 1 M HCl solution especially at high concentrations (100 ppm). The inhibition efficiency of these compounds increase with increase in their concentrations due to the formation of surface film on the metal sheet.
- From the weight loss measurements the inhibition efficiency (%IE) was calculated for all the inhibitors, with and without KI. The inhibitor that showed the best trend and had the highest inhibition efficiency was nPc3. This was confirmed by the electrochemical studies from potentiodynamic polarization data. The plot for nPc3 showed the best trend (with and without KI)
- The addition of potassium Iodide (KI) to the solution increases the inhibition efficiency.
- The adsorption of the naphthalocyanine and phthalocyanine compounds on the aluminium surface obeys Langmuir adsorption isotherm.
- The thermodynamic and kinetic parameters (Gibbs free energy of adsorption, ΔG_{ads}, enthalpy of activation, ΔH_{ads}, entropy of activation, ΔS_{ads} and apparent activation energy, E_a) were obtained from the thermodynamics and kinetic studies. The negative values of ΔG_{ads} show the spontaneity of the adsorption.
- The values of free energy of adsorption and calculated quantum chemical suggest that the inhibition of the phthalocyanine involve two types of interaction, physisorption and chemisorption.
- The E_{HOMO}, E_{LUMO} and ΔE which were derived from the quantum chemical studies on the phthalocyanine. These parameters indicate that the phthalocyanines studied have the ability to donate electrons the metal surface, which confirms that they are good corrosion inhibitors.

REFERENCES

1. Shaw B.A., Kelly R.G. What is Corrosion? *The electrochemical society interface.* 15(2006) 24 – 26.
2. Hussin M.H., Kassim M.J. Electrochemical studies of Mild steel corrosion inhibition in aqueous solution by Uncaria gambir extracts. *Journal of Physical Science.* 21-1(2010) 1-3.
3. Berg H.P. Corrosion Mechanisms and their consequences for nuclear power plants with light water reactors. *R&RATA.* 4(2009) 57-68.
4. GraedeT. E. Corrosion Mechanisms for Silver Exposed to the Atmosphere. *Journal of Electrochemical Society.* 139(1992) 1963-1970.
5. Roberge PR. Corrosion Basics—An Introduction. *2nd ed. Houston, Tex: NACE International*, 2006, 35-47.
6. Watson T.R.B. Why Metals Corrode. *Mater.Prot.* 6(1965) 54.
7. Wranglen G. An Introduction to Corrosion and Protection of Metals. *Anti-corrosion Methods and Materials.* 19(1985) 5-15.
8. Xhang G.X. Galvanic Corrosion. Uhlig's Corrosion Handbook, Third Edition, Edited by R. Winston Revie. Copyright. 2011 John Wiley & Sons, Inc.
9. Little B.J., Mansfeld B.F., Arps P.J., Earthman J.C. Microbiologically Influenced Corrosion. *Material Performance.* Vol 41 (2002) 65.
10. Hoeppner D.W. Pitting Corrosion: Morphology and Characterization. Chapter 5. 1-16 (1976).
11. Yongjun M.T., Revie R.W. Heterogenous Electrode process and localized corrosion. (2013) 3.
12. Rashidi N., Alavi-Soltani S., Asmatulu R. Crevice Corrosion Theory, Mechanisms and Prevention Methods. *Department of Mechanical Engineering, College of Engineering.* (2007). 215-216.
13. Trifunovic Nemanja. Introduction to urban water distribution. (2006) 248.
14. Gerasimov V. V., Rozenfeld I. L. Effect of temperature on the rate of corrosion of metals. *Bulletin of the Academy of Sciences of the USSR, Division of Chemical Science.* 10(1957) 1192-1197.
15. Brondel D. Corrosion in the oil industry. *Oilfield Review.* 6(1994) 3.
16. Trépanier C., Pelton A.R. Effect of Temperature and pH on the Corrosion Resistance of Passivated Nitinol and Stainless Steel. *Nitinol Devices and Components, Fremont, 94539, California, USA.* 2004
17. Nieves-Mendoza D., Gaona-Tiburcio C., Hervert Z H. L., Mendez R. C., Castro-Borges P., Borunda T. A., Zambrano Robledo P., Almeraya-Calderón F. Identifying Factors Influencing the Corrosion Rate of Steel Using Nonparametric Statistics. *Journal of Electrochemical Science.* 7(2012) 6364-6352.
18. Khoma M.S., Sysyn H.M. Influence of Corrosion in media with different pH on local electrode potentials of steels. *Material Science.* 3(2010) 383-388.
19. K.R. Trethewey and J. Chamberlain: "Corrosion for Science and Engineering 2nd Edn.", Longman (UK), 1995.
20. Munger C. Corrosion Prevention by Protective Coatings, Chapter 1, The Corrosion Cell. National Association of Corrosion Engineers, p.28, 1984.
21. Hyung-Suk O., Kwanghyun K., Young-Jin K., Hansung K. Effect of chemical oxidation of CNFs on the electrochemical carbon corrosion in polymer electrolyte membrane fuel cells. International journal of hydrogen energy 35(2010) 701-708.

22. Lister D.H., Davidson R.D., McAlpine E. The mechanism and kinetics of corrosion product release from stainless steel in lithiated high temperature water. *Corrosion Science.* 2(1987) 113-123, 125-140.
23. Torreto M. E., Baraj E., De Pablo J., Gimènez J., Casas I. Kinetics of Corrosion and Dissolution of Uranium Dioxide as a Function of pH. ETSEIB (UPC) Chem. Eng. Depart., Avda. Diagonal 647, 4a planta, 08028 Barcelona, Spain. Received 23 April 1996; accepted 22 July 1996.
24. David E.J. and James D.R. Corrosion Science and technology. (1997) 71.
25. Noor E.A., Al-Moubaraki A. H. Thermodynamic study of metal corrosion and inhibitor adsorption processes in mild steel/1-methyl-4[4'(-X)-styryl pyridinium iodides/hydrochloric acid systems. *Materials Chemistry and Physics.* 110 (2008) 145–154.
26. Jing He., Song H., Liang Z., Fuxing G., Yuh-Shan H. Equlibrium and Thermodynamic Parameter of Adsorption of Methylene Blue onto Rectorite. *Fresenius Environmental Bulletin.* 19(2010) 2651-2656.
27. Khadom A. A., Yaro A. S., AlTaie A. S., Kadum A. A. H. Electrochemical, Activations and Adsorption Studies for the Corrosion Inhibition of Low Carbon Steel in Acidic Media. *Portugaliae Electrochimica Acta.* 6(2009) 699-712.
28. Vasant P. C., Bansal G. K. An Investigation into the Environmental Impacts of Atmospheric Corrosion of Building Materials. *International Journal of Chemical Sciences and Applications.* 4(2013) 1-6.
29. Javaherdashti R. How corrosion affects industry and life. *Anticorrosion methods and materials.* 47(2000) 30-34.
30. Adejo S. O., Yiase S. G., Ahile U. J., Tyohemba T. G., Gbertyo J. A. Inhibitory effect and adsorption parameters of extract of leaves of *Portulaca oleracea* of corrosion of aluminium in H_2SO_4 solution. *Archives of Applied Science Research.* 5(2013) 25-32.
31. Amin A.M., Ahmed M.A., Arida H.A., Arslan T., Saracoglu M., Kandermirli. Monitoring corrosion and corrosion control of iron in HCl by non-ionic surfacants of the TRITON-X series- Part 2. Temperature effect, activation energies and thermodynamics of adsorption. *Corrosion Science.* 53(2011) 540-548.
32. Branzoi V., Golgovici F., Branzoi F. Aluminium corrosion in hydrochloric acid solution and the effect of some organic inhibitors. *Materials Chemistry and Physics.* 78(2002) 122-131.
33. Chai K.Y., Kim S.S. Morphological analysis and classification of types of surface corrosion damage by digital image processing. *Corrosion Science.* 47(2005) 1-15.
34. Eddy N. O., Ita B. I., Ebenso E. E. Experimental and Theoretical Studies on the Corrosion Inhibition Potentials of some Anisole derivatives for Mild Steel. *International Journal of Electrochemical Science.* 6 (2011) 2101 – 2121.
35. Amitha Rani B. E., Basu Bharathi B. J. Green Inhibitors for Corrosion Protection of Metals and Alloys: An Overview. *International Journal of Corrosion.* 2012(2011) 1-15.
36. Saji V. S. A Review on Recent Patents in Corrosion Inhibitors. *Recent Patents on Corrosion Science.* 2(2010) 6-12.
37. Agarwal P., Landolt D.Corrosion Inhibitors. *Corrosion Science.* 260 (1998), 673-691.
38. Prenosil M. Volatile Corrosion Inhibitor coatings. Supplement to Materials Performance. 2001. 14-17.
39. Phanasgaonkar A., Cherry B., Forsyth M. Organic Corrosion inhibitors; how do they inhibit and can they really migrate through concrete. Department of Materials

Engineering and Australian Maritime Engineering Cooperative Research Centre, Monash University.
40. Antonijevic M. M., Petrovic M. B. Copper Corrosion Inhibitors. A review. *International Journal of Electrochemical Science*. 3 (2008) 1-28.
41. Udhayakalaa P., Rajendiranb T. V., Gunasekaranc S. Theoretical approach to the corrosion inhibition efficiency of some pyrimidine derivatives using DFT method. *Journal of Computational Methods in Molecular Design*. 2(2012) 1-15.
42. Özdemir O.K., Aytac A., Atilla D., Durmus M. Corrosion inhibition of aluminium by novel phthalocyanines in hydrochloric acid solution. *Journal of Material Science*. 46(2011) 752-758.
43. Gece G. The use of quantum chemical methods in corrosion inhibitor studies. *Corrosion Science*. 50(2008) 2981-2992.
44. Singh D., Kumar K. Macrocyclic complexes: Synthesis and Characterization. *Journal of the Serbian Chemical Society*. 75(2010) 475-482.
45. Kolthoff M.I. Application of Macrocyclic Compounds in Chemical analysis. *American Chemical Society*. 51(1979) 1-22.
46. Pederson C.J. Cyclic Polyethers and Their Complexes with Metal Salts. *Journal of American Chemical Society*. 89(1967) 7017-7036.
47. Dietrich B., Lehn J.M., Sauvage J.P. Les Crytates. *Tetrahedron Letters*.34(1969) 2889-2892.
48. Ajmal M., Rawat J., Quraishi M.A. Corrosion inhibiting properties of some polyaza macrocyclic compounds on mild steel in acid environments. *Anti-corrosion Methods and Materials*. 45(1998) 419-425.
49. Bentess F.; Lebrini M.; Vezin H.; Chai F.; Traisnel M.; Lagrené M. Ehanced corrosion resistance of carbon steel in normal sulfuric acid medium by some macrocyclic polyether compounds containing a 1,3,4-thiadiazole moiety: AC impedance and computational studies. *Corrosion Science*. 51(2009) 2165-2173.
50. Quraishi M.A.; Rawat J. Inhibition of mild steel corrosion by some macrocyclic compounds in hot and concentrated hydrochloric acid. *Materials Chemistry and Physics*. 73(2002) 118 – 122.
51. McKeown N.B. Phthalocyanine-containing polymers. *Journals of materials Chemistry*. 10(**2000**) 1979-1995.
52. Linstead R.P. Phthalocyanine.Part I. A new type of synthetic colouring matters. *Journal of Chemical Society*. (**1934**), 1016-1017.
53. Sesseler J., Penny brothers, Lee Chang-Hee. Porphyrins and Phthalocyanines. *Chemical Communications*. 50(2013) 6196-6304.
54. Beltran H.I.; Equivel R.; Lozada-Cassou M.; Dominguez-Aguilar M.A.; Sosa-Sánchez A.; Sosa-Sánchez J.L.; Höpfl H.; Barba V.; Luna-Garcia R.; Farfan N.; Zamudio-Rivera L.S. Nano-Shaped Tin Phthalocyanines: Synthesis, Characterization and Corrosion Inhibition Activity. *Chemistry-A European Journal*. 11(2005) 2705 – 2715.
55. Engel M.K.; Hokuku K.R.K. Single-Crystal and solid-state Molecular Structures of Phthalocyanine Complexes. *Kawaura Institute of Chemical Research*. (1997) 11-54.
56. Gregory P. Industrial applications of phthalocyanines. *Journal of Porphyns and Phthalocyanines*. 4(2000) 432-437.
57. van Lier J.E.; Spikes J.D. **2007.** The chemistry, photophysic and photosensitizing properties of phthalocyanines in ciba Foundation Symposium 146-Photosensitizing Compounds: Their Chemistry, Biology and Clinical Use (eds G.Bock and S. Harnett), John Wiley & Sons, Ltd., Chichester, UK.doi:10.1002/9780470513842.ch3.

58. Ohno-Okumura E., Sakamato K. Synthesis and functional properties of phthalocyanine. *Material Science.* 2(2009) 1127-1179.
59. Anees A. K., Aprael S. Y., Abdul Amir H. K., Ahmed S. A.,Ahmed Y. M. The effect of Temperature and Acid Concentration of Corrosion of Low Carbon Steel in Hydrochloric acid media. *American Journal of Applied Science.* 7(2009) 1403-1409.
60. Jing H., Song H., Liang Z., Fuxing G., Yuh-Shan H. Equilibrium and Thermodynamic parameters of adsorption of Methylene blue onto Rectorite. *Fresenius Environmental Bulletin.* 19(2010) 2651-2656.
61. Hettiarachchi S., Chan Y.W.; Wilson R.B., Agarwala V.S. Macrocyclic corrosion inhibitors for mild steel in acid chloride environments. *Corrosion.* 45(1989) 30 -33.
62. Özdemir O.K.; Aytac A.; Atilla D.; Durmus M. Corrosion inhibition of aluminium by novel phthalocyanines in hydrochloric acid solution. *Journal of Material Science.* 46(2011) 752-758.
63. Zhao P., Liang Q., Li Y. Electrochemical, SEM/EDS and quantum chemical study of phthalocyanines as corrosion inhibitors for mild steel in 1 mol/l HCl. *Applied Surface Science.* 252(2005) 1596-1607.
64. Aoki I.V., Seugama P.H. Electrochemical Behavior of Carbon steel pre-Treated with an Organo Functional bis-Silane filled with Copper Phthalocyanine. *Journal of Brazilian Chemical society.* 19(2009) 744-754.
65. Leznoff C. C., Hu M., Nolan K. J. M. The synthesis of phthalocyanine at room temperature. Department of Chemistry, York Universi1,, North York (Toronto), Ontario, Carcda M3J I P3.
66. Jain N.C. The pilgrimage of the Wonder Macromolecule: Phthalocyanine. *Reseacrch Journal of Chemical Sciences.* 3(2011) 1- 5.
67. Kopylovich M. N., Kukushkin V. Y., Haukka M., Luzyanin K. V., Pombeiro A.J.L. An Efficient Synthesis of Phthalocyanines Based on an Unprecedented Double-Addition of Oximes to Phthalonitriles. *Journal of American Chemical Science.* 126 (2004) 15040-15041.
68. Kadish K. M., Smith K. M., Guilard R. The Porphyrin Handbook: Phthalocyanines : properties and materials (2000) 63-72.
69. Sakamoto K., Ohno-Okumura E. Syntheses and Functional Properties of Phthalocyanines. *Materials.* 2(2009) 1127-1179.
70. Nemykin V.N., Lukyanets E.A. Synthesis of Substituted Phthalocyanine. *Special Issue Reviews and Accounts.* i(2010) 136-208.
71. de Souza F.S., Spinelli A. Caffeic acid as a green corrosion inhibitor for mild steel. *Corrosion Science.* 51(2009) 223 – 231.
72. Noor E.A. Temperature effects on corrosion inhibition of mild steel in acidic solution by Aqueous Extracts of Fenugreek leaves. *International Journal of Electrochemical Science* 2(2007) 996 – 1017.
73. Zhang Q.B., Hua X.Y. Corrosion inhibition of mild steel by alkylimidazolium ionic liquids in hydrochloric acid. *Electrochemica Acta* 54(2009) 1881 – 1887.
74. Merino P., Novoa X.R., Pena G., Perez M.C. Electrochemical study on the localized corrosion of SAF2205 duplex stainless steel influence of the σ-phase. (2002) 739.
75. Feng Y., Chen S., Guo W., Liu G., Ma H., Wu L. Electrochemical and molecular simulation studies on the corrosion inhibition of 5,10,15,20-tetraphenylporphyrin adlayers on iron surface. *Applied Surface Science.* 253(2007) 8734-8742.
76. Gece G. The use of quantum chemical methods in corrosion inhibitor studies. *Corrosion Science.* 50(2008) 2981-2992.

77. Kairi N. I,, Kassim J. The Effect of Temperature on the Corrosion Inhibition of Mild Steel in 1 M HCl Solution by *Curcuma Longa* Extracts. *International Journal of Electrochemical Science.* 8(2013) 7138-7155.
78. Soltani N., Behpour M., Ghoreishi S.M., Naeimi H. Corrosion of inhibition of Mild Steel in hydrochloric acid solution by some double Schiff bases. *Corrosion Sciences.* 52(2010) 1351-1361.
79. Khadom A. A., Yaro A.S., AlTaie A.S., Kadum A. A. H. Electrochemical, Activation and Adsorption Studies for the corrosion Inhibition of Low Carbon Steel in Acidic Media. *Portugaliae Electrochimica Acta.* 27(2009) 699-712.
80. Atkins P., De Paula. Physical chemistry. 8th edition. Oxford University express. New York.
81. Fouda A.S., Elewady Y.A., Abd El-Aziz H.K. Corrosion inhibition of carbon steel by cationic surfactants in 0.5 HCl solution. *Journal of Chemical Science and Technology.* 2(2012) 45-53.
82. Hammes-Schiffer S., Anderson C.H. *Ab initio* and semi empirical methods for molecular dynamics simulations based on general Hartree-Fock Theory. *Journal of Chemistry and Physics.* 1(1993) 523-532.
83. Chojnacki H., Kolodziejczyk W., Pruchnik F. Quantuam chemical studies on molecular and electronic structure of platinum and tin adducts with Guanine. *International Journal of Molecular Science.* 2(2001) 148-155.
84. Dewar M. J. S. Thiel W. Ground states of molecules. 38. The MNDO method. Approximations and parameters. *Journal of the American Chemical Society.* 99 (1977) 4899-4907.
85. Dewar M. J. S., Zoebisch E. *G.*, Healy E. F. Stewart J. J. P. **AM1: A** New General Purpose Quantum Mechanical Molecular Model. *Journal of the American Chemical Society.* 107*(*1985) 3902-3909.
86. Stewart J. J. P. Optimization of Parameters for Semi-Empirical Methods III-Extension of PM3 to Be, Mg, Zn, Ga, Ge, As, Se, Cd, In, Sn, Sb Te, Hg, Tl, Pb, and Bi. *Journal of Computational Chemistry.* 12(1991) 320-341.
87. Abreu-Quijano M., Palomar-Pardave M., Cuan A., Romero-Romo M., Negron-Silva G., Alvarez-Bustamante R., Ramirez-Lopez A., Herrera-Hernandez H. Quantum chemical study of 2-Mercaptoimidazole. 2-Mercapto-5-Methylbenzimidazole and 2-Mercapto-5-Nitrobenzimidazole as corrosion inhibitors for steel. *International Journal of Electrochemical Science.* 6(2011) 3729-3742.
88. Kabanda M.M., Morulana L.C., Ozcan M., Karadag F., Dehri I., Obot I.B., Ebenso E.E. Quantum chemical studies on the corrosion inhibition of Mild steel by some triazoles and benzimidazole derivatives in acidic medium. *International Journal of Electrochemical Science.* 7(2012) 5035-5056.
89. Gross E.K.U., Dobson J.F., Petersilka M. Density functional theory of time-dependant phenomena. *Topics in Current Chemistry.* 181(1996) 81-172.
90. Head-Gordon M. Quantum Chemistry and Molecular Processes. *Journal of Physical Chemistry.* 100(1996) 13213–13225.
91. Gaussian 03 User's Reference Manual Version 7, Gaussian Inc. (2003).
92. Lotrich V. F., Bartlett R. J., Grabowski I. Intermolecular Potential Energy Surfaces of Weakly Bound Dimers Computed from *Ab Initio* Density Functional Theory: The Right Answer for the Right Reason. *Chemical Physics Letters.* 405(2005) 43-48.
93. Jensen F., *Introduction to Computational Chemistry*; John Wiley & Sons: Chichester, UK, 2007, 104.

94. Naomi L. H., Quantum chemical Studies of Thermochemistry, Kinetics and Molecular Structure. Doctoral Thesis at the University of Sydney, 2003.
95. Foresman J. B., Frisch A. *Exploring Chemistry with Electronic Structure Methods*, Gaussian, Inc., Pittsburg, PA (USA), 1995.
96. Matta C.F., Gillespie J.R. Understanding and interpreting Molecular electron density distribution. *Journal of Chemical Education.* 9(2002) 1141-1152.
97. Behpour M., Mohammadi N. Use of compounds containing heteroatoms as electrochemical corrosion inhibitors for copper in hydrochloric acid. *Chemical Engineering Communications*. 200(2013) 351-366.
98. Xu F, Duan J, Zhang S, Hou B. The inhibition of mild steel corrosion in 1M hydrochloric acid solutions by triazole derivative. *Materials Letters*. 62(2008) 4072-4074.
99. Kelly P.C., Cramer J.C., Trular D.C. Accurate Partial Atomic charges for high energy molecules using class IV charge models with the MIDI! Basis set. *Theoretical Chemistry Acta*. 113(2005) 133-151.
100. Mulliken R. S. Electronic Structures of Molecules X. Aldehydes, ketones and related molecule, *Journal of Chemical Physics*. 3(1935) 564-572.
101. Mulliken R. S. Electron population analysis on LCAO/MO Molecular wave functions. *Journal of Chemical Physics*. 23(1955) 1833-1841.
102. Mulliken R. S. Criteria for the construction of good self-consistent-field molecular orbital wave functions and the significance of LCAO-MO population analysis. *Journal of Chemical Physics*. 36(1962) 3428-3440.
103. Löwdin P.-O. On the non-orthogonality problem connected with the use of atomic wave functions in the theory of molecules and crystals, *Journal of Chemical Physics*. 18 (1950) 365- 354.
104. Golebiewski A., Rzescowska E. Computational Chemistry, Lowdin Atomic charges. *Acta Physica Polonica.* 45(1974) 563-568.
105. Baker J. Classical chemical concepts from ab initio SCF calculations. *Theoretical Chimica Acta*. 68(1985) 221-229.
106. Kar T., Sannigrahi A. B., Mukherjee D. C. Comparison of atomic charges, valencies and bond orders in some hydrogen-bonded complexes calculated from Mulliken and Lowdin SCF density matrices. *Journal of Molecular Structure (Theochem).* 153 (1987) 93-101.
107. Li W., He Q., Pei C., Hou B. Experimental and theoretical investigation of the adsorption behaviour of new triazole derivatives as inhibitors for mild steel corrosion in acid media. *Electrochimica Acta*. 52(2007) 6386-6394.
108. Cioslowski J., Piskorz P., Guanghua L. Ionization potentials and electron affinities from the extended Koopmans' theorem applied to energy-derivative density matrices: The EKTMP and EKTQCISD methods. *Journal of Chemical Physics*. 107(1997) 6804-6812.
109. Pauling, L. The Nature of the Chemical Bond (Coruell University Press, Ithaca, New York, 1960.
110. Torrent-Sucarrant M., Duran M., Solá. Global hardness evaluation using simplified models for the hardness kernel. *Journal of Physical Chemistry.* 18(2002) 4632-4638.
111. Parr R.G., Pearson R.G. Absolute hardness: companion parameter to absolute electronegativity. *Journal of the American Chemical Society.* 105(1983) 7512-7516.
112. Mert B.D., Mert M.E., Kardaş G., Yazici B. Experimental and theoretical investigation of 3-amino-1,2,4-triazole-5-thiol as a corrosion inhibitor for carbon steel in HCl medium. *Corrosion Science*. 53 (2011) 4265–4272.

113. Arslan T., Kandemirli F., Ebenso E.E., Love I., Alemu H. Quantum chemical studies on the corrosion inhibition of some sulphonamides on mild steel in acidic medium. *Corrosion Science*. 51 (2009) 35–47.
114. Parr R. G., Yang W. Theoretical organic chemistry. *Journal of American Chemical Society*. 106(1984) 4049-4050.
115. Parr R. G., Yang W. Density Functional Theory of Atoms and Molecules, Oxford University Press, New York, 1989.
116. Yang W., Mortier W. J. Intrinsic framework electronegativity: A novel concept in solid state chemistry. *Journal of American Chemical Society*. 108(1986)5708-5717.
117. Zhao P., Qiang Liang Q., Li Y. Electrochemical, SEM/EDS and quantum chemical study of phthalocyanines as corrosion inhibitors for mild steel in 1 mol/l HCl. *Applied Surface Science*. 252 (2005) 1596–1607.
118. Senet P., Yang M. Relation between the Fukui function and the Coulomb hole. *Journal of Chemical Society*. 117(2005) 411-418.
119. Fuentealba P., Florez E., Tiznado W. Topological Analysis of the Fukui Function. *Journal of Chemical Theory and Computation*. 6(2010) 1470-1478.
120. Zarrrouk A., Zarrok H., Salghi R., Hammouti B., Al-Deyab S.S., Touzani R. Bouachrine M., Warad I., Hadda T.B. A theoretical investigation on the corrosion inhibition of Copper by Quinoxaline derivatives in Nitric acid solution. *International Journal of Electrochemical science*. 7 (2012) 6353 – 6364.
121. Abreu-Quijano1 M., Palomar-Pardavé1 M., Cuán1 A., Romero-Romo1 M., Negrón-Silva2 G., Álvarez-Bustamante1 R., Ramírez-López1 A., Herrera-Hernández1 H. Quantum Chemical Study of 2-Mercaptoimidazole, 2-Mercaptobenzimidazole, 2-Mercapto-5-Methylbenzimidazole and 2-Mercapto-5-Nitrobenzimidazole as Corrosion Inhibitors for Steel. *International Journal Electrochemical Science*. 6 (2011) 3729 – 3742.
122. Torrent-Sucarrat M., De Prof. F., Ayersc P. W., Geerlingsa P. On the applicability of local softness and hardness. *Physical Chemistry Chemical Physics*. 12(2010) 1072–1080.
123. Yang W., Parr R.G. Hardness, softness, and the fukui function in the electronic theory of metals and catalysis. *Proceedings of the National Academy of Sciences*. 82 (1985) 6723-6726.
124. Udhayakala1 P., Rajendiran2 T.V., Gunasekaran3 S. Quantum Chemical Studies on the Efficiencies of Vinyl Imidazole Derivatives as Corrosion Inhibitors For Mild Steel. *Journal of Advanced Scientific Research*. 3(2012) 37-44.
125. Pankratov A. N. Quantum-Chemical estimate of dipole moments for tropones and tropolones. *Chemistry of Natural Compounds*. 6 (2003) 553 - 562.
126. Obi-Egbedi, N.O.; Obot, I.B.; El-Khaiary, M.I.; Umoren, S. A.; Ebenso, E. E. Computational Simulation and Statistical Analysis on the Relationship Between Corrosion Inhibition Efficiency and Molecular Structure of Some Phenanthroline Derivatives on Mild Steel Surface. *Internation Journal of Electrochemical Sciences* 6 (2011), 5649–5675.
127. Lukovits, I.; Bakó, I.; Shaban, A.; Kálmán, E. Polynomial model of the inhibition mechanism of thiourea derivatives. *Electrochim. Acta 43 (*1998) 131–136.

Appendix 1

Tables

Table 3.1: Calculated values of corrosion rate ($g.cm^{-2}h^{-1}$) and the inhibition efficiency (%IE) of aluminium in HCl using 1,4,8,11,15,18,22,25-Octabutoxy -29H, 31H Phthalocyanine (Pc1).

Conc.	30°C			40°C			50°C			60°C			70°C		
	%IE	CR		%IE	CR		%IE	CR		%IE	CR		%IE	CR	
M HCL		1.14×10^{-3}			1.19×10^{-3}			1.43×10^{-3}			1.64×10^{-3}			1.78×10^{-3}	
5 ppm	63.7	0.93×10^{-3}	0.637	51.4	1.08×10^{-3}	0.514	48.8	1.16×10^{-3}	0.488	46.5	1.19×10^{-3}	0.465	29.8	1.46×10^{-3}	0.298
0.1%KI	81.8	0.90×10^{-3}	0.818	78.4	1.03×10^{-3}	0.784	67.9	1.11×10^{-3}	0.679	63.6	1.15×10^{-3}	0.636	61.4	1.41×10^{-3}	0.614
0 ppm	65.8	0.88×10^{-3}	0.658	57.4	1.05×10^{-3}	0.574	53.5	1.15×10^{-3}	0.535	52.7	1.19×10^{-3}	0.527	50.3	1.26×10^{-3}	0.503
0.1%KI	87.6	0.84×10^{-3}	0.876	78.8	1.02×10^{-3}	0.788	72.9	1.11×10^{-3}	0.729	72.4	1.15×10^{-3}	0.724	67.4	1.22×10^{-3}	0.674
5 ppm	65.8	0.87×10^{-3}	0.658	60.5	1.05×10^{-3}	0.605	55.2	1.13×10^{-3}	0.552	53.8	1.18×10^{-3}	0.538	53.5	1.23×10^{-3}	0.535
0.1%KI	89.3	0.84×10^{-3}	0.893	84.5	1.01×10^{-3}	0.845	73.4	1.09×10^{-3}	0.734	72.8	1.15×10^{-3}	0.728	69.8	1.18×10^{-3}	0.698
00 ppm	67.6	0.82×10^{-3}	0.676	67.5	0.98×10^{-3}	0.675	64.6	1.04×10^{-3}	0.646	56.8	1.17×10^{-3}	0.568	55.5	1.22×10^{-3}	0.555
0.1%KI	93.3	0.78×10^{-3}	0.933	88.7	0.95×10^{-3}	0.887	84.2	1.01×10^{-3}	0.842	80.6	1.12×10^{-3}	0.806	78.8	1.18×10^{-3}	0.788

Table 3.2: Calculated values of corrosion rate ($g.cm^{-2}h^{-1}$) and the inhibition efficiency (%IE) of aluminium in HCl using 2,3,9,10,16,17,23,24-Octakis (octyloxy)--29H, 31H Phthalocyanine (Pc2).

Conc.	30°C			40°C			50°C			60°C			70°C		
	%IE	CR		%IE	CR		%IE	CR		%IE	CR		%IE	CR	
M HCL		1.14×10^{-3}			1.19×10^{-3}			1.43×10^{-3}			1.64×10^{-3}			1.78×10^{-3}	
5 ppm	41.2	0.89×10^{-3}	0.412	38.4	1.09×10^{-3}	0.384	36.4	1.28×10^{-3}	0.364	29.3	1.43×10^{-3}	0.293	20.1	1.48×10^{-3}	0.201
0.1%KI	62.8	0.84×10^{-3}	0.628	59.3	1.06×10^{-3}	0.593	55.9	1.23×10^{-3}	0.559	50.1	1.39×10^{-3}	0.501	48.4	1.42×10^{-3}	0.484
0 ppm	46.1	0.87×10^{-3}	0.461	38.7	1.09×10^{-3}	0.387	38.5	1.26×10^{-3}	0.385	32.8	1.43×10^{-3}	0.328	23.8	1.48×10^{-3}	0.238
0.1%KI	67.5	0.83×10^{-3}	0.675	64.7	1.04×10^{-3}	0.647	61.6	1.21×10^{-3}	0.616	58.3	1.40×10^{-3}	0.583	54.7	1.44×10^{-3}	0.547
5 ppm	49.4	0.87×10^{-3}	0.494	41.6	1.06×10^{-3}	0.416	40.1	1.24×10^{-3}	0.401	34.1	1.41×10^{-3}	0.341	24.9	1.46×10^{-3}	0.249
0.1%KI	71.4	0.82×10^{-3}	0.714	66.9	1.02×10^{-3}	0.669	63.3	1.19×10^{-3}	0.633	59.1	1.36×10^{-3}	0.591	55.8	1.41×10^{-3}	0.558
00 ppm	52.3	0.86×10^{-3}	0.523	41.8	1.06×10^{-3}	0.418	40.8	1.24×10^{-3}	0.408	37.8	1.38×10^{-3}	0.378	30.2	1.45×10^{-3}	0.302
0.1%KI	76.5	0.81×10^{-3}	0.765	73.8	1.02×10^{-3}	0.738	72.4	1.19×10^{-3}	0.724	69.4	1.34×10^{-3}	0.694	67.8	1.41×10^{-3}	0.678

Table 3.3: Calculated values of corrosion rate ($g.cm^{-2}h^{-1}$) and the inhibition efficiency (%IE) of aluminium in HCl using 2,9,16,23 Tetra-tert-butyl-29H, 31H Phthalocyanine (Pc3).

Conc.	30°C			40°C			50°C			60°C			70°C		
	%IE	CR		%IE	CR		%IE	CR		%IE	CR		%IE	CR	
M HCL		1.14×10^{-3}			1.19×10^{-3}			1.43×10^{-3}			1.64×10^{-3}			1.78×10^{-3}	
5 ppm	43.5	0.90×10^{-3}	0.435	38.8	1.09×10^{-3}	0.388	35.4	1.26×10^{-3}	0.354	29.7	1.46×10^{-3}	0.297	24.9	1.49×10^{-3}	0.249
0.1%KI	66.7	0.86×10^{-3}	0.667	62.5	1.04×10^{-3}	0.625	57.9	1.23×10^{-3}	0.579	54.3	1.42×10^{-3}	0.543	51.0	1.44×10^{-3}	0.510
0 ppm	46.8	0.89×10^{-3}	0.468	40.3	1.09×10^{-3}	0.403	35.8	1.25×10^{-3}	0.358	30.3	1.45×10^{-3}	0.303	26.8	1.48×10^{-3}	0.268
0.1%KI	68.3	0.87×10^{-3}	0.683	66.4	1.04×10^{-3}	0.664	61.8	1.22×10^{-3}	0.618	57.7	1.41×10^{-3}	0.577	54.5	1.45×10^{-3}	0.545
5 ppm	49.2	0.86×10^{-3}	0.492	42.2	1.08×10^{-3}	0.422	42.2	1.23×10^{-3}	0.422	36.3	1.41×10^{-3}	0.369	28.0	1.46×10^{-2}	0.280
0.1%KI	74.3	0.82×10^{-3}	0.743	70.7	1.04×10^{-3}	0.707	67.6	$1.20\times10^{-}$	0.676	62.9	1.37×10^{-3}	0.629	57.8	1.41×10^{-3}	0.578
00 ppm	54.3	0.85×10^{-3}	0.538	43.5	1.08×10^{-3}	0.435	43.2	1.21×10^{-3}	0.432	39.7	1.39×10^{-3}	0.397	36.7	1.40×10^{-3}	0.367
0.1%KI	77.9	0.82×10^{-3}	0.779	77.2	1.03×10^{-3}	0.772	73.0	1.18×10^{-3}	0.730	68.7	1.36×10^{-3}	0.687	64.9	1.37×10^{-3}	0.649

Table 3.4: Calculated values of corrosion rate ($g.cm^{-2}h^{-1}$) and the inhibition efficiency (%IE) of aluminium in HCl using 29H, 31H Phthalocyanine (Pc4).

Conc.	30°C			40°C			50°C			60°C			70°C		
	%IE	CR		%IE	CR		%IE	CR		%IE	CR		%IE	CR	
1M HCL		1.14×10^{-3}			1.19×10^{-3}			1.43×10^{-3}			1.64×10^{-3}			1.78×10^{-3}	
25 ppm	39.6	0.88×10^{-3}	0.396	35.9	1.08×10^{-3}	0.359	35.5	1.29×10^{-3}	0.35	24.1	1.43×10^{-3}	0.241	17.8	1.48×10^{-3}	0.1
+0.1%KI	60.3	0.82×10^{-3}	0.603	55.4	1.05×10^{-3}	0.554	52.9	1.24×10^{-3}	0.529	50.1	1.38×10^{-3}	0.501	46.7	1.46×10^{-3}	0.4
50 ppm	40.8	0.85×10^{-3}	0.408	37.8	1.08×10^{-3}	0.378	36.1	1.27×10^{-3}	0.361	27.3	1.43×10^{-3}	0.273	25.2	1.46×10^{-3}	0.2
+0.1%KI	68.4	0.81×10^{-3}	0.684	62.5	1.06×10^{-3}	0.625	58.3	1.22×10^{-3}	0.583	54.9	1.40×10^{-3}	0.549	51.1	1.41×10^{-3}	0.5
75 ppm	43.2	0.84×10^{-3}	0.432	40.4	1.07×10^{-3}	0.404	36.8	1.25×10^{-3}	0.368	32.7	1.38×10^{-3}	0.327	31.7	1.45×10^{-3}	0.3
+0.1%KI	75.3	0.80×10^{-3}	0.753	69.4	1.05×10^{-3}	0.694	64.2	1.23×10^{-3}	0.642	60.6	1.33×10^{-3}	0.606	54.7	1.41×10^{-3}	0.5
100 ppm	46.3	0.82×10^{-3}	0.463	44.9	1.05×10^{-3}	0.449	44.6	1.24×10^{-3}	0.446	39.7	1.38×10^{-3}	0.397	37.6	1.36×10^{-3}	0.3
+0.1%KI	79.5	0.77×10^{-3}	0.795	72.7	1.02×10^{-3}	0.727	68.9	1.21×10^{-3}	0.689	63.9	1.33×10^{-3}	0.639	59.4	1.34×10^{-3}	0.5

Table 3.5: Calculated values of corrosion rate ($g.cm^{-2}h^{-1}$) and the inhibition efficiency (%IE) of aluminium in HCl using 5,9,14,18,23,27,32,36-Octabutoxy -2,3 naPhthalocyanine (nPc1).

Conc.	30°C			40°C			50°C			60°C			70°C		
	%IE	CR		%IE	CR		%IE	CR		%IE	CR		%IE	CR	
1M HCL		1.14×10^{-3}			1.19×10^{-3}			1.43×10^{-3}			1.64×10^{-3}			1.78×10^{-3}	
25 ppm	45.6	0.88×10^{-3}	0.456	40.9	1.09×10^{-3}	0.409	39.8	1.25×10^{-3}	0.398	37.8	1.35×10^{-3}	0.378	33.5	1.42×10^{-3}	0.335
+0.1%KI	79.4	0.85×10^{-3}	0.794	76.2	1.04×10^{-3}	0.762	68.7	1.21×10^{-3}	0.687	65.8	1.31×10^{-3}	0.658	65.1	1.38×10^{-3}	0.651
50 ppm	49.8	0.88×10^{-3}	0.498	42.7	1.06×10^{-3}	0.427	41.6	1.23×10^{-3}	0.416	41.0	1.34×10^{-3}	0.410	38.3	1.39×10^{-3}	0.383
+0.1%KI	84.6	0.85×10^{-3}	0.846	71.9	1.01×10^{-3}	0.719	71.4	1.20×10^{-3}	0.714	67.2	1.30×10^{-3}	0.672	65.4	1.34×10^{-3}	0.654
75 ppm	53.6	0.85×10^{-3}	0.536	43.3	1.06×10^{-3}	0.433	42.5	1.22×10^{-3}	0.425	41.3	1.33×10^{-3}	0.413	38.9	1.39×10^{-3}	0.389
+0.1%KI	85.4	0.81×10^{-3}	0.854	83.7	1.02×10^{-3}	0.837	80.4	1.17×10^{-3}	0.804	71.8	1.30×10^{-3}	0.718	66.2	1.35×10^{-3}	0.662
100 ppm	56.8	0.82×10^{-3}	0.568	46.9	1.05×10^{-3}	0.469	46.4	1.19×10^{-3}	0.464	46.4	1.29×10^{-3}	0.464	41.1	1.34×10^{-3}	0.411
+0.1%KI	87.3	0.78×10^{-3}	0.873	86.4	1.01×10^{-3}	0.864	85.7	1.14×10^{-3}	0.867	82.9	1.26×10^{-3}	0.829	81.6	1.30×10^{-3}	0.816

Table 3.6: Calculated values of corrosion rate ($g.cm^{-2}h^{-1}$) and the inhibition efficiency (%IE) of aluminium in HCl using 2,11,20,29-Tetra-tert-butyl-2,3-naPhthalocyanine (nPc2).

Conc.	30°C			40°C			50°C			60°C			70°C		
	%IE	CR		%IE	CR		%IE	CR		%IE	CR		%IE	CR	
1M HCL		1.14×10^{-3}			1.19×10^{-3}			1.43×10^{-3}			1.64×10^{-3}			1.78×10^{-3}	
25 ppm	42.6	0.91×10^{-3}	0.426	39.6	1.08×10^{-3}	0.396	38.2	1.25×10^{-3}	0.382	29.1	1.42×10^{-3}	0.291	27.7	1.49×10^{-3}	0.277
+0.1%KI	66.5	0.87×10^{-3}	0.665	63.6	1.06×10^{-3}	0.636	62.1	1.22×10^{-3}	0.621	60.9	1.39×10^{-3}	0.609	57.3	1.47×10^{-3}	0.573
50 ppm	47.2	0.87×10^{-3}	0.472	41.4	1.06×10^{-3}	0.414	38.5	1.24×10^{-3}	0.385	31.7	1.42×10^{-3}	0.317	29.4	1.48×10^{-3}	0.294
+0.1%KI	68.8	0.84×10^{-3}	0.688	65.7	1.02×10^{-3}	0.657	62.7	1.21×10^{-3}	0.627	61.5	1.38×10^{-3}	0.615	58.3	1.45×10^{-3}	0.583
75 ppm	48.3	0.86×10^{-3}	0.483	42.9	1.06×10^{-3}	0.429	39.9	1.22×10^{-3}	0.399	37.0	1.39×10^{-3}	0.370	36.5	1.43×10^{-3}	0.365
+0.1%KI	72.5	0.81×10^{-3}	0.725	67.3	1.02×10^{-3}	0.673	63.5	1.18×10^{-3}	0.635	62.1	1.33×10^{-3}	0.621	61.4	1.40×10^{-3}	0.614
100 ppm	51.7	0.84×10^{-3}	0.517	45.7	1.05×10^{-3}	0.457	44.8	1.21×10^{-3}	0.448	44.1	1.30×10^{-3}	0.441	42.4	1.35×10^{-3}	0.424
+0.1%KI	78.6	0.80×10^{-3}	0.786	75.1	1.02×10^{-3}	0.751	73.6	1.18×10^{-3}	0.736	67.3	1.26×10^{-3}	0.673	65.9	1.33×10^{-3}	0.659

Table 3.: Calculated values of corrosion rate ($g.cm^{-2}h^{-1}$) and the inhibition efficiency (%IE) of aluminium in HCl using 5,9,14,18,23,27,32,36-Octabutoxy -2,3 naPhthalocyanine.

Conc.	30°C			40°C			50°C			60°C			70°C		
	%IE	CR		%IE	CR		%IE	CR		%IE	CR		%IE	CR	
1M HCL		1.14×10^{-3}			1.19×10^{-3}			1.43×10^{-3}			1.64×10^{-3}			1.78×10^{-3}	
25 ppm	45.6	0.88×10^{-3}	0.456	40.9	1.09×10^{-3}	0.409	39.8	1.25×10^{-3}	0.398	37.8	1.35×10^{-3}	0.378	33.5	1.42×10^{-3}	0.3
+0.1%KI	79.4	0.85×10^{-3}	0.794	76.2	1.04×10^{-3}	0.762	68.7	1.21×10^{-3}	0.687	65.8	1.31×10^{-3}	0.658	65.1	1.38×10^{-3}	0.6
50 ppm	49.8	0.88×10^{-3}	0.498	42.7	1.06×10^{-3}	0.427	41.6	1.23×10^{-3}	0.416	41.0	1.34×10^{-3}	0.410	38.3	1.39×10^{-3}	0.3
+0.1%KI	84.6	0.85×10^{-3}	0.846	71.9	1.01×10^{-3}	0.719	71.4	1.20×10^{-3}	0.714	67.2	1.30×10^{-3}	0.672	65.4	1.34×10^{-3}	0.6
75 ppm	53.6	0.85×10^{-3}	0.536	43.3	1.06×10^{-3}	0.433	42.5	1.22×10^{-3}	0.425	41.3	1.33×10^{-3}	0.413	38.9	1.39×10^{-3}	0.3
+0.1%KI	85.4	0.81×10^{-3}	0.854	83.7	1.02×10^{-3}	0.837	80.4	1.17×10^{-3}	0.804	71.8	1.30×10^{-3}	0.718	66.2	1.35×10^{-3}	0.6
100 ppm	56.8	0.82×10^{-3}	0.568	46.9	1.05×10^{-3}	0.469	46.4	1.19×10^{-3}	0.464	46.4	1.29×10^{-3}	0.464	41.1	1.34×10^{-3}	0.4
+0.1%KI	87.3	0.78×10^{-3}	0.873	86.4	1.01×10^{-3}	0.864	85.7	1.14×10^{-3}	0.867	82.9	1.26×10^{-3}	0.829	81.6	1.30×10^{-3}	0.8

Table 3.: Calculated values of corrosion rate ($g.cm^{-2}h^{-1}$) and the inhibition efficiency (%IE) of aluminium in HCl using 5,9,14,18,23,27,32,36-Octabutoxy -2,3 naPhthalocyanine.

Conc.	30°C			40°C			50°C			60°C			70°C		
	%IE	CR		%IE	CR		%IE	CR		%IE	CR		%IE	CR	
1M HCL		1.14×10^{-3}			1.19×10^{-3}			1.43×10^{-3}			1.64×10^{-3}			1.78×10^{-3}	
25 ppm	45.6	0.88×10^{-3}	0.456	40.9	1.09×10^{-3}	0.409	39.8	1.25×10^{-3}	0.398	37.8	1.35×10^{-3}	0.378	33.5	1.42×10^{-3}	0.335
+0.1%KI	79.4	0.85×10^{-3}	0.794	76.2	1.04×10^{-3}	0.762	68.7	1.21×10^{-3}	0.687	65.8	1.31×10^{-3}	0.658	65.1	1.38×10^{-3}	0.651
50 ppm	49.8	0.88×10^{-3}	0.498	42.7	1.06×10^{-3}	0.427	41.6	1.23×10^{-3}	0.416	41.0	1.34×10^{-3}	0.410	38.3	1.39×10^{-3}	0.383
+0.1%KI	84.6	0.85×10^{-3}	0.846	71.9	1.01×10^{-3}	0.719	71.4	1.20×10^{-3}	0.714	67.2	1.30×10^{-3}	0.672	65.4	1.34×10^{-3}	0.654
75 ppm	53.6	0.85×10^{-3}	0.536	43.3	1.06×10^{-3}	0.433	42.5	1.22×10^{-3}	0.425	41.3	1.33×10^{-3}	0.413	38.9	1.39×10^{-3}	0.389
+0.1%KI	85.4	0.81×10^{-3}	0.854	83.7	1.02×10^{-3}	0.837	80.4	1.17×10^{-3}	0.804	71.8	1.30×10^{-3}	0.718	66.2	1.35×10^{-3}	0.662
100 ppm	56.8	0.82×10^{-3}	0.568	46.9	1.05×10^{-3}	0.469	46.4	1.19×10^{-3}	0.464	46.4	1.29×10^{-3}	0.464	41.1	1.34×10^{-3}	0.411
+0.1%KI	87.3	0.78×10^{-3}	0.873	86.4	1.01×10^{-3}	0.864	85.7	1.14×10^{-3}	0.867	82.9	1.26×10^{-3}	0.829	81.6	1.30×10^{-3}	0.816

Appendix 2

Equations used

1. **The corrosion rate** : $\rho = (\Delta W / St)$
2. **Inhibition efficiency (% IE)** : $\% IE = (\rho_1 - \rho_2 / \rho_2) \times 100$
3. **Degree of surface coverage** : $\theta = (\rho_1 - \rho_2 / \rho_2)$
4. **Weight loss (W)** : $W = w_1 - w_2$
5. **Langmuir plot:** $\frac{\theta}{1-\theta} = KC$
6. **Activation Energy calculation:** $\log \frac{\rho_2}{\rho_1} = \frac{E_a}{2.303R}\left(\frac{1}{T_1} - \frac{1}{T_2}\right)$
7. **Heat of adsorption (Q_{ads})**:

$$Q_{ads} = 2.303R\left[\log\left(\frac{\theta_2}{1-\theta_2}\right) - \log\left(\frac{\theta_1}{1-\theta_1}\right)\right] x \left(\frac{T_1 T_2}{T_2 - T_1}\right) kJmol^{-1}$$

8. **Gibbs free energy of adsorption:**

$$k = \frac{1}{55.5}\exp\left[\frac{-\Delta G^{o}_{ads}}{RT}\right]$$

9. **Arrheius equation:**

$$k = Ae^{-E_a / RT}$$

10. **Synergism equation**

$$S_I = \frac{1-I_{1+2}}{1-I\prime_{1+2}}$$

11. **Arrhenius equation (another form):**

$$\log \rho = \log A - \frac{E_a}{2.303RT}$$

12. Van't Hoff equation:

$$\ln K = -\frac{\Delta H^0{}_{ads}}{RT} + Cons\tan t$$

13. Gibbs-Helmholtz equation:

$$\left[\frac{\partial\left(\Delta G^0{}_{ads}/T\right)}{\partial T}\right]_P = -\frac{\Delta H^0{}_{ads}}{T^2}$$

14. Entropy and Enthalpy relationship:

$$\Delta G^0{}_{ads} = \Delta H^0{}_{ads} - T\Delta S^0{}_{ads}$$

15. Equilibrium constant (K_{eq}):

$$RT\ln K_{eq} = -\Delta G^0 = nF\Delta E^0$$

16. Electronegativity:

$$\chi \cong -\tfrac{1}{2}\,(E_{HOMO} + E_{LUMO})$$

17. Global hardness:

$$\eta \cong -\tfrac{1}{2}\,(E_{HOMO} - E_{LUMO})$$

18. Global electrophilicity index:

$$\omega = \chi^2/2\eta$$

19. Global softness:

$$\sigma = 1/\eta \cong -2/(E_{HOMO} - E_{LUMO})$$

20. Electron affinity related to E_{HOMO} :

$$I \cong -E_{HOMO}$$

21. Electron affinity related to E_{LUMO} :

$$A \cong -E_{LUMO}$$

22. Potentiodynamic polarization inhibition efficiency:

$$\mu_{PDP} = \frac{i^0_{corr} - i^i_{corr}}{i^0_{corr}} \times 100$$

23. Electrochemical impedance spectroscopy inhibition efficiency:

$$E_{EIS}\% = \left(1 - \frac{R^{0}_{ct}}{R_{ct}}\right) \times 100$$

24. Transition-state equation:

$$C_R = \frac{RT}{Nh} \exp\left(\frac{\Delta S*}{R}\right) \exp\left(-\frac{\Delta H*}{RT}\right)$$

25. Surface coverage (with thermodynamic parameters):

$$\theta = \frac{K_{ads} C_{inh}}{1 + K_{ads} C_{inh}}$$

26. Surface coverage (with thermodynamic parameters) rearranged:

$$\frac{C_{inh}}{\theta} = \frac{1}{K_{ads}} + C_{inh}$$

27. Current response, constant phase element:

$$Z_{CPE} = Y_0^{-1} (i\omega)^{-n}$$

28. Double layer capacitance:

$$C_{dl} = (Y_0 R_{ct}^{1-n})^{1/n}$$

29. Thickness of the protective layer (d):

$$C_{dl} = \frac{\varepsilon \varepsilon_0}{d}$$

30. Surface coverage (EIS):

$$\theta = 1 - \frac{R^{0}_{ct}}{R_{ct}}$$

31. The number of transferred electrons:

$$\Delta N = X_{Fe} - X_{inh} / 2(\eta_{Fe} - \eta_{inh})$$

32. Nucleophilic Fukui function:

$$f^{+} = q_{(N+1)} - q_N$$

33. Electrophilic Fukui function:

$$f^{-} = q_N - q_{(N-1)}$$

34. Linear multiple regression equation by Lukovits:

$$IE_{theor} = Ax_i C_i + B$$

35. Non-linear multiple regression equation by Lukovits:

$$IE_{theor} = \frac{(AX_i + B)^* C_i}{1 + (AX_i + B)^* C_i} * 100$$

36. Sum of Squared Errors (SSE):

$$SSE = \sqrt{\sum_{i=1}^{n} (IE_{pred} - IE_{exp})^2}$$

37. Root Mean Square Error (RMSE):

$$RMSE = \sqrt{\frac{1}{n} \sum_{j=1}^{n} (IE_{pred} - IE_{exp})^2}$$